

TIME-MEAN VELOCITY MEASUREMENTS  
IN SUDDEN EXPANSION CONFINED  
FLOW WITH TANGENTIAL  
INJECTION

By

WOON DON CHAI

Bachelor of Science in Mechanical Engineering

Sung Kyun Kwan University

Seoul, Korea

1985

Submitted to the Faculty of the  
Graduate College of the  
Oklahoma State University  
in partial fulfillment of  
the requirements for  
the Degree of  
MASTER OF SCIENCE  
MAY, 1988

Thesis  
1988  
C434t  
Cop. 2



TIME-MEAN VELOCITY MEASUREMENTS  
IN SUDDEN EXPANSION CONFINED  
FLOW WITH TANGENTIAL  
INJECTION

Thesis Approved:

*David G. Lilley.*

Thesis Adviser

*A. J. Ghajar*

*P. M. Wood*

*Norman N. Dunham*

Dean of the Graduate College

## ACKNOWLEDGMENTS

The author wishes to express his sincere gratitude to his major adviser, Dr. David G. Lilley for his guidance and encouragement. Appreciation is also extended to other committee members, Dr. Peter M. Moretti and Dr. Afshin J. Ghajar.

Further, gratitude is also extended to Mr. Atef k. Khalil for his assistance with the experiments. Also, many thanks go to Mr. Seong D. Ha and Mr. Ghassan A. Eghneim. Their suggestions and support were very helpful throughout the study.

This study is dedicated to the author's parents, Mr. Chang Shin and Mrs. Jum Soon, for their encouragement and understanding.

Finally, special gratitude is expressed to the author's wife, Myoung Ock, for many sacrifices, prayer and love.

## TABLE OF CONTENTS

Chapter	Page
I. INTRODUCTION . . . . .	1
1.1 The Phenomenon . . . . .	1
1.2 The Problem . . . . .	2
1.3 Previous Studies . . . . .	3
1.4 Objectives . . . . .	7
1.5 Outline of the Thesis . . . . .	8
II. EXPERIMENTAL FACILITIES . . . . .	9
2.1 Test Section . . . . .	9
2.2 Tangential Inlet Arrangements . . . . .	10
2.3 Axial Air Arrangements . . . . .	10
2.4 Five-Hole Pitot Probe Instrumentation . . . . .	11
III. MEASUREMENT AND REDUCTION OF DATA . . . . .	14
3.1 Measurement Procedures . . . . .	14
3.2 Data Reduction . . . . .	16
3.3 Calibration . . . . .	17
IV. RESULTS . . . . .	20
4.1 Case 1 ( $m_t/m_a = 2$ and $w_t/u_{av} = 2.83$ ) . . . . .	22
4.2 Case 2 ( $m_t/m_a = 2$ and $w_t/u_{av} = 5.64$ ) . . . . .	23
4.3 Case 3 ( $m_t/m_a = 4$ and $w_t/u_{av} = 3.39$ ) . . . . .	24
4.4 Case 4 ( $m_t/m_a = 4$ and $w_t/u_{av} = 6.78$ ) . . . . .	25
4.5 Case 5 ( $m_t/m_a = 8$ and $w_t/u_{av} = 3.77$ ) . . . . .	27
4.6 Case 6 ( $m_t/m_a = 8$ and $w_t/u_{av} = 7.51$ ) . . . . .	27
4.7 Case 7 ( $m_t/m_a = 0$ and $w_t/u_{av} = 0$ ) . . . . .	29
4.8 Recirculation Zones . . . . .	29
V. CLOSURE . . . . .	31
5.1 Conclusions . . . . .	31
5.2 Recommendations for Further Work . . . . .	32
REFERENCES . . . . .	33
APPENDICES . . . . .	36
APPENDIX A - TABLES . . . . .	36
APPENDIX B - FIGURES . . . . .	73

Chapter

Page

APPENDIX C - DATA REDUCTION COMPUTER PROGRAM AND CALIBRATION DATA FOR FIVE-HOLE PITOT PROBE MEASUREMENTS. . . . .	95
-------------------------------------------------------------------------------------------------------------------------	----

LIST OF TABLES

Table	Page
I. Test Cases . . . . .	37
II. Velocity Data for Case 1 . . . . .	38
III. Velocity Data for Case 2 . . . . .	43
IV. Velocity Data for Case 3 . . . . .	48
V. Velocity Data for Case 4 . . . . .	53
VI. Velocity Data for Case 5 . . . . .	58
VII. Velocity Data for Case 6 . . . . .	63
VIII. Velocity Data for Case 7 . . . . .	68

## LIST OF FIGURES

Figure	Page
1. The Cyclone Furnace . . . . .	74
2. Photograph of the Overall Facility . . . . .	75
3. Geometry of Strongly Swirling Flow Facility . . . . .	76
4. Tangential Inlet Stilling Chamber. . . . .	77
5. Five-Hole Pitot Probe. . . . .	78
6. Apparatus for Time-Mean Velocity Measurements. Using a Five-Hole Pitot Probe. . . . .	79
7. Manual Traverse Mechanism used for Five-Hole Pitot Probe Measurements . . . . .	80
8. Pitch Angle Calibration Characteristic for Five-Hole Pitot Probe. . . . .	81
9. Velocity Coefficient Calibration Characteristic for Five-Hole Pitot Probe. . . . .	82
10. Velocity Components and Flow Direction Angles Associated with Five-Hole Probe Measurements . . . . .	83
11. Calibration Apparatus with Five-Hole Pitot Probe. . . . .	84
12. Case 1 ( $m_t/m_a = 2$ and $w_t/u_{av} = 2.83$ ). . . . .	85
13. Case 2 ( $m_t/m_a = 2$ and $w_t/u_{av} = 5.64$ ). . . . .	86
14. Case 3 ( $m_t/m_a = 4$ and $w_t/u_{av} = 3.39$ ). . . . .	87
15. Case 4 ( $m_t/m_a = 4$ and $w_t/u_{av} = 6.78$ ). . . . .	88
16. Case 5 ( $m_t/m_a = 8$ and $w_t/u_{av} = 3.77$ ). . . . .	89
17. Case 6 ( $m_t/m_a = 8$ and $w_t/u_{av} = 7.51$ ). . . . .	90
18. Case 7 ( $m_t/m_a = 0$ and $w_t/u_{av} = 0$ ) . . . . .	91
19. Sketch of Recirculation Zones . . . . .	92



## NOMENCLATURE

D	test section diameter
d	axial air inlet diameter
m	mass flow rate
P	time-mean pressure
Re	Reynolds number
u	axial velocity
v	radial velocity
w	tangential velocity
x, r, $\theta$	axial, radial, azimuthal cylindrical polar coordinates
$\beta$	yaw angle of probe = $\tan^{-1}(w/u)$
$\delta$	pitch angle probe = $\tan^{-1}[v/(u^2 + w^2)^{1/2}]$
$\rho$	density
$\psi$	probe rotation angle

## Subscripts

a	relating to axial flow at inlet
C	central location
av	average in the large test section
N,S,E,W	north, south, east, west locations
p	probe sensing tip
t	relating to tangential flow at inlet

## Superscripts

\_\_\_\_\_

time-mean average

'

fluctuating quantity

## CHAPTER I

### INTRODUCTION

#### 1.1 The Phenomenon

Vortex phenomena are described by scientists as one of the most important subjects of research in fluid motion. Today, there has been much interest in the study of swirling flows because numerous application utilizing this phenomenon have been evolved in such specialized fields as heat transfer, gas turbines, swirl atomizers, nuclear reactors, and meteorology.

Swirl flows (1,2) occur in a very wide range of application. In combustion systems, the strong favorable effects of applying swirl to injected air and fuel are extensively used as an aid to stabilization of high intensity combustion process and efficient clean combustion in a variety of practical situation.

Recently, concentrated research effort has been expended on understanding and characterizing the combustion aerodynamics of swirl flow burning processes of gaseous, liquid, and solid fuels. Economical design and operation of practical combustion equipment can be facilitated greatly by estimates made from complementary experimental and modeling studies.

Swirl flows result from the application of a spiraling motion, with a swirl velocity component (also known as a tangential velocity component) being imparted to the flow by the use of swirl vanes, by the use of axial-plus-tangential entry swirl generators or by direct tangential entry into the chambers (3).

A major outcome of the current study is the experimental characterization of the flowfield inside the cyclone chamber for seven basic flowfields. Parameter variations investigated are the ratio of the tangential air mass flow rate to the axial air mass flow rate ( $m_t/m_a$ ) and the ratio of the tangential air velocity to the mean velocity at the cyclone exit flow ( $w_t/u_{av}$ ). In the absence of particles, measurements of time-mean velocity components using a five-hole pitot probe characterized the air flow patterns.

## 1.2 The Problem

The cyclone mixer provides a means to inject solid fuel particles into furnaces for subsequent combustion. Many factors affect the particle distribution and velocity inside the cyclone chamber (4). In design situations, the engineer has to seek an optimum path between alternatives of, for example, efficiency and pollution. Figure 1 shows different cyclone-furnace arrangements:

1. Horizontal cyclone-furnace (or slightly slanting at an angle of 5-20 degrees).
2. Vertical cyclone-furnace not concentric with the furnace.

### 3. Vertical cyclone-furnace concentric.

There are many advantages of the cyclone combustion in comparison to conventional combustion chambers. They arise mainly on a unique flow pattern produced by the dominant circumference velocity component. The strong centrifugal field, created by the tangential inlet, alters the two-dimensional radial-axial flow and aids the combustion processes in several ways. The spiral fluid motion enhances the residence of solid fuel in the chamber, and provides adequate time even for the most "difficult" fuel to be completely burned (5-9).

Many instruments (10) are used for separately measuring the magnitude and direction of fluid velocity. However, there are only a few instruments capable of simultaneously sensing both magnitude and direction. The simplest of these senses pressure at certain location on the surface of a sphere, hemisphere, or some other shape of probe.

The five-hole pressure probe is recommended by Beer and Chigier (3) for mean velocity measurements in turbulent swirling flows and several investigations have successfully used it. The main technique of the five-hole probe depends on the fact that the three pressure measurements on a great circle of a sphere unequal determine the velocity component in that plane (11).

#### 1.3 Previous Studies

Three-dimensional spherical pitot probe has been developed and calibrated by Lee and Ash (12) to measure

static pressure and the magnitude and direction of the velocity vector for any arbitrary flow angle without adjustment of the probe.

Time-mean and turbulent flow quantities downstream of pipe expansions with 15, 30, 45, and 90 degrees for non-swirling flow were measured by Chaturvedi (13). The expansion diameter ratio was 2. Measurements of velocity in regions of high turbulence intensity and where the direction of the velocity vector was unknown were made with a 2.5 mm diameter pitot tube. Mean velocity was also measured with a constant temperature hot-wire anemometer using a single wire. A cross-wire used to measure all the Reynolds stresses.

Ustimenko and Bukham (14) carried out the measurement of fluctuating velocity components by a hot-wire anemometer in a cyclone chamber with four tangential inlets positioned equidistant over the circumference. They showed that symmetry in the cyclone flowfield is obtained not only for the time-mean values but for the turbulent characteristics of the flow.

The experiments of Vatistas et al (15) found the dimensionless core size, pressure drop, and radial pressure distribution depend solely upon the geometrical parameters of cyclone chamber from the analytical model with potential flow assumption and confirmed their findings with experiment.

The detailed experimental measurements on a multi-inlet cyclone combustion under both isothermal and combustion conditions have been done by Styles et al (16). Pressure

drop and processing vortex core frequency were measured for a fuel gas/air mixture model under both conditions using a pressure transducer. Temperature measurements were also obtained in the downstream region of the exit on combustion condition by thermocouples.

The research of Lilley (17) was concerned with experimental and theoretical studies on 2-D axisymmetric geometries under low speed nonreacting, turbulent, swirling flow conditions typical of gas turbine and ramjet combustion chambers. They included recirculation zone characterization, time-mean and turbulence simulation in swirling recirculating flow, sudden and gradual expansion flowfields, and further complexities and parameter influences. The study included the investigations: a complete range of swirl strength; swirler performance; downstream contraction nozzle sizes and combined effects on the test section flowfield were observed, measured and characterized. In addition to hot-wire experiments and theoretical studies, one Ph.D. thesis (18) and two M.S. theses (19,21) evolved during the comprehensive study.

In experiments of Rhode (18), he utilized the five-hole pitot probe technique to measure time-mean velocities  $u$ ,  $v$ ,  $w$  in the large diameter test section with  $D/d = 2$ , low swirl strengths  $\phi = 0, 38$  and  $45$  degrees, and no downstream nozzles. Later, Yoon (19) extended the study to higher swirl strengths  $\phi = 60$  and  $70$  degrees, and downstream nozzle effects with both weak and strong nozzles of area ratios  $A/a = 2$  and  $4$  located at  $x/D = 1$  and  $2$ . The results show that

the presence of a swirler shortens the corner recirculation zone and generates a central recirculation zone followed by a precessing vortex core. The effect of a gradual inlet expansion is to encourage the flow to remain close to the sidewall and shorted the extent of the corner recirculation zone in all cases investigated. And the time-mean and turbulence properties of a confined swirling jet using the six-orientation, single hot-wire technique were obtained by Jackson (20). The test section with expansion ratios  $D/d = 1$  and 2 was equipped with a strong contraction nozzle of area ratio 4 at  $x/D = 2$ . The effect of swirl on time-mean velocities, complete Reynolds stress tensor and dissipation rates were measured.

More recently, Scharrer (21) used the same measurement technique with smaller test section tubes with  $D/d = 1.5$  and 1, again with downstream nozzles and a full range of swirl strengths. Findings included that the corner recirculation zone is prominent in nonswirling expanding flows, but it decreases when swirl is introduced. The presence of swirl results in the formation of a central recirculation zone. Initially increases in inlet swirl strength result in an increase in length of this zone. However, increasing to very high swirl strengths results in a shortening and widening of this zone.

The exit velocities of a cyclone chamber which had axial and tangential inlets with  $D/d = 4.5$  and downstream nozzle at  $x/D = 2$  were measured by Khalil and Lilley (22). And they visualized the particle distribution at the cyclone exit.



They also measured the concentration of particles in a mixed air-particle flow by a direct probe sampling method.

Findings included that extreme high level of swirl reduces the efficiency of the cyclone as a mixing device.

The present study used same facility but without nozzle and extends this earlier study (22) by investigating in detailed the flow development after injection. The earlier thesis work at O.S.U. described in Reference 17 was presented in research papers (23-26).

#### 1.4 Objectives

The present paper describes a logical sequence of experiments which were undertaken to establish the effects on the flowfield of the cyclone chamber with axial and tangential inlets and no downstream nozzle for sudden expansion into large plexiglass pipe  $D/d = 4.5$  for seven basic flowfields.

The parameters to be studied are the ratio of the tangential air mass flow rate to the axial air mass flow rate ( $m_t/m_a$ ) and the ratio of the tangential air velocity to the mean velocity at the cyclone exit flow ( $w_t/u_{av}$ ).

A five-hole pitot probe was used to measure the magnitude and direction of the time-mean velocity.

The experimental research included in this study concentrated on:

- (a) measurements of the magnitude and direction of the flow velocity.

- (b) The effects on geometric parameters on the flow-field in the cyclone chamber.

### 1.5 Outline of the Thesis

In the Section I, the significance and scope of this study are introduced. Section II describes facilities used in the investigation. This section also explains the operation of the five-hole pitot probe which was used to measure the magnitude and direction of the time-mean velocity.

Section III describes the procedures of data measurements and reduction. The raw data measured by a five-hole pitot probe are reduced by a Fortran computer program which was made by Rhode (18). A detailed description of the data reduction computer program is listed in Appendix C. And Reference 19 explains the instruction for its use.

Section IV contains the results obtained for different boundary conditions. Finally Section V summarizes these results and suggests further research.

## CHAPTER II

### EXPERIMENTAL FACILITIES

A complete test facility has been built in the Mechanical Engineering Laboratory at Oklahoma State University by Khalil, and it is described in detail in Reference 22. The major features are recalled here.

A schematic of the overall facility is shown in Figure 2. The test facility consists of a cyclone mixer test section which has two inlets; axial and tangential, air blowing and stilling chamber for the tangential inlet and exhaust system.

#### 2.1 Test Section

The test section is composed of a cyclone mixer assembly. The general arrangement of this is given in Figure 3. According to manufacturing consideration the test section was constructed from different parts and materials, nine inch internal diameter plexiglass tube with 1/8" (0.32 cm) thickness was used. The tangential inlet was made of a box according to the required dimensions and was fixed to an opening made in the 9" (22.86 cm) tube.

Great attention was made in using the different machines to get the same centerline for different concentric parts

within an accuracy 0.01 mm. And two wooden cradle which are mounted on a table supports the test section.

## 2.2 Tangential Inlet Arrangements

The tangential air was supplied by a centrifugal blower directly coupled to a 1.5 horse power motor. The maximum output of this blower is 200 CFM and to control the rate of air volume a system of two coaxial orifices with slots was used to partially block the blower intake.

Next is the stilling chamber. It consists of: jet facing plate; followed by two fine mesh screens. Next is the area reduction section which was designed by the method of Morel (27) to produce a minimum adverse pressure gradient on the boundary layer to avoid the flow unsteadiness phenomenon associated with local separation regions. The slope angle was 5 degrees. The final reduced cross-sectional area was the same like that of the rectangular tangential inlet of the cyclone mixer. Figure 4 illustrated the design of this stilling chamber which ensure the supply of a uniform air velocity to the tangential air inlet of the cyclone.

The dynamic pressure from which the air velocity can be calculated and also the air volume flow rate was measured by a two-hole pitot static pressure probe which had been embedded in the rectangular section just before the cyclone inlet.

## 2.3 Axial Air Arrangements

Air volume flow rate is controlled by a pressure

regulator and measured by a calibrated rotameter. And compressed air is supplied to 2" diameter tube.

A 25 liter pressurized air tank is used to damp any pressure fluctuation in the compressed air line before the pressure regulator. The static pressure is measured by a pressure manometer.

#### 2.4 Five-Hole Pitot Probe Instrumentation

A five-hole pitot probe has been used for instruments capable of measuring both the magnitude and the direction of fluid velocity simultaneously. The five-hole pitot probe used in this study is a model DC-125-12-CD manufactured by United Sensor and Control Corp. The accuracy of this particular probe is well documented in Reference 18 and 19. It is shown schematically in Figure 5 and has a 3.2 mm diameter steel sensing tip and shaft containing five tubes. The sensing head is hook-shaped to allow for probe shaft rotation without altering the probe tip location.

There are three standard method of operating the five-hole pitot probe:

1. To adjust the orientation of the probe in both pitch and yaw so that the probe is aligned with the local flow direction.
2. To determine the flow direction from the calibration relationship between probe pressures and flow direction while maintaining a fixed probe orientation.
3. To align the probe yaw angle with the flow yaw angle

while deducing the pitch angle and total velocity coefficient calibration characteristics.

The third method was employed in this study because it used readily available orientation equipment and relatively simple data reduction procedures.

The five-hole pitot probe is accurate within the approximately 5 percent for most of the measurements (24). This value may increase to 10 percent as the velocity magnitude falls below approximately 2.0 m/s because of the insensitivity of the probe to low dynamic pressure.

The instrumentation assembly, in addition to the five-hole pitot probe, consists of a manual traverse mechanism, two five-way ball valves, a differential pressure transducer, a power supply, and an integrating digital voltmeter. The probe is mounted vertically on the test chamber, as shown in Figure 6, using a manual traverse mechanism, model C 1000-18 from United Sensor and Control Corp. This mechanism, shown in Figure 7, is made entirely of steel with a linear vernier accurately readable within  $\pm 0.25$  mm. This allows the probe to vertically traverse across the chamber radius with the capability of manually rotating the probe about its axis to null the yaw angle felt by the pressure sensing tip. This yaw angle is read from the rotary vernier of the traverse unit which is accurately readable within  $\pm 0.2$  degree. The differential pressure transducer is model 590D from Datametrics, Inc. It has a differential pressure range of from 0 to  $1.3 \times 10^3$  N/m<sup>2</sup>. The pressure transducer output is read as the d.c. signal from the TSI model 1076 integrating voltmeter. Use of

an integrating voltmeter removes pressure fluctuations from the vibrating tygon tubing connecting the probe to the valves and transducer.

Finally, auxiliary equipment is used, including a barometer/thermometer unit from Cenco Corp. for local pressure and temperature readings.

## CHAPTER III

### MEASUREMENT AND REDUCTION OF DATA

#### 3.1 Measurement Procedures

The basic measurement technique entails aerodynamically nulling the yaw in the horizontal plane by rotation of the probe about its vertical shaft and then reading two differential pressures ( $p_N - p_S$  and  $p_C - p_W$ ). These pressures along with the yaw angle  $\beta$  are used to obtain the pitch angle  $\delta$  in the vertical plane and the magnitude of total velocity vector from the calibration characteristics. The data reduction employs two calibration curves which were obtained for a single calibration velocity. The underlying principle is that the calibration is independent of probe Reynolds number  $Re_p$ , which is based on probe tip diameter (18).

Calibration experiments of Rhode et al (22) reveal that this condition exists for  $Re_p \geq 1090$ , or a local velocity of 5.4 m/s. Hence measurements of such low velocities suffer from a necessary calibration error. However, the investigation also shows that this calibration error affects the velocity measurements typically by less than 6 percent for  $Re_p \geq 400$ , corresponding to a local velocity greater than 2.0 m/s. In this study, all calibrations are conducted at



air velocity of 6.01 m/s.

Before the production measurements, five-hole pitot rotary vernier must be zeroed for yaw so that the  $x$  and  $\theta$  axis of the measurement coordinate frame coincide with those of the test section, which are illustrated in Figure 6. This is accomplished by rotating the probe until the yaw is aerodynamically nulled near the center of the test section inlet for nonswirling flow. The radial axes of the probe and the test section coincide since the traverse unit base has been carefully machined to mount vertically on the plexiglass tube. The pressure and yaw angle data are read at 0.3 inch increments up to 3.9 inches in the upper half from the centerline and 4.2 inches in the lower half from the centerline.

After the pressure transducer is zeroed, the measurement procedure for each location within a traverse begins with rotation of the probe until the yaw is aerodynamically nulled. This is indicated by a zero reading for  $p_w - p_E$ , where the pressures are identified in Figure 5. The resulting probe rotation angle is read from the rotary vernier. Then the five-way switching valves are set so that  $p_N - p_S$  is sensed by transducer. Finally, the reading of  $p_C - p_w$  is similarly obtained.

The quantity of air mass flow rate has been previously obtained as illustrated in Section 2.2, 2.3 of the discussion about test facilities. The ambient pressure and temperature were monitored near the facility for the determination of air density.

### 3.2 Data Reduction

The differential pressure reading from the five-hole pitot probe are utilized directly to obtain the square of the vector velocity. The vector velocity of turbulent flow consists of a time-mean velocity and a fluctuating velocity component. Since

$$\overline{V^2} = \overline{V}^2 + \overline{V'^2} \quad (3.1)$$

where  $V'$  is the fluctuating portion of the velocity magnitude and the overbar denote time-averaging, it is slightly incorrect to infer that  $\overline{V^2}$  is equal to the square of the magnitude of the time-mean velocity vector  $\overline{V}$ . However, the fluctuation term  $\overline{V'^2}$  is not known and very little information is available for the effect of turbulence in swirl flows on pressure probes, which is probably considerable for the effect of turbulence in swirl flows on pressure probes, which is probably considerable for turbulence intensities greater than about 20 percent (1). Furthermore, the procedures for making corrections for turbulence levels are long and tedious, and even then the confidence in their applicability is unknown. Therefore, no attempt is presently made to incorporate such corrections, and the deduced velocity is taken to be the time-mean velocity magnitude  $\overline{V}$  which is written without the overbar from here onward.

All data used in this investigation were reduced with a Fortran computer program which is similar to that developed by Rhode (18) by first calculating the pitch coefficient ( $p_N$

$-p_s)/(p_c - p_w)$ . From this value a cubic spline interpolation technique (28) is used to obtain the pitch angle  $\delta$  in the vertical plane from the calibration characteristic presented in Figure 8. The resulting value of  $\delta$  is similarly utilized to determine the velocity coefficient  $\rho V^2/[(p_c - p_w)]$  from the calibration characteristic given in Figure 9.

Values for  $V$  as well as the axial, radial, and swirl velocity components  $u$ ,  $v$ , and  $w$ , shown in Figure 10, are easily calculated from the velocity coefficient, pitch angle, and yaw angle  $\beta$ , which is in the horizontal plane.

The latter angle is given by

$$\beta = 360^\circ - \psi \quad (3.2)$$

where  $\psi$  is the probe rotation angle read on the rotary vernier of the traverse mechanism. The magnitude of the velocity vector is given by

$$V = \left[ \frac{2 \rho V^2}{\rho 2(p_c - p_w)} (p_c - p_w) \right]^{1/2} \quad (3.3)$$

and the velocity components are obtained from

$$u = V \cos\delta \cos\beta \quad (3.4)$$

$$v = V \sin\delta \quad (3.5)$$

and

$$w = V \cos\delta \sin\beta \quad (3.6)$$

### 3.3 Calibration

A five-hole pitot probe must be calibrated carefully to translate the measured quantities  $\beta$ ,  $(p_N - p_s)$ , and  $(p_c - p_w)$  into a velocity magnitude and a direction. The calibration

equipment consists of a small air jet, a rotary table, a probe mounting bracket, and the instrumentation system previously described. The calibration jet supply line consists of a compressed air line, which delivers the desired flow rate through a small pressure regulator and a Fischer and Porter model 10A1735A rotameter. The jet housing consists of an effective flow management section followed by a contoured nozzle with a 3.5 cm diameter throat.

The five-hole pitot probe is rotated by the rotary table model BH-9 from Troyke Manufacturing Co., whose rotary vernier is readable within  $\pm 0.5$  minutes. As shown in Figure 11, the aluminum probe mounting bracket is secured to the rotary table, and it supports the probe which rests in a cylindrical steel collect.

The motion of the rotary table orients the probe at the desired pitch angle, whereas the yaw is aerodynamically nulled. The probe sensing tip remains at the centerline within the potential core of the jet and less than one throat diameter downstream of the nozzle discharge plane. The pitch angle is zeroed by very carefully aligning the probe shaft in a plane parallel to that of the nozzle throat.

The operation of calibration consists of recording the voltage output from the pressure transducer for differential pressure  $p_N - p_s$  and  $p_c - p_w$ , where these pressures are identified in Figure 5. These data are measured at 5 degree increments in  $\delta$  over the range  $-58^\circ \leq \delta \leq 58^\circ$ . The measurement technique requires the entire calibration to be conducted at a constant jet velocity. This is permitted

since the dimensionless calibration coefficients are independent of  $Re_p$  for  $Re_p \geq 1090$  (5.4 m/s) determined by careful calibration experiments (18).

As shown in Figures 8 and 9, the calibration characteristics from which  $\delta$  and velocity coefficient  $\rho V^2/[2(p_o - p_w)]$  are obtained, respectively. Both curves exhibit considerable symmetry, as the five pressure sensing holes are almost symmetrical about the probe tip axis.

## CHAPTER IV

### RESULTS

A number of experiments have been done on the sudden expansion cyclone facility without exit nozzle so as to investigate the flow patterns and velocity distribution inside the flow domain. The geometry of the facility was detailed in Chapter II. Velocity measurements were made with the five-hole pitot probe as described in Chapter III. The effects of two inlet flow parameters on the flowfield were investigated: the ratio of the tangential inlet air mass flow rate to the axial inlet mass flow rate ( $m_t/m_a = 2, 4, 8,$  and  $0$ ) with two values of the tangential inlet velocity in each of the swirling cases. With the lower inlet tangential velocity, Cases 1, 3, and 5 were obtained as the mass flow ratio increased (equal to 2, 4, and 8, respectively). Cases 2, 4, and 6 were corresponding cases with the higher tangential velocity, obtained by blocking half the area of the tangential inlet, so doubling the inlet tangential velocity. Case 7 was for nonswirling flow conditions with no tangential injection. These seven flowfields have ratio of tangential inlet velocity to mean axial velocity (in the downstream region) of  $w_t/u_{av} = 2.83, 5.64, 3.39, 6.78, 3.77, 7.51,$  and  $0$ . Seven axial measurement stations were chosen:

$x/D = 0.25, 0.75, 1.25, 1.75, 2.25, 2.75$  and  $3.75$ , each with up to 27 measurements points across the vertical plane.

Table I illustrates the different parameters investigated for the seven cases covered in the study.

Flow characteristics are tabulated in terms of normalized time-mean  $u$ ,  $v$ , and  $w$  velocity components, yaw angle  $\beta$  and pitch angle  $\delta$  in Tables II through VIII. Axial and swirl velocity profiles for all flowfields are shown in Figures 12 through 18 to illustrate the main findings of the experiments.

All the figures show time-mean velocity measurements at the axial locations  $x/D = 0.25, 0.75, 1.25, 1.75, 2.25, 2.75$  and  $3.75$  respectively. Full traverses were made at the first 5 measurement locations, but because of near axisymmetry, only half traverses were needed at the two furthest downstream locations. Part a of the figures gives the normalized time-mean axial velocity  $u$ ; it presents measurements of  $u/u_{av}$  (time-mean axial velocity normalized by division with the cross-sectional averaged time-mean axial velocity at the test section exit). Part b shows the normalized time-mean swirl velocity  $w$ ; it presents measurements of  $w/u_{av}$  (time-mean swirl velocity normalized by division with the cross-sectional averaged time-mean axial velocity at the test section exist. Radial velocities were consistently much smaller than the axial and swirl components, and are not plotted. These values are available in the tabulated data.

The near-axisymmetry assumption was verified by

additional measurements in the lower half of the tube, with + marking these values on the figures.

#### 4.1 Case 1 ( $m_t/m_a = 2$ and $w_t/u_{av} = 2.83$ )

Figure 12 shows normalized axial and swirl velocity measurements for Case 1. As can be seen from Figure 12(a), the maximum axial velocity occurs close to the centerline at the first upstream location. At  $x/D = 0$  the average inflow has a normalized velocity magnitude of  $u_a/u_{av} = 6.74$  across the central region ( $r/D =$  less than 0.11). In fact this inflow is not of constant velocity, because of the build up of the wall boundary layer will have caused a rounded or peaked velocity profile. The additional mass flow of the tangential injection and other geometric and flow changes causes a normalized velocity magnitude of 8.63 to occur at the first measurement station at  $x/D = 0.25$ . Further, the maximum axial velocity shifts towards the outer boundaries as the flow proceeds in the downstream direction. The negative axial velocities seen at the first station ( $x/D = 0.25$ ) in the lower part of the tube are explained on the basis of the tangential inflow suddenly sensing an area increase on entering the large flow. This is amalgamated with the effects of the axial flow, also tending to recirculate after entry to the large tube (at  $x/D = 0$ ). This nonsymmetrical phenomenon at the upstream station is observed in all the swirl flow cases investigated. It is seen clearly in part a of Figures 12 through 17.

In a similar flow situation with weak swirl strength,



Rhode (18) found the central recirculation zone ending at  $x/D = 1.5$  with swirl vane angle  $\phi = 38$  degrees and  $D/d = 2$  which is smaller than this study ( $D/d = 4.5$ ). The central recirculation zone is caused by a swirl velocity being imparted to the flow via use of swirl vane. The central recirculation zone is defined as the wide reverse flow region encountered near the inlet.

As shown in Figure 12(b), the radial location where the maximum swirl velocity occurs increases in the downstream direction. But the maximum velocities in Rhode (18) exist near the centerline. The swirl velocity along the axis as shown in Figure 12(b) is found to be zero as expected because of symmetry. And the profiles of swirl velocity are beginning to be symmetric starting at location  $x/D = 2.25$ .

#### 4.2 Case 2 ( $m_t/m_a = 2$ and $w_t/u_{av} = 5.64$ )

Case 2 was conducted in the same condition to the Case 1 except that the ratio of the inlet tangential velocity to the mean axial velocity of the cyclone exit flow ( $w_t/u_{av}$ ) was twice that of Case 1.

The corner recirculation zone near the upper and lower half at the location  $x/D = 0.25$  provoked by the rather sudden enlargement of the cross-sectional area and increasing of swirl velocity. It can be seen from the Figure 13(a) that the velocity profiles are changed dramatically at the three upstream locations. This is because the upstream locations are close to the tangential air inlet and the swirl velocity increases.

In Figure 13(a) back flow is seen to occur at three upstream locations ( $x/D = 0.25, 0.75, 1.25$ ) instead of occurring at only one location as in Case 1. Also axial velocity profiles are a symmetric in early upstream locations whereas the maximum axial velocities occur near the wall and centerline in the downstream locations as inlet swirl velocity increases as compared to Case 1.

The swirl velocities are minimal in a large region (almost half the tube width) near the centerline at the three upstream locations because incoming axial velocity is larger than the incoming tangential velocity, see part b of Figure 13. The maximum swirl velocities occur close to the wall since strong centrifugal forces are present in the incoming tangential inlet flow. In a similar flow situation, measurements of Scharrer and Lilley (25) with expansion ratio  $\alpha = 90$  degrees, swirl vane angle  $\phi = 45$  and  $70$  degrees, and  $D/d = 1.5$  shows the swirl velocity profiles are nearly uniform in the near-wall region and the radial location of the maximum swirl velocity moves outward for the strong swirl case due to centrifugal effects. As compared to Case 1, the difference is that the symmetry of the axial velocity profiles is destroyed by the increased swirl velocity.

#### 4.3 Case 3 ( $m_t/m_a = 4$ and $w_t/u_{av} = 3.39$ )

In this case, the ratio of the tangential inlet mass flow rate to the axial inlet mass flow rate was twice that of Case 1. All axial velocities except the first location are positive like Case 1. Therefore increasing the mass flow

rate promotes a very large forward velocity. By looking at the Figure 14(a) one can see that the maximum axial velocities occur near the wall and the minimum occur near the centerline. Further, the profiles of the axial velocity are visibly changing in the downstream locations as compared to Case 1.

Yoon and Lilley (24) with expansion angle  $\alpha = 90$  degrees,  $D/d = 2$ , and swirl vane angle  $\phi = 45$  degrees found a considerable back flow around the hub. However, in this case the back flow did not occur except at the first location, which is caused by increasing the tangential inlet mass flow rate. As shown in Figure 14(a) the profiles of the axial velocities are not symmetric like Case 1. This implies that increasing tangential mass flow ratio does not affect the symmetry of axial velocity profiles.

Swirl velocity profiles are almost similar to those in Case 1. Like Case 1, the maximum swirl velocities are observed close to the wall and the minimum occur near the centerline. Also the profiles of the swirl velocity start being symmetric from location  $x/D = 2.25$ . Hence the symmetry of swirl velocity profile is not affected by increasing tangential mass flow ratio.

#### 4.4 Case 4 ( $m_t/m_a = 4$ and $w_t/u_{av} = 6.78$ )

The tangential air inlet was partially blocked so that the mass flow rate remains the same with the tangential velocity doubled. As shown in Figure 15(a), the reverse flow

occurs much more than Case 2 and 3. This means that back flow increases as the swirl velocity increases. In contrast to Case 2, the locations of the maximum axial velocity moves from the centerline to the wall as one goes in the downstream direction. This effect results from the stronger centrifugal forces present now as compared to Case 2. Also the minimum velocities exist near the  $r/D = 0.3$  like Cases 2 and 3. Rhode and Lilley (23) measured time-mean velocity in the test section with  $D/d = 2$  as the swirl vane angle increase. In their results, the maximum axial velocity occurs near the wall and minimum velocity occurs at the centerline because the large central recirculation region cause the downstream flow to accelerate near the wall. It may be seen that the profiles of the axial velocity are more symmetric than Case 3, which means that the higher inlet swirl velocity affects the axial velocity profile considerably.

Figure 15(b) reveals that this stronger swirl velocity case provides much more symmetric profiles of swirl velocities which is caused by even stronger centrifugal forces. Like other cases, the maximum swirl velocity occurs near the wall and the minimum velocity is zero near the centerline because of symmetry. Rhode and Lilley's (23) results give that the swirl velocities are maximum in a large region from  $r/D = 0.2$  to the wall and the minimum exists near the centerline as the swirl vane angle increases. As illustrated in Figure 15(b) the profiles of the swirl velocity are symmetric in early locations as the swirl velocity increases as compared to the Case 3.

#### 4.5 Case 5 ( $m_t/m_a = 8$ and $w_t/u_{av} = 3.77$ )

This case considers the largest mass flow ratio. Back flows occur in the lower part at the first station and  $r/D = 0.25$  at  $x/D = 1.75$  as shown in Figure 16(a). The maximum axial velocities exist near the outer boundaries. Therefore increasing the tangential inflow keeps the flow near the boundaries with large forward velocities.

The profiles of the axial velocity are not symmetric, see Figure 16(a). Hence increasing of the mass flow ratio does not affect the axial velocity profile and promotes the high positive axial velocity near the wall.

The profiles of the swirl velocity in Figure 16(b) are very symmetric as compared to Case 1 and Case 3. So the mass flow ratio influences the swirl velocity profile very much. It may be seen that the location of the maximum swirl velocity occurs near the wall through all cases, which is caused by large tangential inlet mass flow ratio. Also as shown in Figure 16(b), the swirl velocity along the axis is found to be zero as expected because of symmetry.

#### 4.6 Case 6 ( $m_t/m_a = 8$ and $w_t/u_{av} = 7.51$ )

Here, the strongest inlet swirl velocity was considered. As illustrated in Figure 17(a) a lot of back flow around  $r/D = 0.3$  is observed in the lower half of the domain. But Scharrer (21) with  $D/d = 1.5$  gives a considerable reverse flow near the axis as the largest swirl vane angle  $\phi = 70$  degrees. This difference results from the different inlet

swirl velocity position. However, the maximum axial velocity is observed close to the wall in both cases because of the strong centrifugal forces present in the incoming swirling flow. These keep the majority of the flow near the confining walls with resulting higher velocities.

As shown in Figure 17(a) the symmetry is much more prevalent than the previous cases which leads to the conclusion that profiles get increasingly symmetric with the increasing swirl velocity. Yoon and Lilley's (24) results (with  $D/d = 2$  which is also smaller than this case) show that the radial location where the maximum swirl velocity occurs goes up as the swirl vane angle increases. Figure 17(b) shows that the maximum swirl velocity occurs near the wall, which are caused by the increase of the centrifugal effects. As shown in Figure 17(b), the swirl velocity near the axis is zero because of symmetry like other cases.

The above observances are summarized as follows. It may be seen in Figure 12(b) through 17(b) that the profiles of the normalized swirl velocity become symmetric in early axial locations as the inlet mass flow ratio and swirl velocity increase. And the effect of the increase of the swirl velocity generates a considerable back flow and promotes the symmetry of the normalized axial velocity profiles. However, normalized axial velocity profiles are unaffected by the inlet mass flow ratio ( $m_t/m_a$ ). All axial velocities at the centerline are positive for all cases. And maximum swirl velocities occur near the outer boundaries in

all cases.

#### 4.7 Case 7 ( $m_t/m_a = 0$ and $w_t/u_{av} = 0$ )

Figure 18 shows normalized axial velocity for nonswirling flow for comparison with all the other cases which contained swirl. A nearly flat axial velocity profile is seen in the entrance region of the test section. As expected, there was no measurable swirl velocity and it is therefore not plotted. The corner recirculation zone extends to about  $x/D = 0.75$ , which is about two step-heights downstream of the inlet expansion. Yoon and Lilley (24) measured the reattachment point in a test section with an expansion ratio  $D/d = 2$ , which is different from the present study (with  $= 4.5$ ). The result yields a value of  $x/D = 2$  as a reattachment point, which corresponds to an attachment point approximately eight step-heights downstream. This is much greater than the present study. Therefore large expansion ratio shortens step-heights toward upstream direction.

Although a corner recirculation zone is present, there is no evidence of a central torridly recirculation zone. Indeed there is no swirl-induced centrifugal force to encourage its formation. As shown in Figure 18(a), the axial velocity profiles are almost symmetric.

#### 4.8 Recirculation Zones

General observations of recirculation zones in the test section are given in Figure 19 for all cases. As shown in

Figure 19, recirculation zones are generally more prominent in the lower part of domain than the top part. This is because of greater centrifugal effects near the lower part of the tube close to the incoming tangential flow.

The recirculation zones of Cases 1, 3, and 5 appear only in the bottom of the tube. However Cases 2, 4, and 6 with stronger incoming swirl velocity provide additional recirculation zones in the half of the tube, and larger zones in the lower half.



## CHAPTER V

### CLOSURE

#### 5.1 Conclusions

The present research is concerned with the time-mean velocity measurements of a nonreacting, swirling flowfields. Three velocity components normalized with the average axial velocity at the test section exit are tabulated along with yaw and pitch angles.

Many factors affect the velocity distribution in cyclone chamber such as degree of inlet swirl and choice of geometric parameters. A major outcome of the current study is the experimental characterization of these factors for seven basic flowfields. Parameter variations which define these flow conditions are the ratio of the tangential air mass flow rate to the axial mass flow rate ( $m_t/m_a$ ) and the ratio of the tangential inlet air velocity to the mean velocity of the test section exit ( $w_t/u_{av}$ ).

The detailed experiment involved of the measurement of time-mean velocity components using a five-hole pitot probe. These measurements provided a complete understanding of each flowfield and an extensive data base for latter verification of a theoretical simulation of the complex turbulent flow.

Recirculation increases for a fixed ratio of the tangential inlet mass flow rate to axial inlet mass flow rate ( $m_t/m_a$ ) as tangential inlet velocity increases. All axial velocities at the centerline are positive for all cases. The normalized axial velocity profile become more uniform in the downstream direction. And normalized axial velocity profiles were unaffected by the inlet mass flow ratio ( $m_t/m_a$ ). On the other hand, the normalized swirl velocity profiles are almost unaffected by downstream locations, or inlet mass flow ratio, or magnitude of inlet swirl velocity. Maximum swirl velocities occurred near the outer boundary in all cases.

## 5.2 Recommendations for Further Work

Fundamental research should be continued in swirling flows in several areas. First, additional flow visualization and computational studies would be useful in helping to understand the flowfield. Second, more realistic geometry could be achieved by changing the sudden expansion to gradual expansion and putting a downstream contraction nozzle in place. Third, further details of the flowfields are needed to allow a more complete fundamental understanding. These should consist of turbulence quantity measurements, including all of the Reynolds stresses. This would allow the deduction of more sophisticated turbulence models relating turbulent shear stresses with time-mean velocity gradients and useful for prediction study.

## REFERENCES

- (1) Gupta, A. K., Lilley, D. G., and Syred, N. Swirl Flows. Abacus Press, Turnbrige Wells, England, 1982.
- (2) Lilley, D. G. "Swirl Flows in Combustion:A Review." Paper AIAA-77-405, San Diego, Calif., July 14-16, 1976.
- (3) Beer, J. M. and Chigier, N. A. Combustion Aerodynamics. London:Applied Science, and New York: Halsted-wiley, 1972.
- (4) Stambuleanu, A. Flame Combustion Processes in Industry. Abacus Press, 1980.
- (5) Rietema, K. and Verver, C. G. Cyclones in Industry. Elsevier Pub. Co., New York, 1961.
- (6) Priestly, G. and Stephens, H. S. "Hydrocyclones." International Conference on Hydrocyclones, Cambridge, England, October 1-3, 1980.
- (7) Bradley, D. The Hydrocyclone. Technomic Pub. Co., New York, 1984.
- (8) Svarovsky, L. Hydrocyclone. Pergamon Press, New York, 1965.
- (9) Poole, J. B. and Doyle, D. Solid-liquid Separation Chemical Pub. Co., New York, 1968.
- (10) Bryer, D. W. and Pankhurst, R. C. Pressure-Probe Methods for Determining Wind Speed and Flow Direction. Her Majesty Stationary Office, London, 1971.
- (11) Hiett, G. F. and Powell, G. E. "Three-Dimensional Probe for Investigation of flow Patterns." The Engineer (January, 1962), pp. 165-170.
- (12) Lee, J. C. and Ash, J. E. "A Three-Dimensional Spherical Pitot Probe." Transactions, ASME (April, 1956), pp. 603-608.
- (13) Chaturvedi, M. C. "Flow Characteristics of

- Axisymmetric Expansions." Proceedings, Journal of the Hydraulics Division, ASCE, Vol. 89, No. HY3 (1963), pp. 61-92.
- (14) Ustimenko, B. P. and Bukhman, M. A. "Turbulent Flow Structure in a Cyclone Chamber." Thermal Engineering, Vol. 15, No. 2, 1968, pp.90-94.
- (15) Vatistas, G. H., Lin, S., and Kwok, C. K. "Theoretical and Experimental Studies on Vortex Chamber Flows." AIAA Journal, Vol. 24, No. 4, April 1986, pp.635-642.
- (16) Styles, A. C., Syred, N., and Najim, S. E., "A Study of Modulatable Cyclone Combustors Using Gaseous Fuel." Paper presented at Spring Meeting of Central Section, The Combustion Institute, NASA Lewis Research Center, OH, March 1977.
- (17) Lilley, D. G. "Investigations of Flowfields Found in Typical Combustor Geometries." NASA Contractor Report 3869, February, 1985.
- (18) Rhode, D. L. "Predictions and Measurements of Isothermal Flowfields in Axisymmetric Combustion Geometries." Ph.D. Thesis (December, 1981), Oklahoma State University.
- (19) Yoon, H. K. "Five-Hole Pitot Probe Time-Mean Velocity Measurement in Confined Swirling Flows." M.S. Thesis (July, 1982), Oklahoma State University.
- (20) Jackson, T. W. "Turbulence Characteristics of Swirling Flowfields" Ph.D. Thesis (December, 1983), Oklahoma State University.
- (21) Scharrer, G. L. "Swirl Expansion Ratio and Blockage Effects on Confined Turbulent Flow." M.S. Thesis (May, 1984), Oklahoma State University
- (22) Khalil, A. H. and Lilley, D. G. "Experimental Study of Exit Velocity and Relative Particle Concentration Distributions from Two-Phase Flow in a Cyclone Mixer." Report, 1987, Oklahoma State University.
- (23) Rhode, D. L., Lilley, D. G., and McLaughlin, D. K. "Mean Flowfields in Axisymmetric Combustion Geometries with Swirl." Paper AIAA, Orlando, Florida, Jan 11-14, 1982
- (24) Yoon, H. K. and Lilley, D. G. "Five-Hole Pitot Probe Time-Mean Velocity Measurements in Confined Swirling Flows." Paper AIAA-85-0315, Reno, Nevada, Jan 10-13, 1983.

- (25) Scharrer, G. L. and Lilley, D. G. "Five-Hole Pitot Probe Measurements of Swirl Confinement and Nozzle Effects on Confined Turbulent Flow." Paper AIAA-84-1605, Snowmass, Colorado, June 25-27, 1984.
- (26) Jackson, T. W. and Lilley, D. G. "Single-Wire Swirl Flow Turbulence Measurements", Paper AIAA-83-1202, Seattle, Washington, June 27-29, 1983.
- (27) Morel, T. "Comprehensive Design of Axisymmetric Wind Tunnel Constructions" ASME paper 75-FE-17, Minneapolis, Minn, May 5-7, 1975.
- (28) Gerald, C. F. and Wheatley, O. W. Applied Numerical Analysis, Addison-Wesley Publishing Company, 1985.

APPENDIX A

TABLES

TABLE I TEST CASES

Investigated Case	$m_t/m_a$	$w_t/u_{av}$	$m_t$ (CFM)	$m_a$ (CFM)	$w_t$ (m/s)	$u_a$ (m/s)	$u_{av}$ (m/s)
Case 1	2	2.82	70	35	3.41	8.15	1.21
Case 2	2	5.64	70	35	6.82	8.15	1.21
Case 3	4	3.39	80	20	3.90	4.66	1.15
Case 4	4	6.78	80	20	7.80	4.66	1.15
Case 5	8	3.77	144	18	7.01	4.19	1.86
Case 6	8	7.51	128	16	12.47	3.73	1.66
Case 7	0	0	0	38.5	0	6.99	0.44

TABLE II  
VELOCITY DATA FOR CASE 1

	I =	1	2	3	4	5	6	7
J	X =	0.0063	0.0190	0.0318	0.0444	0.0572	0.0698	0.0952
	Y							
27	0.0914	0.273E+03	0.294E+03	0.302E+03	0.307E+03	0.302E+03	0.290E+03	0.299E+03
26	0.0838	0.277E+03	0.302E+03	0.303E+03	0.305E+03	0.303E+03	0.290E+03	0.298E+03
25	0.0762	0.278E+03	0.311E+03	0.305E+03	0.303E+03	0.303E+03	0.291E+03	0.298E+03
24	0.0686	0.280E+03	0.324E+03	0.309E+03	0.301E+03	0.302E+03	0.292E+03	0.297E+03
23	0.0610	0.285E+03	0.335E+03	0.315E+03	0.301E+03	0.304E+03	0.294E+03	0.297E+03
22	0.0533	0.300E+03	0.344E+03	0.322E+03	0.302E+03	0.305E+03	0.296E+03	0.298E+03
21	0.0457	0.330E+03	0.347E+03	0.327E+03	0.302E+03	0.307E+03	0.300E+03	0.302E+03
20	0.0381	0.356E+03	0.349E+03	0.330E+03	0.304E+03	0.310E+03	0.311E+03	0.308E+03
19	0.0305	0.220E+01	0.350E+03	0.332E+03	0.310E+03	0.316E+03	0.325E+03	0.317E+03
18	0.0229	0.380E+01	0.350E+03	0.332E+03	0.318E+03	0.324E+03	0.340E+03	0.330E+03
17	0.0152	0.300E+01	0.351E+03	0.332E+03	0.335E+03	0.336E+03	0.357E+03	0.350E+03
16	0.0076	0.300E+01	0.351E+03	0.332E+03	0.353E+03	0.350E+03	0.110E+02	0.100E+02
15	0.0000	0.400E+00	0.351E+03	0.334E+03	0.000E+00	0.360E+03	0.200E+02	0.240E+02
14	-0.0076	0.000E+00	0.200E+01	0.334E+03	0.160E+02	0.340E+02		
13	-0.0152	0.200E+01	0.360E+02	0.334E+03	0.300E+02	0.450E+02		
12	-0.0229	0.450E+02	0.750E+02	0.134E+03	0.420E+02	0.500E+02		
11	-0.0305	0.106E+03	0.860E+02	0.000E+00	0.440E+02	0.600E+02		
10	-0.0381	0.102E+03	0.820E+02	0.860E+02	0.490E+02	0.660E+02		
9	-0.0457	0.990E+02	0.780E+02	0.778E+02	0.520E+02	0.680E+02	0.570E+02	0.620E+02
8	-0.0533	0.960E+02	0.750E+02	0.870E+02	0.530E+02	0.700E+02		
7	-0.0610	0.960E+02	0.736E+02	0.840E+02	0.560E+02	0.700E+02		
6	-0.0686	0.959E+02	0.736E+02	0.856E+02	0.580E+02	0.660E+02		
5	-0.0762	0.959E+02	0.760E+02	0.856E+02	0.620E+02	0.656E+02		
4	-0.0838	0.970E+02	0.800E+02	0.842E+02	0.650E+02	0.630E+02		
3	-0.0914	0.976E+02	0.800E+02	0.842E+02	0.680E+02	0.600E+02	0.590E+02	0.600E+02
2	-0.0991	0.980E+02	0.806E+02	0.856E+02	0.690E+02	0.590E+02		
1	-0.1067	0.960E+02	0.808E+02	0.856E+02	0.698E+02	0.580E+02		

(a) Yaw Angle



TABLE II (Continued)

I =		1	2	3	4	5	6	7
X =		0.0063	0.0190	0.0318	0.0444	0.0572	0.0698	0.0952
J	Y							
27	0.0914	-0.770E+01	-0.561E+00	-0.128E+02	-0.481E+01	-0.195E+02	-0.707E+01	-0.645E+01
26	0.0838	-0.773E+01	0.378E+01	-0.181E+02	-0.439E+01	-0.238E+02	-0.725E+01	-0.605E+01
25	0.0762	-0.853E+01	0.858E+01	-0.205E+02	-0.382E+01	-0.273E+02	-0.957E+01	-0.248E+01
24	0.0686	-0.101E+02	0.149E+02	-0.267E+02	-0.332E+01	-0.330E+02	-0.129E+02	-0.147E+01
23	0.0610	-0.100E+02	0.147E+02	-0.367E+02	-0.254E+01	-0.346E+02	-0.132E+02	0.000E+00
22	0.0533	-0.465E+01	0.161E+02	-0.419E+02	-0.295E+01	-0.378E+02	-0.188E+02	0.194E+01
21	0.0457	0.384E+02	0.122E+02	-0.388E+02	-0.479E+01	-0.433E+02	-0.286E+02	0.249E+01
20	0.0381	0.306E+02	0.854E+01	-0.413E+02	-0.628E+01	-0.485E+02	-0.393E+02	0.912E+01
19	0.0305	0.220E+02	0.673E+01	-0.402E+02	-0.636E+01	-0.510E+02	-0.478E+02	0.211E+02
18	0.0229	0.136E+02	0.362E+01	-0.433E+02	-0.147E+02	-0.525E+02	0.000E+00	0.341E+02
17	0.0152	0.121E+02	0.257E+01	-0.483E+02	-0.165E+02	-0.549E+02	0.000E+00	0.428E+02
16	0.0076	0.112E+02	0.585E+00	-0.489E+02	-0.165E+02	-0.510E+02	-0.465E+02	0.527E+02
15	0.0000	0.889E+01	0.000E+00	-0.496E+02	-0.315E+02	-0.478E+02	-0.433E+02	0.560E+02
14	-0.0076	0.542E+01	0.000E+00	-0.510E+02	-0.218E+02	-0.147E+02		
13	-0.0152	0.177E+01	0.000E+00	0.000E+00	-0.188E+02	-0.100E+02		
12	-0.0229	0.161E+02	0.102E+02	0.000E+00	-0.218E+02	-0.605E+01		
11	-0.0305	0.147E+02	0.912E+01	0.000E+00	-0.210E+02	-0.266E+01		
10	-0.0381	0.102E+02	0.673E+01	0.264E+02	-0.212E+02	0.000E+00		
9	-0.0457	0.783E+01	0.585E+01	0.211E+02	-0.228E+02	0.000E+00	-0.110E+02	0.178E+02
8	-0.0533	0.766E+01	0.498E+01	0.217E+02	-0.192E+02	0.000E+00		
7	-0.0610	0.676E+01	0.447E+01	0.200E+02	-0.189E+02	-0.107E+01		
6	-0.0686	0.726E+01	0.409E+01	0.144E+02	-0.165E+02	-0.930E+00		
5	-0.0762	0.720E+01	0.384E+01	0.102E+02	-0.134E+02	-0.185E+01		
4	-0.0838	0.720E+01	0.415E+01	0.736E+01	-0.105E+02	-0.237E+01		
3	-0.0914	0.619E+01	0.354E+01	0.423E+01	-0.721E+01	-0.287E+01	-0.906E+00	0.947E+00
2	-0.0991	0.533E+01	0.306E+01	0.650E+00	-0.499E+01	-0.387E+01		
1	-0.1067	0.306E+01	0.188E+01	-0.693E+00	-0.188E+01	-0.340E+01		

(b) Pitch Angle

TABLE II (Continued)

I =		1	2	3	4	5	6	7
X =		0.0278	0.0833	0.1389	0.1944	0.2500	0.3056	0.4167
J	Y							
27	0.4000	0.206E+00	0.129E+01	0.145E+01	0.173E+01	0.125E+01	0.855E+00	0.118E+01
26	0.3667	0.516E+00	0.161E+01	0.127E+01	0.161E+01	0.125E+01	0.773E+00	0.110E+01
25	0.3333	0.544E+00	0.191E+01	0.117E+01	0.150E+01	0.118E+01	0.722E+00	0.997E+00
24	0.3000	0.620E+00	0.245E+01	0.106E+01	0.136E+01	0.103E+01	0.672E+00	0.898E+00
23	0.2667	0.760E+00	0.318E+01	0.986E+00	0.135E+01	0.103E+01	0.680E+00	0.829E+00
22	0.2333	0.110E+01	0.380E+01	0.978E+00	0.129E+01	0.956E+00	0.600E+00	0.771E+00
21	0.2000	0.161E+01	0.420E+01	0.108E+01	0.115E+01	0.827E+00	0.517E+00	0.760E+00
20	0.1667	0.378E+01	0.467E+01	0.112E+01	0.104E+01	0.756E+00	0.516E+00	0.779E+00
19	0.1333	0.632E+01	0.459E+01	0.122E+01	0.103E+01	0.720E+00	0.497E+00	0.821E+00
18	0.1000	0.823E+01	0.417E+01	0.115E+01	0.829E+00	0.681E+00	0.530E+00	0.794E+00
17	0.0667	0.863E+01	0.368E+01	0.998E+00	0.821E+00	0.646E+00	0.563E+00	0.776E+00
16	0.0333	0.858E+01	0.300E+01	0.925E+00	0.734E+00	0.664E+00	0.514E+00	0.661E+00
15	0.0000	0.820E+01	0.204E+01	0.815E+00	0.339E+00	0.607E+00	0.577E+00	0.603E+00
14	-0.0333	0.624E+01	0.125E+01	0.661E+00	0.602E+00	0.925E+00		
13	-0.0667	0.344E+01	0.000E+00	0.619E+00	0.838E+00	0.849E+00		
12	-0.1000	0.556E+00	0.251E+00	0.000E+00	0.806E+00	0.867E+00		
11	-0.1333	-0.393E+00	0.124E+00	0.000E+00	0.976E+00	0.738E+00		
10	-0.1667	-0.474E+00	0.335E+00	0.538E-01	0.981E+00	0.688E+00		
9	-0.2000	-0.479E+00	0.600E+00	0.236E+00	0.991E+00	0.701E+00	0.101E+01	0.870E+00
8	-0.2333	-0.374E+00	0.888E+00	0.686E-01	0.108E+01	0.735E+00		
7	-0.2667	-0.408E+00	0.107E+01	0.160E+00	0.104E+01	0.791E+00		
6	-0.3000	-0.414E+00	0.112E+01	0.141E+00	0.104E+01	0.101E+01		
5	-0.3333	-0.424E+00	0.992E+00	0.166E+00	0.993E+00	0.103E+01		
4	-0.3667	-0.502E+00	0.709E+00	0.247E+00	0.987E+00	0.123E+01		
3	-0.4000	-0.527E+00	0.684E+00	0.267E+00	0.963E+00	0.142E+01	0.129E+01	0.119E+01
2	-0.4333	-0.518E+00	0.630E+00	0.221E+00	0.101E+01	0.154E+01		
1	-0.4667	-0.357E+00	0.595E+00	0.219E+00	0.105E+01	0.155E+01		

(c)  $u/u_{av}$

TABLE II (Continued)

		I =	1	2	3	4	5	6	7
		X =	0.0278	0.0833	0.1389	0.1944	0.2500	0.3056	0.4167
J	Y								
27	0.4000	-0.531E+00	-0.309E-01	-0.623E+00	-0.242E+00	-0.838E+00	-0.304E+00	-0.274E+00	
26	0.3667	-0.544E+00	0.201E+00	-0.754E+00	-0.215E+00	-0.101E+01	-0.287E+00	-0.247E+00	
25	0.3333	-0.586E+00	0.439E+00	-0.763E+00	-0.184E+00	-0.112E+01	-0.340E+00	-0.935E-01	
24	0.3000	-0.637E+00	0.806E+00	-0.840E+00	-0.153E+00	-0.125E+01	-0.411E+00	-0.506E-01	
23	0.2667	-0.518E+00	0.921E+00	-0.104E+01	-0.116E+00	-0.127E+01	-0.392E+00	0.000E+00	
22	0.2333	-0.180E+00	0.114E+01	-0.112E+01	-0.125E+00	-0.129E+01	-0.465E+00	0.557E-01	
21	0.2000	0.147E+01	0.933E+00	-0.104E+01	-0.182E+00	-0.130E+01	-0.563E+00	0.627E-01	
20	0.1667	0.224E+01	0.715E+00	-0.113E+01	-0.205E+00	-0.133E+01	-0.644E+00	0.203E+00	
19	0.1333	0.256E+01	0.550E+00	-0.116E+01	-0.179E+00	-0.124E+01	-0.670E+00	0.434E+00	
18	0.1000	0.200E+01	0.268E+00	-0.122E+01	-0.292E+00	-0.110E+01	0.000E+00	0.620E+00	
17	0.0667	0.184E+01	0.167E+00	-0.127E+01	-0.268E+00	-0.101E+01	0.000E+00	0.731E+00	
16	0.0333	0.171E+01	0.311E-01	-0.120E+01	-0.219E+00	-0.833E+00	-0.553E+00	0.881E+00	
15	0.0000	0.128E+01	0.000E+00	-0.107E+01	-0.208E+00	-0.670E+00	-0.579E+00	0.978E+00	
14	-0.0333	0.593E+00	0.000E+00	-0.907E+00	-0.250E+00	-0.292E+00			
13	-0.0667	0.106E+00	0.000E+00	0.000E+00	-0.329E+00	-0.212E+00			
12	-0.1000	0.227E+00	0.174E+00	0.000E+00	-0.434E+00	-0.143E+00			
11	-0.1333	0.372E+00	0.286E+00	0.000E+00	-0.522E+00	-0.686E-01			
10	-0.1667	0.411E+00	0.284E+00	0.383E+00	-0.579E+00	0.000E+00			
9	-0.2000	0.421E+00	0.296E+00	0.433E+00	-0.677E+00	0.000E+00	-0.360E+00	0.593E+00	
8	-0.2333	0.481E+00	0.299E+00	0.521E+00	-0.621E+00	0.000E+00			
7	-0.2667	0.463E+00	0.296E+00	0.556E+00	-0.640E+00	-0.432E-01			
6	-0.3000	0.513E+00	0.284E+00	0.474E+00	-0.578E+00	-0.402E-01			
5	-0.3333	0.521E+00	0.275E+00	0.390E+00	-0.503E+00	-0.806E-01			
4	-0.3667	0.521E+00	0.296E+00	0.315E+00	-0.432E+00	-0.112E+00			
3	-0.4000	0.432E+00	0.244E+00	0.196E+00	-0.325E+00	-0.143E+00	-0.397E-01	0.395E-01	
2	-0.4333	0.347E+00	0.206E+00	0.327E-01	-0.245E+00	-0.202E+00			
1	-0.4667	0.183E+00	0.122E+00	-0.345E-01	-0.996E-01	-0.173E+00			

(d)  $v/u_{av}$

TABLE II (Continued)

	I =	1	2	3	4	5	6	7
J	X =	0.0278	0.0833	0.1389	0.1944	0.2500	0.3056	0.4167
Y								
27	0.4000	-0.393E+01	-0.289E+01	-0.232E+01	-0.229E+01	-0.200E+01	-0.230E+01	-0.212E+01
26	0.3667	-0.397E+01	-0.257E+01	-0.193E+01	-0.229E+01	-0.192E+01	-0.212E+01	-0.206E+01
25	0.3333	-0.387E+01	-0.219E+01	-0.167E+01	-0.231E+01	-0.182E+01	-0.188E+01	-0.192E+01
24	0.3000	-0.352E+01	-0.179E+01	-0.129E+01	-0.226E+01	-0.164E+01	-0.166E+01	-0.176E+01
23	0.2667	-0.284E+01	-0.148E+01	-0.986E+00	-0.224E+01	-0.152E+01	-0.153E+01	-0.163E+01
22	0.2333	-0.191E+01	-0.112E+01	-0.770E+00	-0.206E+01	-0.137E+01	-0.123E+01	-0.145E+01
21	0.2000	-0.928E+00	-0.984E+00	-0.693E+00	-0.185E+01	-0.110E+01	-0.895E+00	-0.122E+01
20	0.1667	-0.264E+00	-0.892E+00	-0.647E+00	-0.155E+01	-0.902E+00	-0.593E+00	-0.997E+00
19	0.1333	0.243E+00	-0.809E+00	-0.646E+00	-0.123E+01	-0.695E+00	-0.348E+00	-0.766E+00
18	0.1000	0.547E+00	-0.735E+00	-0.601E+00	-0.747E+00	-0.495E+00	-0.193E+00	-0.458E+00
17	0.0667	0.452E+00	-0.596E+00	-0.531E+00	-0.383E+00	-0.288E+00	-0.295E-01	-0.137E+00
16	0.0333	0.449E+00	-0.476E+00	-0.492E+00	-0.901E-01	-0.117E+00	0.100E+00	0.117E+00
15	0.0000	0.572E-01	-0.308E+00	-0.397E+00	0.000E+00	-0.106E-02	0.210E+00	0.268E+00
14	-0.0333	0.000E+00	0.438E-01	-0.322E+00	0.173E+00	0.624E+00		
13	-0.0667	0.120E+00	0.000E+00	-0.299E+00	0.484E+00	0.849E+00		
12	-0.1000	0.556E+00	0.936E+00	0.000E+00	0.726E+00	0.103E+01		
11	-0.1333	0.136E+01	0.178E+01	0.000E+00	0.943E+00	0.128E+01		
10	-0.1667	0.223E+01	0.238E+01	0.770E+00	0.113E+01	0.155E+01		
9	-0.2000	0.302E+01	0.282E+01	0.109E+01	0.127E+01	0.173E+01	0.155E+01	0.164E+01
8	-0.2333	0.355E+01	0.331E+01	0.131E+01	0.143E+01	0.202E+01		
7	-0.2667	0.388E+01	0.363E+01	0.152E+01	0.155E+01	0.217E+01		
6	-0.3000	0.400E+01	0.381E+01	0.183E+01	0.166E+01	0.226E+01		
5	-0.3333	0.410E+01	0.398E+01	0.216E+01	0.187E+01	0.228E+01		
4	-0.3667	0.409E+01	0.402E+01	0.243E+01	0.212E+01	0.241E+01		
3	-0.4000	0.395E+01	0.388E+01	0.263E+01	0.238E+01	0.246E+01	0.215E+01	0.207E+01
2	-0.4333	0.368E+01	0.380E+01	0.288E+01	0.263E+01	0.256E+01		
1	-0.4667	0.340E+01	0.367E+01	0.284E+01	0.285E+01	0.248E+01		

(e)  $w/u_{av}$

TABLE III  
VELOCITY DATA FOR CASE 2

		I =	1	2	3	4	5	6	7
		X =	0.0063	0.0190	0.0318	0.0444	0.0572	0.0698	0.0952
J	Y								
27	0.0914	0.278E+03	0.280E+03	0.280E+03	0.280E+03	0.289E+03	0.282E+03	0.280E+03	0.285E+03
26	0.0838	0.280E+03	0.277E+03	0.277E+03	0.277E+03	0.283E+03	0.280E+03	0.280E+03	0.282E+03
25	0.0762	0.278E+03	0.272E+03	0.272E+03	0.276E+03	0.278E+03	0.280E+03	0.285E+03	0.280E+03
24	0.0686	0.272E+03	0.271E+03	0.289E+03	0.274E+03	0.274E+03	0.282E+03	0.291E+03	0.279E+03
23	0.0610	0.264E+03	0.307E+03	0.314E+03	0.272E+03	0.272E+03	0.287E+03	0.300E+03	0.281E+03
22	0.0533	0.261E+03	0.344E+03	0.340E+03	0.340E+03	0.275E+03	0.297E+03	0.310E+03	0.290E+03
21	0.0457	0.283E+03	0.352E+03	0.350E+03	0.350E+03	0.299E+03	0.316E+03	0.320E+03	0.301E+03
20	0.0381	0.338E+03	0.355E+03	0.354E+03	0.340E+03	0.340E+03	0.332E+03	0.326E+03	0.317E+03
19	0.0305	0.100E+00	0.356E+03	0.356E+03	0.359E+03	0.342E+03	0.329E+03	0.329E+03	0.336E+03
18	0.0229	0.380E+01	0.356E+03	0.356E+03	0.700E+01	0.350E+03	0.335E+03	0.335E+03	0.349E+03
17	0.0152	0.300E+01	0.356E+03	0.355E+03	0.800E+01	0.352E+03	0.339E+03	0.339E+03	0.359E+03
16	0.0076	0.240E+01	0.356E+03	0.354E+03	0.100E+02	0.355E+03	0.343E+03	0.343E+03	0.600E+01
15	0.0000	0.200E+01	0.354E+03	0.353E+03	0.120E+02	0.356E+03	0.345E+03	0.345E+03	0.700E+01
14	-0.0076	0.200E+01	0.152E+03	0.353E+03	0.160E+02	0.400E+01			
13	-0.0152	0.300E+01	0.146E+03	0.354E+03	0.180E+02	0.700E+01			
12	-0.0229	0.110E+02	0.126E+03	0.100E+00	0.220E+02	0.110E+02			
11	-0.0305	0.890E+02	0.200E+03	0.260E+02	0.280E+02	0.180E+02			
10	-0.0381	0.107E+03	0.138E+03	0.170E+03	0.340E+02	0.350E+02			
9	-0.0457	0.970E+02	0.110E+03	0.150E+03	0.470E+02	0.550E+02	0.778E+02	0.620E+02	
8	-0.0533	0.940E+02	0.970E+02	0.125E+03	0.560E+02	0.780E+02			
7	-0.0610	0.920E+02	0.899E+02	0.112E+03	0.690E+02	0.870E+02			
6	-0.0686	0.920E+02	0.850E+02	0.102E+03	0.800E+02	0.890E+02			
5	-0.0762	0.921E+02	0.802E+02	0.950E+02	0.850E+02	0.870E+02			
4	-0.0838	0.930E+02	0.782E+02	0.890E+02	0.870E+02	0.830E+02			
3	-0.0914	0.103E+03	0.800E+02	0.840E+02	0.850E+02	0.790E+02	0.720E+02	0.768E+02	
2	-0.0991	0.945E+02	0.860E+02	0.790E+02	0.810E+02	0.740E+02			
1	-0.1067	0.940E+02	0.880E+02	0.758E+02	0.780E+02	0.710E+02			

(a) Yaw Angle

TABLE III (Continued)

		I =	1	2	3	4	5	6	7
		X =	0.0063	0.0190	0.0318	0.0444	0.0572	0.0698	0.0952
J	Y								
27	0.0914	-0.680E+01	-0.857E+01	-0.750E+01	-0.594E+01	-0.152E+02	-0.112E+02	-0.801E+01	
26	0.0838	-0.863E+01	-0.109E+02	-0.913E+01	-0.657E+01	-0.181E+02	-0.116E+02	-0.843E+01	
25	0.0762	-0.107E+02	-0.150E+02	-0.110E+02	-0.707E+01	-0.202E+02	-0.105E+02	-0.919E+01	
24	0.0686	-0.122E+02	-0.171E+02	-0.137E+02	-0.817E+01	-0.214E+02	-0.107E+02	-0.978E+01	
23	0.0610	-0.139E+02	0.000E+00	-0.150E+02	-0.982E+01	-0.200E+02	-0.788E+01	-0.122E+02	
22	0.0533	-0.132E+02	0.607E+01	-0.325E+01	-0.141E+02	-0.132E+02	-0.739E+01	-0.891E+01	
21	0.0457	0.233E+01	0.391E+01	-0.682E+01	0.000E+00	-0.465E+01	-0.605E+01	-0.605E+01	
20	0.0381	0.344E+02	0.368E+01	-0.734E+01	-0.165E+02	0.442E+01	-0.439E+01	-0.415E+01	
19	0.0305	0.203E+02	0.235E+01	-0.878E+01	-0.110E+02	0.756E+01	-0.232E+01	0.000E+00	
18	0.0229	0.109E+02	0.143E+01	-0.106E+02	-0.144E+02	0.756E+01	-0.232E+01	0.391E+01	
17	0.0152	0.741E+01	0.143E+00	-0.133E+02	-0.124E+02	0.867E+01	-0.248E+01	0.391E+01	
16	0.0076	0.617E+01	-0.140E+01	-0.163E+02	-0.141E+02	0.842E+01	-0.266E+01	0.673E+01	
15	0.0000	0.461E+01	-0.366E+01	-0.196E+02	-0.136E+02	0.712E+01	-0.652E+01	0.116E+02	
14	-0.0076	0.316E+01	0.310E+02	-0.255E+02	-0.195E+02	0.146E+01			
13	-0.0152	0.127E+00	-0.433E+02	-0.343E+02	-0.209E+02	0.000E+00			
12	-0.0229	-0.465E+01	-0.244E+02	-0.451E+02	-0.221E+02	-0.195E+01			
11	-0.0305	0.545E+02	0.000E+00	-0.465E+02	-0.226E+02	-0.494E+01			
10	-0.0381	0.112E+02	0.135E+02	-0.259E+02	-0.262E+02	-0.340E+01			
9	-0.0457	0.564E+01	0.658E+01	-0.141E+02	-0.197E+02	-0.415E+01	-0.853E+01	-0.185E+01	
8	-0.0533	0.451E+01	0.536E+01	-0.494E+01	-0.173E+02	0.000E+00			
7	-0.0610	0.395E+01	0.469E+01	0.000E+00	-0.141E+02	0.152E+01			
6	-0.0686	0.489E+01	0.354E+01	0.198E+01	-0.989E+01	0.855E+00			
5	-0.0762	0.554E+01	0.291E+01	0.322E+01	-0.539E+01	0.541E+00			
4	-0.0838	0.528E+01	0.256E+01	0.280E+01	-0.283E+01	0.391E+00			
3	-0.0914	0.511E+01	0.256E+01	0.188E+01	-0.107E+01	0.296E+00	-0.403E+01	-0.143E+01	
2	-0.0991	0.435E+01	0.268E+01	0.376E+00	-0.757E+00	-0.240E+00			
1	-0.1067	0.301E+01	0.203E+01	-0.102E+01	-0.889E+00	-0.721E+00			

(b) Pitch Angle

TABLE III (Continued)

I =		1	2	3	4	5	6	7
X =		0.0278	0.0833	0.1389	0.1944	0.2500	0.3056	0.4167
J	Y							
27	0.4000	0.850E+00	0.914E+00	0.781E+00	0.155E+01	0.748E+00	0.557E+00	0.905E+00
26	0.3667	0.965E+00	0.461E+00	0.432E+00	0.965E+00	0.532E+00	0.485E+00	0.670E+00
25	0.3333	0.689E+00	0.964E-01	0.302E+00	0.516E+00	0.435E+00	0.610E+00	0.502E+00
24	0.3000	0.162E+00	0.322E-01	0.599E+00	0.208E+00	0.408E+00	0.724E+00	0.386E+00
23	0.2667	-0.394E+00	0.241E+00	0.861E+00	0.779E-01	0.453E+00	0.913E+00	0.373E+00
22	0.2333	-0.470E+00	0.194E+01	0.178E+01	0.122E+00	0.540E+00	0.109E+01	0.566E+00
21	0.2000	0.477E+00	0.356E+01	0.264E+01	0.195E+00	0.800E+00	0.128E+01	0.696E+00
20	0.1667	0.214E+01	0.482E+01	0.317E+01	0.495E+00	0.943E+00	0.135E+01	0.862E+00
19	0.1333	0.519E+01	0.576E+01	0.363E+01	0.114E+01	0.109E+01	0.137E+01	0.103E+01
18	0.1000	0.795E+01	0.611E+01	0.380E+01	0.149E+01	0.138E+01	0.144E+01	0.111E+01
17	0.0667	0.894E+01	0.626E+01	0.369E+01	0.183E+01	0.150E+01	0.144E+01	0.114E+01
16	0.0333	0.901E+01	0.574E+01	0.337E+01	0.196E+01	0.171E+01	0.142E+01	0.121E+01
15	0.0000	0.889E+01	0.469E+01	0.286E+01	0.215E+01	0.167E+01	0.126E+01	0.111E+01
14	-0.0333	0.854E+01	-0.336E+00	0.228E+01	0.215E+01	0.192E+01		
13	-0.0667	0.664E+01	-0.361E+00	0.168E+01	0.208E+01	0.182E+01		
12	-0.1000	0.267E+01	-0.419E+00	0.105E+01	0.188E+01	0.170E+01		
11	-0.1333	0.577E-02	0.000E+00	0.670E+00	0.163E+01	0.145E+01		
10	-0.1667	-0.386E+00	-0.778E+00	-0.778E+00	0.134E+01	0.108E+01		
9	-0.2000	-0.256E+00	-0.663E+00	-0.859E+00	0.112E+01	0.679E+00	0.284E+00	0.831E+00
8	-0.2333	-0.195E+00	-0.371E+00	-0.872E+00	0.904E+00	0.301E+00		
7	-0.2667	-0.125E+00	0.721E-02	-0.809E+00	0.616E+00	0.984E-01		
6	-0.3000	-0.161E+00	0.455E+00	-0.590E+00	0.345E+00	0.442E-01		
5	-0.3333	-0.214E+00	0.104E+01	-0.312E+00	0.219E+00	0.168E+00		
4	-0.3667	-0.348E+00	0.137E+01	0.753E-01	0.169E+00	0.461E+00		
3	-0.4000	-0.159E+01	0.119E+01	0.527E+00	0.351E+00	0.831E+00	0.124E+01	0.794E+00
2	-0.4333	-0.607E+00	0.513E+00	0.104E+01	0.748E+00	0.134E+01		
1	-0.4667	-0.533E+00	0.257E+00	0.131E+01	0.106E+01	0.159E+01		

(c)  $u/u_{av}$

TABLE III (Continued)

		I =	1	2	3	4	5	6	7
		X =	0.0278	0.0833	0.1389	0.1944	0.2500	0.3056	0.4167
J	Y								
27	0.4000	-0.729E+00	-0.794E+00	-0.575E+00	-0.495E+00	-0.981E+00	-0.634E+00	-0.492E+00	
26	0.3667	-0.861E+00	-0.764E+00	-0.570E+00	-0.494E+00	-0.100E+01	-0.574E+00	-0.474E+00	
25	0.3333	-0.962E+00	-0.739E+00	-0.528E+00	-0.460E+00	-0.922E+00	-0.436E+00	-0.459E+00	
24	0.3000	-0.955E+00	-0.569E+00	-0.449E+00	-0.427E+00	-0.769E+00	-0.380E+00	-0.421E+00	
23	0.2667	-0.901E+00	0.000E+00	-0.332E+00	-0.387E+00	-0.565E+00	-0.253E+00	-0.423E+00	
22	0.2333	-0.681E+00	0.215E+00	-0.108E+00	-0.353E+00	-0.279E+00	-0.221E+00	-0.262E+00	
21	0.2000	0.862E-01	0.246E+00	-0.320E+00	0.000E+00	-0.905E-01	-0.177E+00	-0.143E+00	
20	0.1667	0.158E+01	0.312E+00	-0.411E+00	-0.156E+00	0.825E-01	-0.125E+00	-0.855E-01	
19	0.1333	0.192E+01	0.237E+00	-0.562E+00	-0.222E+00	0.152E+00	-0.646E-01	0.000E+00	
18	0.1000	0.153E+01	0.153E+00	-0.713E+00	-0.386E+00	0.186E+00	-0.646E-01	0.776E-01	
17	0.0667	0.116E+01	0.156E-01	-0.872E+00	-0.406E+00	0.230E+00	-0.668E-01	0.776E-01	
16	0.0333	0.974E+00	-0.140E+00	-0.989E+00	-0.500E+00	0.254E+00	-0.693E-01	0.143E+00	
15	0.0000	0.718E+00	-0.302E+00	-0.103E+01	-0.529E+00	0.209E+00	-0.149E+00	0.231E+00	
14	-0.0333	0.472E+00	0.228E+00	-0.109E+01	-0.791E+00	0.489E-01			
13	-0.0667	0.148E-01	-0.411E+00	-0.115E+01	-0.837E+00	0.000E+00			
12	-0.1000	-0.221E+00	-0.323E+00	-0.105E+01	-0.823E+00	-0.589E-01			
11	-0.1333	0.463E+00	0.000E+00	-0.786E+00	-0.769E+00	-0.131E+00			
10	-0.1667	0.262E+00	0.252E+00	-0.384E+00	-0.797E+00	-0.780E-01			
9	-0.2000	0.207E+00	0.224E+00	-0.250E+00	-0.587E+00	-0.859E-01	-0.201E+00	-0.571E-01	
8	-0.2333	0.220E+00	0.285E+00	-0.131E+00	-0.504E+00	0.000E+00			
7	-0.2667	0.247E+00	0.339E+00	0.000E+00	-0.433E+00	0.499E-01			
6	-0.3000	0.395E+00	0.323E+00	0.979E-01	-0.347E+00	0.378E-01			
5	-0.3333	0.566E+00	0.310E+00	0.201E+00	-0.237E+00	0.302E-01			
4	-0.3667	0.615E+00	0.299E+00	0.211E+00	-0.159E+00	0.258E-01			
3	-0.4000	0.623E+00	0.305E+00	0.166E+00	-0.753E-01	0.225E-01	-0.282E+00	-0.867E-01	
2	-0.4333	0.590E+00	0.344E+00	0.358E-01	-0.632E-01	-0.204E-01			
1	-0.4667	0.402E+00	0.262E+00	-0.948E-01	-0.792E-01	-0.616E-01			

(d)  $v/u_{av}$



TABLE III (Continued)

I =		1	2	3	4	5	6	7
X =		0.0278	0.0833	0.1389	0.1944	0.2500	0.3056	0.4167
J	Y							
27	0.4000	-0.605E+01	-0.518E+01	-0.430E+01	-0.450E+01	-0.352E+01	-0.316E+01	-0.338E+01
26	0.3667	-0.559E+01	-0.393E+01	-0.352E+01	-0.418E+01	-0.302E+01	-0.275E+01	-0.313E+01
25	0.3333	-0.503E+01	-0.276E+01	-0.269E+01	-0.367E+01	-0.247E+01	-0.228E+01	-0.279E+01
24	0.3000	-0.442E+01	-0.185E+01	-0.174E+01	-0.297E+01	-0.192E+01	-0.189E+01	-0.241E+01
23	0.2667	-0.363E+01	-0.319E+00	-0.891E+00	-0.223E+01	-0.148E+01	-0.158E+01	-0.192E+01
22	0.2333	-0.287E+01	-0.557E+00	-0.650E+00	-0.140E+01	-0.106E+01	-0.130E+01	-0.157E+01
21	0.2000	-0.206E+01	-0.500E+00	-0.451E+00	-0.351E+00	-0.773E+00	-0.107E+01	-0.116E+01
20	0.1667	-0.866E+00	-0.422E+00	-0.333E+00	-0.180E+00	-0.501E+00	-0.911E+00	-0.804E+00
19	0.1333	0.907E-02	-0.403E+00	-0.285E+00	-0.199E-01	-0.354E+00	-0.821E+00	-0.460E+00
18	0.1000	0.528E+00	-0.427E+00	-0.279E+00	0.183E+00	-0.244E+00	-0.674E+00	-0.217E+00
17	0.0667	0.469E+00	-0.405E+00	-0.323E+00	0.258E+00	-0.200E+00	-0.553E+00	-0.198E-01
16	0.0333	0.377E+00	-0.381E+00	-0.354E+00	0.345E+00	-0.149E+00	-0.436E+00	0.127E+00
15	0.0000	0.310E+00	-0.477E+00	-0.352E+00	0.456E+00	-0.117E+00	-0.337E+00	0.137E+00
14	-0.0333	0.298E+00	0.178E+00	-0.280E+00	0.615E+00	0.134E+00		
13	-0.0667	0.348E+00	0.244E+00	-0.176E+00	0.677E+00	0.224E+00		
12	-0.1000	0.519E+00	0.576E+00	0.183E-02	0.758E+00	0.331E+00		
11	-0.1333	0.331E+00	0.000E+00	0.327E+00	0.868E+00	0.470E+00		
10	-0.1667	0.126E+01	0.700E+00	0.137E+00	0.906E+00	0.753E+00		
9	-0.2000	0.208E+01	0.182E+01	0.496E+00	0.120E+01	0.969E+00	0.131E+01	0.156E+01
8	-0.2333	0.278E+01	0.302E+01	0.124E+01	0.134E+01	0.141E+01		
7	-0.2667	0.357E+01	0.412E+01	0.200E+01	0.161E+01	0.188E+01		
6	-0.3000	0.462E+01	0.520E+01	0.277E+01	0.196E+01	0.253E+01		
5	-0.3333	0.583E+01	0.601E+01	0.356E+01	0.251E+01	0.320E+01		
4	-0.3667	0.664E+01	0.654E+01	0.431E+01	0.322E+01	0.375E+01		
3	-0.4000	0.679E+01	0.673E+01	0.501E+01	0.402E+01	0.427E+01	0.380E+01	0.339E+01
2	-0.4333	0.772E+01	0.734E+01	0.535E+01	0.472E+01	0.468E+01		
1	-0.4667	0.763E+01	0.737E+01	0.516E+01	0.499E+01	0.462E+01		

(e)  $w/u_{av}$

TABLE IV  
VELOCITY DATA FOR CASE 3

J	I =		1	2	3	4	5	6	7
	X =		0.0063	0.0190	0.0318	0.0444	0.0572	0.0698	0.0952
	Y.								
27	0.0914	0.282E+03	0.290E+03	0.290E+03	0.295E+03	0.290E+03	0.297E+03	0.298E+03	
26	0.0838	0.283E+03	0.291E+03	0.284E+03	0.292E+03	0.290E+03	0.293E+03	0.297E+03	
25	0.0762	0.284E+03	0.290E+03	0.278E+03	0.290E+03	0.290E+03	0.288E+03	0.294E+03	
24	0.0686	0.284E+03	0.291E+03	0.273E+03	0.287E+03	0.290E+03	0.284E+03	0.292E+03	
23	0.0610	0.292E+03	0.292E+03	0.270E+03	0.286E+03	0.291E+03	0.279E+03	0.289E+03	
22	0.0533	0.308E+03	0.296E+03	0.267E+03	0.290E+03	0.292E+03	0.277E+03	0.287E+03	
21	0.0457	0.330E+03	0.312E+03	0.270E+03	0.295E+03	0.294E+03	0.277E+03	0.287E+03	
20	0.0381	0.344E+03	0.335E+03	0.277E+03	0.302E+03	0.297E+03	0.280E+03	0.288E+03	
19	0.0305	0.350E+03	0.356E+03	0.295E+03	0.310E+03	0.300E+03	0.287E+03	0.291E+03	
18	0.0229	0.352E+03	0.800E+01	0.322E+03	0.314E+03	0.308E+03	0.300E+03	0.295E+03	
17	0.0152	0.352E+03	0.800E+01	0.358E+03	0.317E+03	0.317E+03	0.322E+03	0.305E+03	
16	0.0076	0.352E+03	0.800E+01	0.200E+02	0.322E+03	0.332E+03	0.357E+03	0.317E+03	
15	0.0000	0.348E+03	0.800E+01	0.375E+02	0.328E+03	0.351E+03	0.250E+02	0.351E+03	
14	-0.0076	0.000E+00	0.300E+02	0.430E+02	0.345E+03	0.700E+01			
13	-0.0152	0.122E+03	0.450E+02	0.430E+02	0.200E+02	0.360E+02			
12	-0.0229	0.122E+03	0.800E+02	0.480E+02	0.600E+02	0.530E+02			
11	-0.0305	0.104E+03	0.924E+02	0.490E+02	0.780E+02	0.650E+02			
10	-0.0381	0.997E+02	0.890E+02	0.520E+02	0.840E+02	0.750E+02			
9	-0.0457	0.960E+02	0.870E+02	0.560E+02	0.840E+02	0.800E+02	0.702E+02	0.838E+02	
8	-0.0533	0.960E+02	0.830E+02	0.600E+02	0.840E+02	0.860E+02			
7	-0.0610	0.960E+02	0.797E+02	0.650E+02	0.802E+02	0.890E+02			
6	-0.0686	0.962E+02	0.787E+02	0.710E+02	0.770E+02	0.880E+02			
5	-0.0762	0.970E+02	0.820E+02	0.740E+02	0.735E+02	0.840E+02			
4	-0.0838	0.962E+02	0.822E+02	0.760E+02	0.700E+02	0.800E+02			
3	-0.0914	0.958E+02	0.830E+02	0.770E+02	0.670E+02	0.750E+02	0.660E+02	0.600E+02	
2	-0.0991	0.940E+02	0.840E+02	0.760E+02	0.640E+02	0.700E+02			
1	-0.1067	0.938E+02	0.840E+02	0.760E+02	0.630E+02	0.670E+02			

(a) Yaw Angle

TABLE IV (Continued)

I =		1	2	3	4	5	6	7
X =		0.0063	0.0190	0.0318	0.0444	0.0572	0.0698	0.0952
J	Y							
27	0.0914	0.577E+01	-0.618E+01	-0.384E+00	-0.798E+01	-0.362E+01	-0.769E+01	-0.707E+01
26	0.0838	0.595E+01	-0.752E+01	-0.852E+00	-0.845E+01	-0.465E+01	-0.938E+01	-0.783E+01
25	0.0762	0.660E+01	-0.916E+01	-0.139E+01	-0.890E+01	-0.594E+01	-0.109E+02	-0.853E+01
24	0.0686	0.100E+02	-0.118E+02	-0.110E+01	-0.977E+01	-0.665E+01	-0.127E+02	-0.973E+01
23	0.0610	0.273E+02	-0.186E+02	-0.311E+01	-0.914E+01	-0.853E+01	-0.145E+02	-0.104E+02
22	0.0533	0.380E+02	-0.333E+02	-0.122E+01	-0.773E+01	-0.110E+02	-0.165E+02	-0.121E+02
21	0.0457	0.364E+02	0.000E+00	0.000E+00	-0.400E+01	-0.158E+02	-0.160E+02	-0.122E+02
20	0.0381	0.319E+02	0.000E+00	0.318E+01	-0.176E+01	-0.197E+02	-0.186E+02	-0.136E+02
19	0.0305	0.263E+02	0.000E+00	0.277E+02	0.000E+00	-0.277E+02	-0.218E+02	-0.165E+02
18	0.0229	0.206E+02	0.000E+00	0.506E+02	0.194E+01	-0.362E+02	-0.252E+02	-0.174E+02
17	0.0152	0.176E+02	0.000E+00	0.000E+00	0.269E+01	-0.448E+02	-0.393E+02	-0.208E+02
16	0.0076	0.157E+02	0.000E+00	0.520E+02	0.673E+01	-0.540E+02	-0.315E+02	-0.269E+02
15	0.0000	0.104E+02	0.000E+00	0.336E+02	0.125E+02	0.000E+00	-0.165E+02	-0.315E+02
14	-0.0076	0.000E+00	-0.565E+02	0.175E+02	0.310E+02	-0.549E+02		
13	-0.0152	-0.510E+02	0.000E+00	0.129E+02	0.545E+02	-0.373E+02		
12	-0.0229	0.000E+00	-0.605E+01	0.720E+01	0.355E+02	-0.218E+02		
11	-0.0305	0.000E+00	0.116E+02	0.140E+01	0.246E+02	-0.147E+02		
10	-0.0381	0.295E+02	0.922E+01	-0.136E+01	0.161E+02	-0.110E+02		
9	-0.0457	0.228E+02	0.100E+02	-0.257E+01	0.116E+02	-0.415E+01	-0.981E+00	0.189E+01
8	-0.0533	0.149E+02	0.820E+01	-0.374E+01	0.803E+01	-0.153E+01		
7	-0.0610	0.130E+02	0.584E+01	-0.340E+01	0.526E+01	-0.107E+01		
6	-0.0686	0.125E+02	0.472E+01	-0.185E+01	0.363E+01	-0.768E+00		
5	-0.0762	0.105E+02	0.494E+01	-0.153E+01	0.149E+01	0.000E+00		
4	-0.0838	0.912E+01	0.475E+01	-0.579E+00	0.359E+00	-0.459E+00		
3	-0.0914	0.744E+01	0.426E+01	0.000E+00	-0.109E+01	-0.426E+00	-0.478E+00	-0.981E+00
2	-0.0991	0.569E+01	0.269E+01	-0.388E+00	-0.195E+01	-0.126E+01		
1	-0.1067	0.252E+01	0.119E+01	-0.384E+00	-0.169E+01	-0.137E+01		

(b) Pitch Angle

TABLE IV (Continued)

I =		1	2	3	4	5	6	7
X =		0.0278	0.0833	0.1389	0.1944	0.2500	0.3056	0.4167
J	Y							
27	0.4000	0.851E+00	0.151E+01	0.139E+01	0.165E+01	0.114E+01	0.173E+01	0.150E+01
26	0.3667	0.907E+00	0.147E+01	0.939E+00	0.145E+01	0.108E+01	0.147E+01	0.147E+01
25	0.3333	0.899E+00	0.123E+01	0.519E+00	0.124E+01	0.100E+01	0.113E+01	0.130E+01
24	0.3000	0.765E+00	0.106E+01	0.179E+00	0.955E+00	0.938E+00	0.796E+00	0.113E+01
23	0.2667	0.978E+00	0.786E+00	-0.138E-04	0.777E+00	0.880E+00	0.468E+00	0.912E+00
22	0.2333	0.143E+01	0.557E+00	-0.120E+00	0.844E+00	0.825E+00	0.305E+00	0.750E+00
21	0.2000	0.241E+01	0.559E+00	-0.830E-05	0.935E+00	0.770E+00	0.276E+00	0.693E+00
20	0.1667	0.333E+01	0.378E+00	0.164E+00	0.102E+01	0.788E+00	0.325E+00	0.663E+00
19	0.1333	0.413E+01	0.931E+00	0.386E+00	0.119E+01	0.692E+00	0.436E+00	0.662E+00
18	0.1000	0.439E+01	0.131E+01	0.399E+00	0.122E+01	0.688E+00	0.563E+00	0.684E+00
17	0.0667	0.444E+01	0.137E+01	0.423E+00	0.108E+01	0.620E+00	0.467E+00	0.736E+00
16	0.0333	0.399E+01	0.131E+01	0.582E+00	0.102E+01	0.551E+00	0.509E+00	0.667E+00
15	0.0000	0.304E+01	0.101E+01	0.836E+00	0.798E+00	0.727E+00	0.504E+00	0.357E+00
14	-0.0333	0.000E+00	0.644E+00	0.111E+01	0.675E+00	0.529E+00		
13	-0.0667	-0.167E+00	0.417E+00	0.126E+01	0.330E+00	0.566E+00		
12	-0.1000	-0.221E+00	0.173E+00	0.131E+01	0.396E+00	0.568E+00		
11	-0.1333	-0.142E+00	-0.695E-01	0.136E+01	0.274E+00	0.502E+00		
10	-0.1667	-0.307E+00	0.420E-01	0.134E+01	0.196E+00	0.361E+00		
9	-0.2000	-0.314E+00	0.170E+00	0.126E+01	0.250E+00	0.308E+00	0.870E+00	0.272E+00
8	-0.2333	-0.417E+00	0.503E+00	0.114E+01	0.314E+00	0.144E+00		
7	-0.2667	-0.478E+00	0.842E+00	0.101E+01	0.583E+00	0.430E-01		
6	-0.3000	-0.512E+00	0.963E+00	0.864E+00	0.847E+00	0.101E+00		
5	-0.3333	-0.598E+00	0.699E+00	0.802E+00	0.114E+01	0.350E+00		
4	-0.3667	-0.515E+00	0.665E+00	0.803E+00	0.143E+01	0.650E+00		
3	-0.4000	-0.470E+00	0.570E+00	0.857E+00	0.165E+01	0.101E+01	0.149E+01	0.182E+01
2	-0.4333	-0.303E+00	0.479E+00	0.979E+00	0.180E+01	0.135E+01		
1	-0.4667	-0.263E+00	0.465E+00	0.984E+00	0.178E+01	0.147E+01		

(c)  $u/u_{av}$

TABLE IV (Continued)

I =		1	2	3	4	5	6	7
X =		0.0278	0.0833	0.1389	0.1944	0.2500	0.3056	0.4167
J	Y							
27	0.4000	0.414E+00	-0.478E+00	-0.273E-01	-0.549E+00	-0.209E+00	-0.515E+00	-0.398E+00
26	0.3667	0.420E+00	-0.552E+00	-0.577E-01	-0.573E+00	-0.254E+00	-0.622E+00	-0.446E+00
25	0.3333	0.430E+00	-0.580E+00	-0.906E-01	-0.571E+00	-0.302E+00	-0.701E+00	-0.476E+00
24	0.3000	0.559E+00	-0.614E+00	-0.658E-01	-0.562E+00	-0.317E+00	-0.753E+00	-0.516E+00
23	0.2667	0.135E+01	-0.707E+00	-0.158E+00	-0.453E+00	-0.368E+00	-0.771E+00	-0.513E+00
22	0.2333	0.182E+01	-0.835E+00	-0.489E-01	-0.335E+00	-0.429E+00	-0.772E+00	-0.548E+00
21	0.2000	0.205E+01	0.000E+00	0.000E+00	-0.155E+00	-0.534E+00	-0.648E+00	-0.514E+00
20	0.1667	0.216E+01	0.000E+00	0.746E-01	-0.591E-01	-0.621E+00	-0.628E+00	-0.520E+00
19	0.1333	0.207E+01	0.000E+00	0.479E+00	0.000E+00	-0.726E+00	-0.596E+00	-0.547E+00
18	0.1000	0.167E+01	0.000E+00	0.616E+00	0.593E-01	-0.817E+00	-0.531E+00	-0.508E+00
17	0.0667	0.142E+01	0.000E+00	0.000E+00	0.692E-01	-0.842E+00	-0.485E+00	-0.488E+00
16	0.0333	0.113E+01	0.000E+00	0.793E+00	0.152E+00	-0.858E+00	-0.313E+00	-0.464E+00
15	0.0000	0.571E+00	0.000E+00	0.701E+00	0.209E+00	0.000E+00	-0.164E+00	-0.221E+00
14	-0.0333	0.000E+00	-0.112E+01	0.476E+00	0.420E+00	-0.758E+00		
13	-0.0667	-0.389E+00	0.000E+00	0.396E+00	0.491E+00	-0.534E+00		
12	-0.1000	0.000E+00	-0.106E+00	0.248E+00	0.564E+00	-0.377E+00		
11	-0.1333	0.000E+00	0.342E+00	0.506E-01	0.603E+00	-0.311E+00		
10	-0.1667	0.103E+01	0.390E+00	-0.516E-01	0.541E+00	-0.272E+00		
9	-0.2000	0.127E+01	0.575E+00	-0.101E+00	0.492E+00	-0.129E+00	-0.440E-01	0.830E-01
8	-0.2333	0.106E+01	0.595E+00	-0.149E+00	0.423E+00	-0.552E-01		
7	-0.2667	0.106E+01	0.482E+00	-0.142E+00	0.315E+00	-0.460E-01		
6	-0.3000	0.106E+01	0.406E+00	-0.855E-01	0.239E+00	-0.389E-01		
5	-0.3333	0.913E+00	0.434E+00	-0.777E-01	0.105E+00	0.000E+00		
4	-0.3667	0.765E+00	0.407E+00	-0.336E-01	0.262E-01	-0.300E-01		
3	-0.4000	0.607E+00	0.348E+00	0.000E+00	-0.804E-01	-0.289E-01	-0.306E-01	-0.623E-01
2	-0.4333	0.433E+00	0.215E+00	-0.274E-01	-0.139E+00	-0.866E-01		
1	-0.4667	0.175E+00	0.922E-01	-0.273E-01	-0.116E+00	-0.905E-01		

(d)  $v/u_{av}$

TABLE IV (Continued)

J	Y	I =	1	2	3	4	5	6	7
		X =	0.0278	0.0833	0.1389	0.1944	0.2500	0.3056	0.4167
27	0.4000	-0.401E+01	-0.414E+01	-0.382E+01	-0.355E+01	-0.310E+01	-0.340E+01	-0.283E+01	
26	0.3667	-0.393E+01	-0.392E+01	-0.377E+01	-0.358E+01	-0.293E+01	-0.347E+01	-0.289E+01	
25	0.3333	-0.361E+01	-0.338E+01	-0.370E+01	-0.343E+01	-0.273E+01	-0.346E+01	-0.289E+01	
24	0.3000	-0.307E+01	-0.275E+01	-0.341E+01	-0.312E+01	-0.255E+01	-0.324E+01	-0.279E+01	
23	0.2667	-0.242E+01	-0.195E+01	-0.290E+01	-0.271E+01	-0.229E+01	-0.296E+01	-0.265E+01	
22	0.2333	-0.183E+01	-0.114E+01	-0.230E+01	-0.232E+01	-0.204E+01	-0.259E+01	-0.245E+01	
21	0.2000	-0.139E+01	-0.620E+00	-0.174E+01	-0.200E+01	-0.173E+01	-0.225E+01	-0.227E+01	
20	0.1667	-0.954E+00	-0.176E+00	-0.133E+01	-0.164E+01	-0.155E+01	-0.184E+01	-0.204E+01	
19	0.1333	-0.727E+00	-0.651E-01	-0.828E+00	-0.142E+01	-0.120E+01	-0.143E+01	-0.173E+01	
18	0.1000	-0.601E+00	0.184E+00	-0.311E+00	-0.126E+01	-0.881E+00	-0.975E+00	-0.147E+01	
17	0.0667	-0.608E+00	0.193E+00	-0.148E-01	-0.101E+01	-0.578E+00	-0.365E+00	-0.105E+01	
16	0.0333	-0.568E+00	0.184E+00	0.212E+00	-0.793E+00	-0.293E+00	-0.267E-01	-0.622E+00	
15	0.0000	-0.646E+00	0.142E+00	0.642E+00	-0.499E+00	-0.115E+00	0.235E+00	-0.565E-01	
14	-0.0333	0.000E+00	0.372E+00	0.103E+01	-0.181E+00	0.649E-01			
13	-0.0667	0.267E+00	0.417E+00	0.118E+01	0.120E+00	0.411E+00			
12	-0.1000	0.353E+00	0.983E+00	0.146E+01	0.686E+00	0.754E+00			
11	-0.1333	0.571E+00	0.166E+01	0.156E+01	0.129E+01	0.108E+01			
10	-0.1667	0.180E+01	0.241E+01	0.172E+01	0.187E+01	0.135E+01			
9	-0.2000	0.299E+01	0.325E+01	0.187E+01	0.237E+01	0.175E+01	0.242E+01	0.250E+01	
8	-0.2333	0.397E+01	0.409E+01	0.198E+01	0.298E+01	0.206E+01			
7	-0.2667	0.454E+01	0.464E+01	0.217E+01	0.337E+01	0.246E+01			
6	-0.3000	0.471E+01	0.482E+01	0.251E+01	0.367E+01	0.290E+01			
5	-0.3333	0.487E+01	0.497E+01	0.280E+01	0.386E+01	0.333E+01			
4	-0.3667	0.474E+01	0.485E+01	0.322E+01	0.393E+01	0.369E+01			
3	-0.4000	0.462E+01	0.464E+01	0.371E+01	0.388E+01	0.375E+01	0.335E+01	0.315E+01	
2	-0.4333	0.433E+01	0.456E+01	0.393E+01	0.369E+01	0.370E+01			
1	-0.4667	0.396E+01	0.443E+01	0.395E+01	0.350E+01	0.347E+01			

(e)  $w/u_{av}$

TABLE V  
VELOCITY DATA FOR CASE 4

J	Y	I =	1	2	3	4	5	6	7
		X =	0.0063	0.0190	0.0318	0.0444	0.0572	0.0698	0.0952
27	0.0914	0.280E+03	0.282E+03	0.276E+03	0.282E+03	0.282E+03	0.282E+03	0.282E+03	0.282E+03
26	0.0838	0.282E+03	0.279E+03	0.270E+03	0.278E+03	0.278E+03	0.278E+03	0.278E+03	0.278E+03
25	0.0762	0.280E+03	0.276E+03	0.266E+03	0.277E+03	0.274E+03	0.274E+03	0.274E+03	0.274E+03
24	0.0686	0.276E+03	0.272E+03	0.262E+03	0.276E+03	0.272E+03	0.272E+03	0.272E+03	0.272E+03
23	0.0610	0.272E+03	0.272E+03	0.260E+03	0.278E+03	0.270E+03	0.270E+03	0.270E+03	0.270E+03
22	0.0533	0.270E+03	0.276E+03	0.264E+03	0.283E+03	0.270E+03	0.270E+03	0.270E+03	0.270E+03
21	0.0457	0.283E+03	0.294E+03	0.284E+03	0.290E+03	0.272E+03	0.274E+03	0.272E+03	0.272E+03
20	0.0381	0.336E+03	0.323E+03	0.312E+03	0.302E+03	0.280E+03	0.280E+03	0.276E+03	0.276E+03
19	0.0305	0.355E+03	0.352E+03	0.341E+03	0.313E+03	0.300E+03	0.294E+03	0.284E+03	0.284E+03
18	0.0229	0.359E+03	0.359E+03	0.354E+03	0.324E+03	0.327E+03	0.310E+03	0.293E+03	0.293E+03
17	0.0152	0.359E+03	0.180E+01	0.400E+01	0.327E+03	0.347E+03	0.323E+03	0.313E+03	0.313E+03
16	0.0076	0.358E+03	0.200E+01	0.800E+01	0.333E+03	0.400E+01	0.342E+03	0.346E+03	0.346E+03
15	0.0000	0.356E+03	0.300E+01	0.140E+02	0.338E+03	0.100E+02	0.360E+03	0.700E+01	0.700E+01
14	-0.0076	0.356E+03	0.180E+01	0.190E+02	0.345E+03	0.200E+02			
13	-0.0152	0.353E+03	0.180E+01	0.250E+02	0.353E+03	0.310E+02			
12	-0.0229	0.351E+03	0.800E+01	0.350E+02	0.100E+02	0.400E+02			
11	-0.0305	0.351E+03	0.240E+02	0.450E+02	0.460E+02	0.510E+02			
10	-0.0381	0.112E+03	0.900E+02	0.570E+02	0.770E+02	0.650E+02			
9	-0.0457	0.104E+03	0.101E+03	0.670E+02	0.910E+02	0.760E+02	0.800E+02	0.800E+02	0.800E+02
8	-0.0533	0.102E+03	0.990E+02	0.750E+02	0.970E+02	0.830E+02			
7	-0.0610	0.972E+02	0.950E+02	0.810E+02	0.960E+02	0.870E+02			
6	-0.0686	0.940E+02	0.902E+02	0.830E+02	0.937E+02	0.870E+02			
5	-0.0762	0.923E+02	0.859E+02	0.840E+02	0.893E+02	0.835E+02			
4	-0.0838	0.937E+02	0.822E+02	0.830E+02	0.843E+02	0.810E+02			
3	-0.0914	0.941E+02	0.827E+02	0.807E+02	0.790E+02	0.767E+02	0.761E+02	0.730E+02	0.730E+02
2	-0.0991	0.939E+02	0.870E+02	0.780E+02	0.737E+02	0.727E+02			
1	-0.1067	0.100E+03	0.880E+02	0.760E+02	0.688E+02	0.700E+02			

(a) Yaw Angle

TABLE V (Continued)

		I =	1	2	3	4	5	6	7
		X =	0.0063	0.0190	0.0318	0.0444	0.0572	0.0698	0.0952
J	Y								
27	0.0914	-0.564E+01	-0.605E+01	-0.388E+01	-0.666E+01	-0.555E+01	-0.794E+01	-0.493E+01	
26	0.0838	-0.698E+01	-0.786E+01	-0.465E+01	-0.775E+01	-0.646E+01	-0.955E+01	-0.641E+01	
25	0.0762	-0.757E+01	-0.100E+02	-0.523E+01	-0.793E+01	-0.794E+01	-0.105E+02	-0.739E+01	
24	0.0686	-0.729E+01	-0.129E+02	-0.521E+01	-0.720E+01	-0.937E+01	-0.114E+02	-0.853E+01	
23	0.0610	-0.605E+01	-0.190E+02	-0.356E+01	-0.672E+01	-0.111E+02	-0.119E+02	-0.996E+01	
22	0.0533	0.000E+00	-0.280E+02	0.000E+00	-0.640E+01	-0.145E+02	-0.115E+02	-0.114E+02	
21	0.0457	0.231E+02	-0.465E+02	0.351E+01	-0.374E+01	-0.184E+02	-0.957E+01	-0.147E+02	
20	0.0381	0.455E+02	-0.549E+02	0.231E+02	-0.356E+01	-0.252E+02	-0.563E+01	-0.158E+02	
19	0.0305	0.318E+02	-0.359E+02	0.287E+02	-0.415E+01	-0.404E+02	-0.465E+01	-0.192E+02	
18	0.0229	0.204E+02	-0.297E+02	0.333E+02	-0.439E+01	-0.354E+02	0.000E+00	-0.244E+02	
17	0.0152	0.150E+02	-0.275E+02	0.310E+02	-0.527E+01	-0.315E+02	0.000E+00	-0.315E+02	
16	0.0076	0.120E+02	-0.256E+02	0.231E+02	-0.798E+01	-0.218E+02	0.161E+02	-0.315E+02	
15	0.0000	0.958E+01	-0.288E+02	0.212E+02	-0.707E+01	-0.110E+02	0.310E+02	-0.315E+02	
14	-0.0076	0.436E+01	-0.315E+02	0.151E+02	-0.465E+01	-0.773E+01			
13	-0.0152	0.103E+01	-0.445E+02	0.121E+02	-0.132E+02	-0.100E+02			
12	-0.0229	0.000E+00	0.000E+00	0.796E+01	-0.165E+02	-0.652E+01			
11	-0.0305	0.000E+00	0.000E+00	0.579E+01	0.000E+00	-0.563E+01			
10	-0.0381	0.410E+02	0.000E+00	0.391E+01	0.102E+02	-0.605E+01			
9	-0.0457	0.141E+02	0.474E+01	0.205E+01	0.125E+02	-0.430E+01	0.108E+02	0.269E+01	
8	-0.0533	0.875E+01	0.479E+01	0.731E+00	0.879E+01	-0.254E+01			
7	-0.0610	0.710E+01	0.506E+01	0.000E+00	0.682E+01	-0.107E+01			
6	-0.0686	0.648E+01	0.462E+01	0.000E+00	0.548E+01	-0.357E+00			
5	-0.0762	0.614E+01	0.388E+01	-0.264E+00	0.459E+01	-0.752E+00			
4	-0.0838	0.570E+01	0.300E+01	-0.200E+00	0.343E+01	-0.386E+00			
3	-0.0914	0.542E+01	0.262E+01	-0.151E+00	0.235E+01	-0.333E+00	0.132E+01	0.256E+01	
2	-0.0991	0.426E+01	0.263E+01	-0.244E+00	0.130E+01	-0.652E+00			
1	-0.1067	0.266E+01	0.153E+01	0.000E+00	0.766E+00	-0.536E+00			

(b) Pitch Angle



TABLE V (Continued)

I =		1	2	3	4	5	6	7
X =		0.0278	0.0833	0.1389	0.1944	0.2500	0.3056	0.4167
J	Y							
27	0.4000	0.124E+01	0.150E+01	0.722E+00	0.125E+01	0.128E+01	0.114E+01	0.103E+01
26	0.3667	0.137E+01	0.960E+00	0.210E-01	0.786E+00	0.791E+00	0.725E+00	0.614E+00
25	0.3333	0.105E+01	0.473E+00	-0.372E+00	0.574E+00	0.376E+00	0.356E+00	0.315E+00
24	0.3000	0.515E+00	0.139E+00	-0.535E+00	0.428E+00	0.133E+00	0.143E+00	0.140E+00
23	0.2667	0.129E+00	0.915E-01	-0.474E+00	0.479E+00	-0.180E-04	-0.161E-04	0.124E-01
22	0.2333	-0.121E-04	0.186E+00	-0.194E+00	0.626E+00	-0.144E-04	-0.129E-04	-0.142E-04
21	0.2000	0.287E+00	0.395E+00	0.311E+00	0.785E+00	0.792E-01	0.150E+00	0.829E-01
20	0.1667	0.113E+01	0.604E+00	0.693E+00	0.102E+01	0.276E+00	0.260E+00	0.198E+00
19	0.1333	0.278E+01	0.141E+01	0.102E+01	0.121E+01	0.477E+00	0.479E+00	0.326E+00
18	0.1000	0.420E+01	0.193E+01	0.113E+01	0.139E+01	0.728E+00	0.668E+00	0.296E+00
17	0.0667	0.458E+01	0.217E+01	0.134E+01	0.130E+01	0.784E+00	0.587E+00	0.348E+00
16	0.0333	0.464E+01	0.232E+01	0.162E+01	0.132E+01	0.939E+00	0.564E+00	0.350E+00
15	0.0000	0.439E+01	0.198E+01	0.165E+01	0.121E+01	0.968E+00	0.571E+00	0.358E+00
14	-0.0333	0.362E+01	0.162E+01	0.174E+01	0.114E+01	0.114E+01	0.116E+01	
13	-0.0667	0.244E+01	0.969E+00	0.163E+01	0.885E+00	0.109E+01		
12	-0.1000	0.127E+01	0.597E+00	0.154E+01	0.549E+00	0.105E+01		
11	-0.1333	0.000E+00	0.000E+00	0.140E+01	0.512E+00	0.940E+00		
10	-0.1667	-0.249E+00	0.135E-05	0.114E+01	0.234E+00	0.742E+00		
9	-0.2000	-0.444E+00	-0.295E+00	0.944E+00	-0.285E-01	0.514E+00	0.447E+00	0.512E+00
8	-0.2333	-0.647E+00	-0.450E+00	0.756E+00	-0.321E+00	0.339E+00		
7	-0.2667	-0.538E+00	-0.380E+00	0.559E+00	-0.379E+00	0.182E+00		
6	-0.3000	-0.398E+00	-0.205E-01	0.517E+00	-0.299E+00	0.221E+00		
5	-0.3333	-0.287E+00	0.515E+00	0.517E+00	0.678E-01	0.573E+00		
4	-0.3667	-0.532E+00	0.114E+01	0.693E+00	0.630E+00	0.899E+00		
3	-0.4000	-0.635E+00	0.113E+01	0.106E+01	0.132E+01	0.142E+01	0.136E+01	0.147E+01
2	-0.4333	-0.667E+00	0.502E+00	0.151E+01	0.201E+01	0.187E+01		
1	-0.4667	-0.170E+01	0.333E+00	0.179E+01	0.252E+01	0.205E+01		

(c)  $u/u_{av}$

TABLE V (Continued)

I =		1	2	3	4	5	6	7
X =		0.0278	0.0833	0.1389	0.1944	0.2500	0.3056	0.4167
J	Y							
27	0.4000	-0.708E+00	-0.765E+00	-0.468E+00	-0.718E+00	-0.595E+00	-0.775E+00	-0.428E+00
26	0.3667	-0.806E+00	-0.812E+00	-0.491E+00	-0.741E+00	-0.644E+00	-0.876E+00	-0.529E+00
25	0.3333	-0.787E+00	-0.828E+00	-0.454E+00	-0.655E+00	-0.716E+00	-0.881E+00	-0.571E+00
24	0.3000	-0.630E+00	-0.828E+00	-0.351E+00	-0.516E+00	-0.739E+00	-0.827E+00	-0.601E+00
23	0.2667	-0.392E+00	-0.901E+00	-0.170E+00	-0.406E+00	-0.745E+00	-0.716E+00	-0.623E+00
22	0.2333	0.000E+00	-0.945E+00	0.000E+00	-0.312E+00	-0.787E+00	-0.552E+00	-0.601E+00
21	0.2000	0.544E+00	-0.102E+01	0.788E-01	-0.150E+00	-0.754E+00	-0.362E+00	-0.621E+00
20	0.1667	0.125E+01	-0.108E+01	0.442E+00	-0.120E+00	-0.749E+00	-0.148E+00	-0.534E+00
19	0.1333	0.173E+01	-0.103E+01	0.594E+00	-0.129E+00	-0.810E+00	-0.957E-01	-0.468E+00
18	0.1000	0.156E+01	-0.110E+01	0.748E+00	-0.132E+00	-0.616E+00	0.000E+00	-0.343E+00
17	0.0667	0.123E+01	-0.113E+01	0.808E+00	-0.143E+00	-0.493E+00	0.000E+00	-0.313E+00
16	0.0333	0.990E+00	-0.111E+01	0.699E+00	-0.208E+00	-0.376E+00	0.171E+00	-0.221E+00
15	0.0000	0.742E+00	-0.109E+01	0.658E+00	-0.162E+00	-0.191E+00	0.343E+00	-0.221E+00
14	-0.0333	0.277E+00	-0.994E+00	0.497E+00	-0.959E-01	-0.167E+00		
13	-0.0667	0.442E-01	-0.953E+00	0.386E+00	-0.209E+00	-0.225E+00		
12	-0.1000	0.000E+00	0.000E+00	0.263E+00	-0.165E+00	-0.157E+00		
11	-0.1333	0.000E+00	0.000E+00	0.200E+00	0.000E+00	-0.147E+00		
10	-0.1667	0.578E+00	0.000E+00	0.144E+00	0.187E+00	-0.186E+00		
9	-0.2000	0.451E+00	0.128E+00	0.866E-01	0.362E+00	-0.160E+00	0.492E+00	0.138E+00
8	-0.2333	0.479E+00	0.241E+00	0.373E-01	0.408E+00	-0.123E+00		
7	-0.2667	0.535E+00	0.386E+00	0.000E+00	0.433E+00	-0.649E-01		
6	-0.3000	0.648E+00	0.474E+00	0.000E+00	0.445E+00	-0.263E-01		
5	-0.3333	0.768E+00	0.489E+00	-0.228E-01	0.445E+00	-0.664E-01		
4	-0.3667	0.823E+00	0.439E+00	-0.198E-01	0.381E+00	-0.388E-01		
3	-0.4000	0.843E+00	0.407E+00	-0.172E-01	0.284E+00	-0.360E-01	0.131E+00	0.224E+00
2	-0.4333	0.730E+00	0.441E+00	-0.309E-01	0.163E+00	-0.714E-01		
1	-0.4667	0.446E+00	0.255E+00	0.000E+00	0.931E-01	-0.560E-01		

(d)  $v/u_{av}$

TABLE V (Continued)

		I =	1	2	3	4	5	6	7
		X =	0.0278	0.0833	0.1389	0.1944	0.2500	0.3056	0.4167
J	Y								
27	0.4000	-0.705E+01	-0.706E+01	-0.687E+01	-0.602E+01	-0.598E+01	-0.543E+01	-0.486E+01	
26	0.3667	-0.644E+01	-0.580E+01	-0.603E+01	-0.539E+01	-0.563E+01	-0.516E+01	-0.467E+01	
25	0.3333	-0.583E+01	-0.466E+01	-0.494E+01	-0.467E+01	-0.512E+01	-0.474E+01	-0.439E+01	
24	0.3000	-0.490E+01	-0.362E+01	-0.381E+01	-0.407E+01	-0.448E+01	-0.409E+01	-0.400E+01	
23	0.2667	-0.370E+01	-0.262E+01	-0.269E+01	-0.341E+01	-0.378E+01	-0.339E+01	-0.355E+01	
22	0.2333	-0.254E+01	-0.177E+01	-0.185E+01	-0.271E+01	-0.304E+01	-0.272E+01	-0.298E+01	
21	0.2000	-0.124E+01	-0.887E+00	-0.125E+01	-0.216E+01	-0.227E+01	-0.214E+01	-0.237E+01	
20	0.1667	-0.502E+00	-0.455E+00	-0.770E+00	-0.163E+01	-0.156E+01	-0.147E+01	-0.188E+01	
19	0.1333	-0.243E+00	-0.198E+00	-0.353E+00	-0.130E+01	-0.826E+00	-0.108E+01	-0.131E+01	
18	0.1000	-0.734E-01	-0.338E-01	-0.119E+00	-0.101E+01	-0.473E+00	-0.796E+00	-0.696E+00	
17	0.0667	-0.800E-01	0.681E-01	0.938E-01	-0.847E+00	-0.181E+00	-0.442E+00	-0.373E+00	
16	0.0333	-0.162E+00	0.810E-01	0.228E+00	-0.673E+00	0.656E-01	-0.183E+00	-0.872E-01	
15	0.0000	-0.307E+00	0.104E+00	0.412E+00	-0.490E+00	0.171E+00	-0.344E-05	0.439E-01	
14	-0.0333	-0.253E+00	0.509E-01	0.598E+00	-0.305E+00	0.421E+00			
13	-0.0667	-0.300E+00	0.305E-01	0.760E+00	-0.109E+00	0.657E+00			
12	-0.1000	-0.201E+00	0.840E-01	0.108E+01	0.967E-01	0.881E+00			
11	-0.1333	0.000E+00	0.000E+00	0.140E+01	0.530E+00	0.116E+01			
10	-0.1667	0.616E+00	0.427E+00	0.176E+01	0.101E+01	0.159E+01			
9	-0.2000	0.174E+01	0.152E+01	0.222E+01	0.163E+01	0.206E+01	0.253E+01	0.290E+01	
8	-0.2333	0.304E+01	0.284E+01	0.282E+01	0.262E+01	0.276E+01			
7	-0.2667	0.426E+01	0.434E+01	0.353E+01	0.360E+01	0.347E+01			
6	-0.3000	0.569E+01	0.587E+01	0.421E+01	0.463E+01	0.422E+01			
5	-0.3333	0.714E+01	0.718E+01	0.492E+01	0.554E+01	0.503E+01			
4	-0.3667	0.823E+01	0.831E+01	0.564E+01	0.632E+01	0.568E+01			
3	-0.4000	0.886E+01	0.880E+01	0.645E+01	0.678E+01	0.602E+01	0.549E+01	0.480E+01	
2	-0.4333	0.979E+01	0.957E+01	0.712E+01	0.688E+01	0.599E+01			
1	-0.4667	0.947E+01	0.955E+01	0.717E+01	0.649E+01	0.563E+01			

(e)  $w/u_{nv}$

TABLE VI  
VELOCITY DATA FOR CASE 5

J	I =		1	2	3	4	5	6	7
	X =		0.0063	0.0190	0.0318	0.0444	0.0572	0.0698	0.0952
	Y								
27	0.0914	0.283E+03	0.288E+03	0.290E+03	0.289E+03	0.291E+03	0.277E+03	0.290E+03	
26	0.0838	0.286E+03	0.288E+03	0.285E+03	0.286E+03	0.286E+03	0.282E+03	0.285E+03	
25	0.0762	0.288E+03	0.288E+03	0.280E+03	0.284E+03	0.282E+03	0.278E+03	0.280E+03	
24	0.0686	0.290E+03	0.285E+03	0.276E+03	0.282E+03	0.277E+03	0.275E+03	0.276E+03	
23	0.0610	0.293E+03	0.282E+03	0.273E+03	0.281E+03	0.274E+03	0.272E+03	0.273E+03	
22	0.0533	0.303E+03	0.279E+03	0.274E+03	0.281E+03	0.272E+03	0.272E+03	0.272E+03	
21	0.0457	0.316E+03	0.278E+03	0.278E+03	0.282E+03	0.272E+03	0.274E+03	0.273E+03	
20	0.0381	0.328E+03	0.278E+03	0.286E+03	0.282E+03	0.274E+03	0.276E+03	0.276E+03	
19	0.0305	0.334E+03	0.284E+03	0.295E+03	0.285E+03	0.278E+03	0.280E+03	0.280E+03	
18	0.0229	0.336E+03	0.310E+03	0.305E+03	0.288E+03	0.288E+03	0.289E+03	0.286E+03	
17	0.0152	0.336E+03	0.358E+03	0.320E+03	0.295E+03	0.305E+03	0.300E+03	0.295E+03	
16	0.0076	0.336E+03	0.300E+02	0.344E+03	0.306E+03	0.329E+03	0.324E+03	0.318E+03	
15	0.0000	0.348E+03	0.420E+02	0.200E+01	0.327E+03	0.000E+00	0.600E+01	0.700E+01	
14	-0.0076	0.718E+02	0.500E+02	0.360E+02	0.355E+03	0.300E+02			
13	-0.0152	0.102E+03	0.567E+02	0.570E+02	0.360E+02	0.540E+02			
12	-0.0229	0.102E+03	0.630E+02	0.680E+02	0.620E+02	0.650E+02			
11	-0.0305	0.100E+03	0.710E+02	0.750E+02	0.760E+02	0.737E+02			
10	-0.0381	0.980E+02	0.800E+02	0.800E+02	0.840E+02	0.783E+02			
9	-0.0457	0.960E+02	0.870E+02	0.820E+02	0.900E+02	0.810E+02	0.822E+02	0.822E+02	
8	-0.0533	0.956E+02	0.890E+02	0.830E+02	0.920E+02	0.810E+02			
7	-0.0610	0.960E+02	0.870E+02	0.820E+02	0.917E+02	0.803E+02			
6	-0.0686	0.982E+02	0.859E+02	0.810E+02	0.880E+02	0.790E+02			
5	-0.0762	0.999E+02	0.863E+02	0.797E+02	0.815E+02	0.762E+02			
4	-0.0838	0.980E+02	0.879E+02	0.780E+02	0.760E+02	0.732E+02			
3	-0.0914	0.940E+02	0.870E+02	0.758E+02	0.714E+02	0.700E+02	0.769E+02	0.659E+02	
2	-0.0991	0.900E+02	0.860E+02	0.743E+02	0.675E+02	0.670E+02			
1	-0.1067	0.879E+02	0.860E+02	0.738E+02	0.650E+02	0.650E+02			

(a) Yaw Angle

TABLE VI (Continued)

		I =	1	2	3	4	5	6	7
		X =	0.0063	0.0190	0.0318	0.0444	0.0572	0.0698	0.0952
J	Y								
27	0.0914	0.333E+01	-0.312E+01	-0.203E+01	-0.605E+01	-0.790E+01	-0.703E+01	-0.360E+01	
26	0.0838	0.360E+01	-0.359E+01	-0.280E+01	-0.674E+01	-0.956E+01	-0.840E+01	-0.480E+01	
25	0.0762	0.434E+01	-0.460E+01	-0.345E+01	-0.692E+01	-0.114E+02	-0.920E+01	-0.577E+01	
24	0.0686	0.583E+01	-0.630E+01	-0.276E+01	-0.751E+01	-0.135E+02	-0.102E+02	-0.667E+01	
23	0.0610	0.807E+01	-0.857E+01	-0.206E+01	-0.741E+01	-0.156E+02	-0.102E+02	-0.727E+01	
22	0.0533	0.128E+02	-0.137E+02	-0.271E+01	-0.790E+01	-0.185E+02	-0.110E+02	-0.849E+01	
21	0.0457	0.218E+02	-0.208E+02	-0.173E+01	-0.865E+01	-0.212E+02	-0.131E+02	-0.108E+02	
20	0.0381	0.240E+02	-0.348E+02	-0.599E+00	-0.105E+02	-0.249E+02	-0.144E+02	-0.112E+02	
19	0.0305	0.220E+02	-0.568E+02	0.835E+00	-0.125E+02	-0.311E+02	-0.168E+02	-0.141E+02	
18	0.0229	0.249E+02	0.000E+00	0.607E+01	-0.178E+02	-0.411E+02	-0.183E+02	-0.184E+02	
17	0.0152	0.304E+02	0.000E+00	0.179E+02	-0.225E+02	-0.518E+02	-0.248E+02	-0.297E+02	
16	0.0076	0.406E+02	-0.524E+02	0.287E+02	-0.239E+02	0.000E+00	-0.957E+01	-0.565E+02	
15	0.0000	0.000E+00	-0.328E+02	0.491E+02	-0.165E+02	-0.565E+02	0.756E+01	-0.315E+02	
14	-0.0076	0.000E+00	-0.221E+02	0.431E+02	-0.110E+02	-0.165E+02			
13	-0.0152	0.000E+00	-0.169E+02	0.326E+02	0.391E+01	-0.340E+01			
12	-0.0229	0.373E+02	-0.129E+02	0.269E+02	0.712E+01	-0.906E+00			
11	-0.0305	0.289E+02	-0.652E+01	0.176E+02	0.431E+01	0.000E+00			
10	-0.0381	0.207E+02	-0.968E+00	0.119E+02	0.550E+01	0.391E+00			
9	-0.0457	0.158E+02	0.335E+01	0.717E+01	0.582E+01	0.306E+00	0.355E+01	0.383E+01	
8	-0.0533	0.135E+02	0.549E+01	0.428E+01	0.521E+01	0.251E+00			
7	-0.0610	0.123E+02	0.586E+01	0.227E+01	0.479E+01	0.213E+00			
6	-0.0686	0.111E+02	0.543E+01	0.129E+01	0.394E+01	0.178E+00			
5	-0.0762	0.973E+01	0.547E+01	0.560E+00	0.244E+01	0.000E+00			
4	-0.0838	0.833E+01	0.531E+01	0.125E+00	0.160E+01	-0.136E+00			
3	-0.0914	0.668E+01	0.474E+01	-0.348E+00	0.103E+01	-0.532E+00	-0.178E+01	0.109E+01	
2	-0.0991	0.458E+01	0.395E+01	-0.461E+00	0.640E+00	-0.140E+01			
1	-0.1067	0.183E+01	0.157E+01	-0.127E+00	0.704E+00	-0.109E+01			

(b) Pitch Angle

TABLE VI (Continued)

J	Y	I =						
		1	2	3	4	5	6	7
X =		0.0278	0.0833	0.1389	0.1944	0.2500	0.3056	0.4167
27	0.4000	0.108E+01	0.158E+01	0.162E+01	0.136E+01	0.154E+01	0.469E+00	0.135E+01
26	0.3667	0.131E+01	0.158E+01	0.125E+01	0.114E+01	0.116E+01	0.864E+00	0.102E+01
25	0.3333	0.138E+01	0.148E+01	0.832E+00	0.938E+00	0.802E+00	0.537E+00	0.674E+00
24	0.3000	0.132E+01	0.111E+01	0.434E+00	0.749E+00	0.454E+00	0.290E+00	0.371E+00
23	0.2667	0.120E+01	0.733E+00	0.200E+00	0.618E+00	0.229E+00	0.139E+00	0.174E+00
22	0.2333	0.119E+01	0.407E+00	0.201E+00	0.569E+00	0.887E-01	0.103E+00	0.117E+00
21	0.2000	0.128E+01	0.268E+00	0.333E+00	0.559E+00	0.851E-01	0.171E+00	0.138E+00
20	0.1667	0.156E+01	0.170E+00	0.557E+00	0.507E+00	0.148E+00	0.225E+00	0.211E+00
19	0.1333	0.175E+01	0.166E+00	0.707E+00	0.532E+00	0.230E+00	0.308E+00	0.316E+00
18	0.1000	0.162E+01	0.238E+00	0.831E+00	0.512E+00	0.358E+00	0.469E+00	0.385E+00
17	0.0667	0.122E+01	0.524E+00	0.890E+00	0.539E+00	0.447E+00	0.477E+00	0.353E+00
16	0.0333	0.710E+00	0.510E+00	0.904E+00	0.529E+00	0.628E+00	0.533E+00	0.199E+00
15	0.0000	0.256E+00	0.718E+00	0.545E+00	0.494E+00	0.377E+00	0.524E+00	0.219E+00
14	-0.0333	0.141E+00	0.850E+00	0.620E+00	0.424E+00	0.588E+00		
13	-0.0667	-0.163E+00	0.832E+00	0.647E+00	0.597E+00	0.705E+00		
12	-0.1000	-0.334E+00	0.758E+00	0.594E+00	0.508E+00	0.689E+00		
11	-0.1333	-0.448E+00	0.618E+00	0.516E+00	0.379E+00	0.586E+00		
10	-0.1667	-0.527E+00	0.392E+00	0.419E+00	0.214E+00	0.495E+00		
9	-0.2000	-0.485E+00	0.153E+00	0.393E+00	0.806E-05	0.433E+00	0.410E+00	0.419E+00
8	-0.2333	-0.502E+00	0.671E-01	0.386E+00	-0.106E+00	0.478E+00		
7	-0.2667	-0.556E+00	0.253E+00	0.479E+00	-0.104E+00	0.559E+00		
6	-0.3000	-0.774E+00	0.398E+00	0.591E+00	0.138E+00	0.694E+00		
5	-0.3333	-0.935E+00	0.367E+00	0.734E+00	0.641E+00	0.940E+00		
4	-0.3667	-0.734E+00	0.205E+00	0.913E+00	0.111E+01	0.121E+01		
3	-0.4000	-0.353E+00	0.279E+00	0.112E+01	0.150E+01	0.145E+01	0.923E+00	0.157E+01
2	-0.4333	0.152E-04	0.359E+00	0.124E+01	0.178E+01	0.163E+01		
1	-0.4667	0.164E+00	0.347E+00	0.122E+01	0.187E+01	0.166E+01		

(c)  $u/u_{av}$

TABLE VI (Continued)

I =		1	2	3	4	5	6	7
X =		0.0278	0.0833	0.1389	0.1944	0.2500	0.3056	0.4167
J	Y							
27	0.4000	0.279E+00	-0.277E+00	-0.166E+00	-0.456E+00	-0.601E+00	-0.511E+00	-0.250E+00
26	0.3667	0.301E+00	-0.319E+00	-0.235E+00	-0.491E+00	-0.711E+00	-0.609E+00	-0.332E+00
25	0.3333	0.341E+00	-0.386E+00	-0.281E+00	-0.471E+00	-0.810E+00	-0.625E+00	-0.388E+00
24	0.3000	0.399E+00	-0.468E+00	-0.200E+00	-0.475E+00	-0.898E+00	-0.634E+00	-0.429E+00
23	0.2667	0.435E+00	-0.531E+00	-0.125E+00	-0.433E+00	-0.944E+00	-0.598E+00	-0.438E+00
22	0.2333	0.496E+00	-0.657E+00	-0.136E+00	-0.425E+00	-0.100E+01	-0.578E+00	-0.457E+00
21	0.2000	0.713E+00	-0.779E+00	-0.724E-01	-0.419E+00	-0.995E+00	-0.584E+00	-0.500E+00
20	0.1667	0.820E+00	-0.906E+00	-0.211E-01	-0.444E+00	-0.988E+00	-0.551E+00	-0.435E+00
19	0.1333	0.787E+00	-0.105E+01	0.244E-01	-0.457E+00	-0.994E+00	-0.530E+00	-0.458E+00
18	0.1000	0.824E+00	0.000E+00	0.154E+00	-0.532E+00	-0.101E+01	-0.475E+00	-0.463E+00
17	0.0667	0.787E+00	0.000E+00	0.376E+00	-0.523E+00	-0.989E+00	-0.441E+00	-0.476E+00
16	0.0333	0.666E+00	-0.763E+00	0.515E+00	-0.398E+00	0.000E+00	-0.111E+00	-0.404E+00
15	0.0000	0.000E+00	-0.622E+00	0.629E+00	-0.174E+00	-0.569E+00	0.700E-01	-0.135E+00
14	-0.0333	0.000E+00	-0.537E+00	0.717E+00	-0.829E-01	-0.201E+00		
13	-0.0667	0.000E+00	-0.460E+00	0.759E+00	0.504E-01	-0.713E-01		
12	-0.1000	0.120E+01	-0.382E+00	0.805E+00	0.135E+00	-0.258E-01		
11	-0.1333	0.143E+01	-0.217E+00	0.633E+00	0.118E+00	0.000E+00		
10	-0.1667	0.143E+01	-0.382E-01	0.509E+00	0.197E+00	0.167E-01		
9	-0.2000	0.131E+01	0.171E+00	0.355E+00	0.259E+00	0.148E-01	0.188E+00	0.207E+00
8	-0.2333	0.124E+01	0.370E+00	0.237E+00	0.277E+00	0.134E-01		
7	-0.2667	0.115E+01	0.495E+00	0.136E+00	0.293E+00	0.124E-01		
6	-0.3000	0.107E+01	0.530E+00	0.851E-01	0.272E+00	0.113E-01		
5	-0.3333	0.932E+00	0.545E+00	0.401E-01	0.185E+00	0.000E+00		
4	-0.3667	0.772E+00	0.520E+00	0.955E-02	0.128E+00	-0.993E-02		
3	-0.4000	0.593E+00	0.443E+00	-0.278E-01	0.848E-01	-0.394E-01	-0.127E+00	0.730E-01
2	-0.4333	0.383E+00	0.355E+00	-0.370E-01	0.521E-01	-0.102E+00		
1	-0.4667	0.143E+00	0.137E+00	-0.966E-02	0.545E-01	-0.750E-01		

(d)  $v/u_{av}$

TABLE VI (Continued)

I =		1	2	3	4	5	6	7
X =		0.0278	0.0833	0.1389	0.1944	0.2500	0.3056	0.4167
J	Y							
27	0.4000	-0.467E+01	-0.482E+01	-0.441E+01	-0.408E+01	-0.405E+01	-0.412E+01	-0.373E+01
26	0.3667	-0.460E+01	-0.482E+01	-0.465E+01	-0.399E+01	-0.406E+01	-0.403E+01	-0.382E+01
25	0.3333	-0.429E+01	-0.456E+01	-0.458E+01	-0.376E+01	-0.394E+01	-0.382E+01	-0.378E+01
24	0.3000	-0.368E+01	-0.410E+01	-0.413E+01	-0.352E+01	-0.370E+01	-0.352E+01	-0.365E+01
23	0.2667	-0.282E+01	-0.345E+01	-0.347E+01	-0.327E+01	-0.336E+01	-0.332E+01	-0.343E+01
22	0.2333	-0.183E+01	-0.266E+01	-0.287E+01	-0.301E+01	-0.299E+01	-0.296E+01	-0.306E+01
21	0.2000	-0.124E+01	-0.203E+01	-0.237E+01	-0.270E+01	-0.257E+01	-0.251E+01	-0.263E+01
20	0.1667	-0.975E+00	-0.129E+01	-0.194E+01	-0.235E+01	-0.212E+01	-0.214E+01	-0.219E+01
19	0.1333	-0.854E+00	-0.668E+00	-0.152E+01	-0.198E+01	-0.163E+01	-0.173E+01	-0.179E+01
18	0.1000	-0.720E+00	-0.284E+00	-0.119E+01	-0.157E+01	-0.110E+01	-0.136E+01	-0.134E+01
17	0.0667	-0.545E+00	-0.183E-01	-0.746E+00	-0.114E+01	-0.638E+00	-0.826E+00	-0.757E+00
16	0.0333	-0.316E+00	0.294E+00	-0.259E+00	-0.727E+00	-0.378E+00	-0.388E+00	-0.179E+00
15	0.0000	-0.544E-01	0.647E+00	0.190E-01	-0.321E+00	0.000E+00	0.551E-01	0.269E-01
14	-0.0333	0.430E+00	0.101E+01	0.450E+00	-0.371E-01	0.340E+00		
13	-0.0667	0.767E+00	0.127E+01	0.996E+00	0.434E+00	0.970E+00		
12	-0.1000	0.155E+01	0.149E+01	0.147E+01	0.955E+00	0.148E+01		
11	-0.1333	0.254E+01	0.179E+01	0.193E+01	0.152E+01	0.201E+01		
10	-0.1667	0.375E+01	0.222E+01	0.237E+01	0.203E+01	0.239E+01		
9	-0.2000	0.462E+01	0.292E+01	0.280E+01	0.254E+01	0.273E+01	0.299E+01	0.306E+01
8	-0.2333	0.512E+01	0.384E+01	0.315E+01	0.303E+01	0.302E+01		
7	-0.2667	0.529E+01	0.482E+01	0.341E+01	0.350E+01	0.327E+01		
6	-0.3000	0.537E+01	0.556E+01	0.373E+01	0.395E+01	0.357E+01		
5	-0.3333	0.536E+01	0.568E+01	0.404E+01	0.429E+01	0.383E+01		
4	-0.3667	0.522E+01	0.560E+01	0.430E+01	0.445E+01	0.400E+01		
3	-0.4000	0.505E+01	0.533E+01	0.444E+01	0.445E+01	0.399E+01	0.397E+01	0.351E+01
2	-0.4333	0.478E+01	0.513E+01	0.443E+01	0.430E+01	0.383E+01		
1	-0.4667	0.446E+01	0.497E+01	0.420E+01	0.402E+01	0.356E+01		

(e)  $w/u_{av}$



TABLE VII  
VELOCITY DATA FOR CASE 6

	I =	1	2	3	4	5	6	7
J	X =	0.0063	0.0190	0.0318	0.0444	0.0572	0.0698	0.0952
	Y							
27	0.0914	0.276E+03	0.275E+03	0.274E+03	0.279E+03	0.281E+03	0.282E+03	0.282E+03
26	0.0838	0.278E+03	0.272E+03	0.269E+03	0.276E+03	0.277E+03	0.279E+03	0.278E+03
25	0.0762	0.279E+03	0.268E+03	0.266E+03	0.274E+03	0.273E+03	0.276E+03	0.274E+03
24	0.0686	0.278E+03	0.263E+03	0.263E+03	0.273E+03	0.270E+03	0.273E+03	0.270E+03
23	0.0610	0.278E+03	0.260E+03	0.262E+03	0.272E+03	0.268E+03	0.272E+03	0.268E+03
22	0.0533	0.280E+03	0.260E+03	0.265E+03	0.272E+03	0.266E+03	0.272E+03	0.268E+03
21	0.0457	0.288E+03	0.262E+03	0.272E+03	0.274E+03	0.267E+03	0.272E+03	0.268E+03
20	0.0381	0.307E+03	0.268E+03	0.285E+03	0.276E+03	0.270E+03	0.275E+03	0.268E+03
19	0.0305	0.326E+03	0.284E+03	0.297E+03	0.281E+03	0.276E+03	0.277E+03	0.269E+03
18	0.0229	0.337E+03	0.310E+03	0.308E+03	0.290E+03	0.287E+03	0.281E+03	0.271E+03
17	0.0152	0.342E+03	0.337E+03	0.320E+03	0.303E+03	0.303E+03	0.288E+03	0.278E+03
16	0.0076	0.344E+03	0.358E+03	0.333E+03	0.318E+03	0.324E+03	0.298E+03	0.280E+03
15	0.0000	0.345E+03	0.120E+02	0.350E+03	0.337E+03	0.200E+01	0.320E+03	0.400E+02
14	-0.0076	0.350E+03	0.220E+02	0.900E+01	0.800E+00	0.370E+02		
13	-0.0152	0.358E+03	0.300E+02	0.362E+02	0.300E+02	0.550E+02		
12	-0.0229	0.460E+02	0.400E+02	0.567E+02	0.500E+02	0.680E+02		
11	-0.0305	0.840E+02	0.520E+02	0.700E+02	0.680E+02	0.770E+02		
10	-0.0381	0.980E+02	0.680E+02	0.780E+02	0.820E+02	0.827E+02		
9	-0.0457	0.987E+02	0.810E+02	0.820E+02	0.890E+02	0.850E+02	0.890E+02	0.860E+02
8	-0.0533	0.962E+02	0.865E+02	0.850E+02	0.920E+02	0.874E+02		
7	-0.0610	0.940E+02	0.872E+02	0.858E+02	0.925E+02	0.880E+02		
6	-0.0686	0.902E+02	0.857E+02	0.847E+02	0.908E+02	0.877E+02		
5	-0.0762	0.889E+02	0.820E+02	0.828E+02	0.880E+02	0.860E+02		
4	-0.0838	0.900E+02	0.790E+02	0.801E+02	0.840E+02	0.830E+02		
3	-0.0914	0.925E+02	0.785E+02	0.773E+02	0.795E+02	0.800E+02	0.784E+02	0.743E+02
2	-0.0991	0.920E+02	0.825E+02	0.740E+02	0.740E+02	0.774E+02		
1	-0.1067	0.893E+02	0.830E+02	0.721E+02	0.688E+02	0.760E+02		

(a) Yaw Angle

TABLE VII (Continued)

I =		1	2	3	4	5	6	7
X =		0.0063	0.0190	0.0318	0.0444	0.0572	0.0698	0.0952
J	Y							
27	0.0914	-0.137E+01	-0.569E+01	-0.774E+01	-0.472E+01	-0.754E+01	-0.701E+01	-0.455E+01
26	0.0838	-0.234E+01	-0.730E+01	-0.840E+01	-0.550E+01	-0.874E+01	-0.812E+01	-0.545E+01
25	0.0762	-0.276E+01	-0.917E+01	-0.848E+01	-0.649E+01	-0.102E+02	-0.927E+01	-0.599E+01
24	0.0686	-0.162E+00	-0.119E+02	-0.809E+01	-0.761E+01	-0.110E+02	-0.990E+01	-0.647E+01
23	0.0610	0.143E+01	-0.151E+02	-0.755E+01	-0.853E+01	-0.127E+02	-0.927E+01	-0.641E+01
22	0.0533	0.260E+01	-0.198E+02	-0.661E+01	-0.979E+01	-0.143E+02	-0.976E+01	-0.727E+01
21	0.0457	0.573E+01	-0.267E+02	-0.517E+01	-0.109E+02	-0.184E+02	-0.109E+02	-0.663E+01
20	0.0381	0.989E+01	-0.424E+02	-0.114E+01	-0.135E+02	-0.212E+02	-0.115E+02	-0.692E+01
19	0.0305	0.736E+01	-0.552E+02	0.000E+00	-0.165E+02	-0.296E+02	-0.128E+02	-0.883E+01
18	0.0229	0.653E+01	0.000E+00	0.184E+01	-0.137E+02	-0.401E+02	-0.121E+02	-0.539E+01
17	0.0152	0.588E+01	-0.454E+02	0.269E+01	-0.218E+02	-0.465E+02	-0.155E+02	-0.218E+01
16	0.0076	0.456E+01	-0.346E+02	0.756E+01	-0.269E+02	-0.565E+02	-0.110E+02	-0.316E+02
15	0.0000	0.491E+01	-0.213E+02	0.389E+02	-0.510E+02	-0.315E+02	-0.316E+02	0.000E+00
14	-0.0076	0.548E+01	-0.165E+02	0.520E+02	-0.315E+02	0.510E+01		
13	-0.0152	0.125E+02	-0.150E+02	0.382E+02	0.607E+01	0.442E+01		
12	-0.0229	0.478E+02	-0.124E+02	0.320E+02	0.269E+01	0.328E+01		
11	-0.0305	0.418E+02	-0.107E+02	0.248E+02	0.607E+01	0.259E+01		
10	-0.0381	0.257E+02	-0.605E+01	0.153E+02	0.665E+01	0.194E+01		
9	-0.0457	0.118E+02	-0.484E+00	0.111E+02	0.578E+01	0.179E+01	0.560E+01	0.505E+01
8	-0.0533	0.752E+01	0.112E+01	0.532E+01	0.480E+01	0.123E+01		
7	-0.0610	0.589E+01	0.297E+01	0.387E+01	0.446E+01	0.803E+00		
6	-0.0686	0.512E+01	0.384E+01	0.218E+01	0.426E+01	0.219E+00		
5	-0.0762	0.486E+01	0.404E+01	0.814E+00	0.345E+01	0.179E+00		
4	-0.0838	0.466E+01	0.351E+01	-0.619E-01	0.261E+01	0.744E-01		
3	-0.0914	0.457E+01	0.295E+01	-0.415E+00	0.184E+01	-0.646E-01	0.126E+01	0.103E+01
2	-0.0991	0.336E+01	0.172E+01	-0.507E+00	0.111E+01	-0.563E+00		
1	-0.1067	0.110E+01	0.113E+01	-0.462E-01	0.639E+00	-0.538E+00		

(b) Pitch Angle

TABLE VII (Continued)

I =		1	2	3	4	5	6	7
X =		0.0278	0.0833	0.1389	0.1944	0.2500	0.3056	0.4167
J	Y							
27	0.4000	0.861E+00	0.700E+00	0.459E+00	0.115E+01	0.125E+01	0.130E+01	0.122E+01
26	0.3667	0.108E+01	0.239E+00	-0.116E+00	0.689E+00	0.770E+00	0.892E+00	0.778E+00
25	0.3333	0.107E+01	-0.209E+00	-0.439E+00	0.418E+00	0.313E+00	0.549E+00	0.330E+00
24	0.3000	0.855E+00	-0.584E+00	-0.560E+00	0.269E+00	0.181E-01	0.295E+00	0.345E-01
23	0.2667	0.676E+00	-0.639E+00	-0.494E+00	0.154E+00	-0.162E+00	0.165E+00	-0.136E+00
22	0.2333	0.592E+00	-0.513E+00	-0.221E+00	0.130E+00	-0.240E+00	0.139E+00	-0.165E+00
21	0.2000	0.761E+00	-0.285E+00	0.712E-01	0.213E+00	-0.143E+00	0.139E+00	-0.139E+00
20	0.1667	0.103E+01	-0.408E-01	0.435E+00	0.260E+00	-0.961E-05	0.230E+00	-0.119E+00
19	0.1333	0.150E+01	0.171E+00	0.628E+00	0.339E+00	0.137E+00	0.275E+00	-0.420E-01
18	0.1000	0.195E+01	0.501E+00	0.771E+00	0.464E+00	0.228E+00	0.325E+00	0.320E-01
17	0.0667	0.222E+01	0.646E+00	0.785E+00	0.507E+00	0.298E+00	0.347E+00	0.166E+00
16	0.0333	0.222E+01	0.957E+00	0.752E+00	0.472E+00	0.245E+00	0.319E+00	0.432E-01
15	0.0000	0.202E+01	0.125E+01	0.529E+00	0.292E+00	0.250E+00	0.191E+00	0.317E+00
14	-0.0333	0.182E+01	0.143E+01	0.427E+00	0.251E+00	0.580E+00		
13	-0.0667	0.113E+01	0.136E+01	0.655E+00	0.579E+00	0.636E+00		
12	-0.1000	0.391E+00	0.120E+01	0.652E+00	0.661E+00	0.596E+00		
11	-0.1333	0.906E-01	0.100E+01	0.576E+00	0.501E+00	0.469E+00		
10	-0.1667	-0.242E+00	0.698E+00	0.496E+00	0.267E+00	0.345E+00		
9	-0.2000	-0.423E+00	0.395E+00	0.431E+00	0.464E-01	0.293E+00	0.603E-01	0.277E+00
8	-0.2333	-0.426E+00	0.221E+00	0.346E+00	-0.123E+00	0.185E+00		
7	-0.2667	-0.367E+00	0.241E+00	0.350E+00	-0.203E+00	0.164E+00		
6	-0.3000	-0.232E-01	0.474E+00	0.518E+00	-0.786E-01	0.211E+00		
5	-0.3333	0.158E+00	0.108E+01	0.795E+00	0.229E+00	0.406E+00		
4	-0.3667	0.296E-04	0.173E+01	0.121E+01	0.757E+00	0.781E+00		
3	-0.4000	-0.423E+00	0.194E+01	0.170E+01	0.141E+01	0.120E+01	0.133E+01	0.158E+01
2	-0.4333	-0.367E+00	0.136E+01	0.226E+01	0.221E+01	0.153E+01		
1	-0.4667	0.126E+00	0.126E+01	0.251E+01	0.283E+01	0.164E+01		

(c)  $u/u_{av}$

TABLE VII (Continued)

J	I =		X =						
	Y	1	2	3	4	5	6	7	
		0.0278	0.0833	0.1389	0.1944	0.2500	0.3056	0.4167	
27	0.4000	-0.198E+00	-0.800E+00	-0.102E+01	-0.586E+00	-0.884E+00	-0.765E+00	-0.467E+00	
26	0.3667	-0.314E+00	-0.877E+00	-0.978E+00	-0.624E+00	-0.971E+00	-0.841E+00	-0.540E+00	
25	0.3333	-0.337E+00	-0.920E+00	-0.834E+00	-0.665E+00	-0.104E+01	-0.887E+00	-0.568E+00	
24	0.3000	-0.173E-01	-0.985E+00	-0.653E+00	-0.687E+00	-0.101E+01	-0.868E+00	-0.561E+00	
23	0.2667	0.123E+00	-0.100E+01	-0.483E+00	-0.663E+00	-0.100E+01	-0.736E+00	-0.516E+00	
22	0.2333	0.163E+00	-0.103E+01	-0.320E+00	-0.643E+00	-0.921E+00	-0.684E+00	-0.524E+00	
21	0.2000	0.247E+00	-0.103E+01	-0.185E+00	-0.589E+00	-0.908E+00	-0.666E+00	-0.422E+00	
20	0.1667	0.298E+00	-0.107E+01	-0.330E-01	-0.571E+00	-0.785E+00	-0.574E+00	-0.376E+00	
19	0.1333	0.233E+00	-0.102E+01	0.000E+00	-0.526E+00	-0.746E+00	-0.512E+00	-0.373E+00	
18	0.1000	0.243E+00	0.000E+00	0.402E-01	-0.332E+00	-0.655E+00	-0.367E+00	-0.173E+00	
17	0.0667	0.241E+00	-0.711E+00	0.481E-01	-0.372E+00	-0.578E+00	-0.312E+00	-0.456E-01	
16	0.0333	0.184E+00	-0.661E+00	0.112E+00	-0.323E+00	-0.457E+00	-0.133E+00	-0.153E+00	
15	0.0000	0.180E+00	-0.501E+00	0.433E+00	-0.391E+00	-0.153E+00	-0.153E+00	0.000E+00	
14	-0.0333	0.177E+00	-0.456E+00	0.553E+00	-0.154E+00	0.649E-01			
13	-0.0667	0.250E+00	-0.422E+00	0.638E+00	0.712E-01	0.857E-01			
12	-0.1000	0.620E+00	-0.343E+00	0.741E+00	0.482E-01	0.913E-01			
11	-0.1333	0.776E+00	-0.308E+00	0.780E+00	0.142E+00	0.943E-01			
10	-0.1667	0.839E+00	-0.197E+00	0.652E+00	0.223E+00	0.920E-01			
9	-0.2000	0.586E+00	-0.213E-01	0.609E+00	0.269E+00	0.105E+00	0.339E+00	0.352E+00	
8	-0.2333	0.521E+00	0.708E-01	0.370E+00	0.297E+00	0.874E-01			
7	-0.2667	0.543E+00	0.256E+00	0.323E+00	0.362E+00	0.660E-01			
6	-0.3000	0.597E+00	0.424E+00	0.214E+00	0.419E+00	0.201E-01			
5	-0.3333	0.701E+00	0.548E+00	0.901E-01	0.395E+00	0.182E-01			
4	-0.3667	0.761E+00	0.557E+00	-0.762E-02	0.330E+00	0.831E-02			
3	-0.4000	0.776E+00	0.501E+00	-0.559E-01	0.249E+00	-0.777E-02	0.145E+00	0.105E+00	
2	-0.4333	0.617E+00	0.313E+00	-0.726E-01	0.155E+00	-0.691E-01			
1	-0.4667	0.198E+00	0.203E+00	-0.658E-02	0.874E-01	-0.636E-01			

(d)  $v/u_{av}$

TABLE VII (Continued)

J	Y	I =						
		1	2	3	4	5	6	7
X =		0.0278	0.0833	0.1389	0.1944	0.2500	0.3056	0.4167
27	0.4000	-0.819E+01	-0.800E+01	-0.750E+01	-0.700E+01	-0.656E+01	-0.608E+01	-0.574E+01
26	0.3667	-0.761E+01	-0.684E+01	-0.662E+01	-0.645E+01	-0.627E+01	-0.583E+01	-0.561E+01
25	0.3333	-0.691E+01	-0.569E+01	-0.557E+01	-0.583E+01	-0.579E+01	-0.540E+01	-0.540E+01
24	0.3000	-0.608E+01	-0.462E+01	-0.456E+01	-0.514E+01	-0.519E+01	-0.497E+01	-0.495E+01
23	0.2667	-0.487E+01	-0.366E+01	-0.361E+01	-0.441E+01	-0.442E+01	-0.451E+01	-0.459E+01
22	0.2333	-0.354E+01	-0.282E+01	-0.275E+01	-0.372E+01	-0.361E+01	-0.398E+01	-0.410E+01
21	0.2000	-0.234E+01	-0.203E+01	-0.204E+01	-0.304E+01	-0.273E+01	-0.346E+01	-0.363E+01
20	0.1667	-0.136E+01	-0.117E+01	-0.160E+01	-0.235E+01	-0.202E+01	-0.280E+01	-0.309E+01
19	0.1333	-0.101E+01	-0.686E+00	-0.123E+01	-0.175E+01	-0.131E+01	-0.224E+01	-0.240E+01
18	0.1000	-0.835E+00	-0.597E+00	-0.987E+00	-0.128E+01	-0.744E+00	-0.167E+01	-0.183E+01
17	0.0667	-0.721E+00	-0.274E+00	-0.658E+00	-0.780E+00	-0.459E+00	-0.107E+01	-0.118E+01
16	0.0333	-0.636E+00	-0.334E-01	-0.383E+00	-0.425E+00	-0.178E+00	-0.601E+00	-0.245E+00
15	0.0000	-0.541E+00	0.267E+00	-0.933E-01	-0.124E+00	0.873E-02	-0.160E+00	0.266E+00
14	-0.0333	-0.321E+00	0.578E+00	0.676E-01	0.351E-02	0.437E+00		
13	-0.0667	-0.393E-01	0.787E+00	0.479E+00	0.335E+00	0.908E+00		
12	-0.1000	0.405E+00	0.101E+01	0.992E+00	0.788E+00	0.148E+01		
11	-0.1333	0.862E+00	0.128E+01	0.158E+01	0.124E+01	0.203E+01		
10	-0.1667	0.172E+01	0.173E+01	0.233E+01	0.190E+01	0.269E+01		
9	-0.2000	0.277E+01	0.249E+01	0.307E+01	0.266E+01	0.334E+01	0.345E+01	0.397E+01
8	-0.2333	0.392E+01	0.361E+01	0.395E+01	0.354E+01	0.408E+01		
7	-0.2667	0.525E+01	0.493E+01	0.476E+01	0.464E+01	0.470E+01		
6	-0.3000	0.666E+01	0.631E+01	0.558E+01	0.563E+01	0.525E+01		
5	-0.3333	0.823E+01	0.768E+01	0.629E+01	0.655E+01	0.581E+01		
4	-0.3667	0.934E+01	0.891E+01	0.694E+01	0.720E+01	0.636E+01		
3	-0.4000	0.970E+01	0.953E+01	0.754E+01	0.760E+01	0.678E+01	0.648E+01	0.561E+01
2	-0.4333	0.105E+02	0.104E+02	0.789E+01	0.769E+01	0.686E+01		
1	-0.4667	0.103E+02	0.102E+02	0.777E+01	0.730E+01	0.658E+01		

(e)  $w/u_{av}$

TABLE VIII  
VELOCITY DATA FOR CASE 7

		I =	1	2	3	4	5	6	7
		X =	0.0063	0.0190	0.0318	0.0444	0.0572	0.0698	0.0952
J	Y								
27	0.0914	0.250E+03	0.000E+00	0.895E+02	0.230E+02	0.360E+03	0.340E+02	0.360E+03	
26	0.0838	0.234E+03	0.000E+00	0.895E+02	0.330E+02	0.000E+00	0.340E+02	0.360E+03	
25	0.0762	0.234E+03	0.200E+00	0.895E+02	0.540E+01	0.360E+03	0.340E+02	0.360E+03	
24	0.0686	0.229E+03	0.000E+00	0.395E+02	0.350E+01	0.360E+03	0.260E+02	0.360E+03	
23	0.0610	0.210E+03	0.000E+00	0.400E+01	0.350E+01	0.360E+03	0.260E+02	0.000E+00	
22	0.0533	0.204E+03	0.000E+00	0.400E+01	0.140E+01	0.360E+03	0.800E+01	0.360E+03	
21	0.0457	0.100E+02	0.000E+00	0.100E+01	0.140E+01	0.360E+03	0.800E+01	0.360E+03	
20	0.0381	0.400E+01	0.200E+00	0.100E+01	0.360E+03	0.360E+03	0.800E+01	0.360E+03	
19	0.0305	0.400E+01	0.200E+00	0.100E+01	0.360E+03	0.360E+03	0.800E+01	0.360E+03	
18	0.0229	0.200E+01	0.360E+03	0.100E+01	0.360E+03	0.360E+03	0.360E+03	0.360E+03	
17	0.0152	0.200E+00	0.360E+03	0.360E+03	0.360E+03	0.360E+03	0.360E+03	0.360E+03	
16	0.0076	0.100E+00	0.100E+00	0.360E+03	0.360E+03	0.360E+03	0.360E+03	0.360E+03	
15	0.0000	0.360E+03	0.360E+03	0.360E+03	0.360E+03	0.360E+03	0.360E+03	0.360E+03	
14	-0.0076	0.000E+00	0.360E+03	0.360E+03	0.360E+03	0.360E+03			
13	-0.0152	0.000E+00	0.360E+03	0.360E+03	0.359E+03	0.360E+03			
12	-0.0229	0.000E+00	0.360E+03	0.360E+03	0.359E+03	0.360E+03			
11	-0.0305	0.100E+01	0.360E+03	0.360E+03	0.359E+03	0.360E+03			
10	-0.0381	0.200E+01	0.360E+03	0.360E+03	0.359E+03	0.360E+03			
9	-0.0457	0.000E+00	0.360E+03	0.360E+03	0.359E+03	0.360E+03	0.800E+01	0.360E+03	
8	-0.0533	0.152E+03	0.170E+01	0.100E+01	0.359E+03	0.360E+03			
7	-0.0610	0.161E+03	0.000E+00	0.100E+01	0.359E+03	0.360E+03			
6	-0.0686	0.161E+03	0.100E+03	0.100E+01	0.359E+03	0.360E+03			
5	-0.0762	0.000E+00	0.138E+03	0.100E+01	0.000E+00	0.360E+03			
4	-0.0838	0.161E+03	0.138E+03	0.100E+01	0.000E+00	0.360E+03			
3	-0.0914	0.161E+03	0.138E+03	0.200E+01	0.000E+00	0.360E+03	0.800E+01	0.360E+03	
2	-0.0991	0.161E+03	0.138E+03	0.110E+02	0.000E+00	0.360E+03			
1	-0.1067	0.161E+03	0.138E+03	0.110E+02	0.000E+00	0.360E+03			

(a) Yaw Angle

TABLE VIII (Continued)

I =		1	2	3	4	5	6	7
X =		0.0063	0.0190	0.0318	0.0444	0.0572	0.0698	0.0952
J	Y							
27	0.0914	0.000E+00	0.000E+00	-0.433E+02	-0.165E+02	0.000E+00	-0.315E+02	0.000E+00
26	0.0838	0.000E+00	0.000E+00	-0.510E+02	-0.165E+02	0.000E+00	-0.218E+02	0.000E+00
25	0.0762	-0.510E+02	0.000E+00	0.000E+00	0.000E+00	0.310E+02	-0.165E+02	0.000E+00
24	0.0686	-0.510E+02	0.000E+00	-0.707E+01	0.351E+01	0.161E+02	-0.132E+02	0.000E+00
23	0.0610	-0.510E+02	0.000E+00	-0.287E+01	0.474E+01	0.756E+01	-0.527E+01	0.000E+00
22	0.0533	-0.315E+02	0.000E+00	0.318E+01	0.280E+01	0.116E+02	0.000E+00	0.000E+00
21	0.0457	0.000E+00	0.000E+00	0.463E+01	0.420E+01	0.102E+02	0.000E+00	0.000E+00
20	0.0381	0.000E+00	0.607E+01	0.415E+01	0.391E+01	0.756E+01	0.000E+00	0.000E+00
19	0.0305	0.867E+01	0.607E+01	0.341E+01	0.238E+01	0.511E+01	0.000E+00	0.000E+00
18	0.0229	0.339E+01	0.318E+01	0.235E+01	0.152E+01	0.366E+01	0.000E+00	0.000E+00
17	0.0152	0.512E+00	0.820E+00	-0.235E+01	-0.248E+01	0.198E+01	0.000E+00	0.000E+00
16	0.0076	-0.860E+00	-0.853E+00	0.512E+00	0.275E+00	0.558E+00	0.000E+00	0.000E+00
15	0.0000	-0.204E+01	-0.403E+01	-0.768E+00	-0.774E+00	0.000E+00	0.000E+00	0.000E+00
14	-0.0076	-0.299E+01	-0.289E+01	-0.304E+01	-0.432E+01	-0.170E+01		
13	-0.0152	-0.357E+01	-0.567E+01	-0.588E+01	-0.652E+01	-0.359E+01		
12	-0.0229	-0.581E+01	-0.758E+01	-0.805E+01	-0.773E+01	-0.494E+01		
11	-0.0305	-0.125E+02	-0.107E+02	-0.113E+02	-0.957E+01	-0.682E+01		
10	-0.0381	0.000E+00	-0.807E+01	-0.100E+02	-0.128E+02	-0.107E+02		
9	-0.0457	0.000E+00	-0.152E+02	-0.165E+02	-0.150E+02	-0.119E+02	-0.179E+02	-0.315E+02
8	-0.0533	0.000E+00	-0.315E+02	-0.315E+02	-0.197E+02	-0.116E+02		
7	-0.0610	0.000E+00	0.000E+00	-0.315E+02	0.000E+00	-0.197E+02		
6	-0.0686	0.000E+00	0.000E+00	-0.510E+02	-0.315E+02	-0.315E+02		
5	-0.0762	0.000E+00	0.000E+00	-0.315E+02	0.000E+00	-0.244E+02		
4	-0.0838	-0.315E+02	0.000E+00	0.000E+00	0.000E+00	-0.315E+02		
3	-0.0914	0.000E+00	0.000E+00	-0.315E+02	0.000E+00	-0.315E+02	-0.315E+02	0.000E+00
2	-0.0991	0.000E+00	0.000E+00	-0.315E+02	0.000E+00	0.000E+00		
1	-0.1067	0.000E+00	0.000E+00	-0.315E+02	0.000E+00	0.000E+00		

(b) Pitch Angle

TABLE VIII (Continued)

	I =	1	2	3	4	5	6	7
J	X =	0.0278	0.0833	0.1389	0.1944	0.2500	0.3056	0.4167
	Y							
27	0.4000	0.000E+00	0.000E+00	0.132E+01	0.132E+01	0.109E+01	0.109E+01	0.109E+01
26	0.3667	-0.644E+00	0.000E+00	0.120E+01	0.120E+01	0.000E+00	0.142E+01	0.109E+01
25	0.3333	-0.487E+00	0.000E+00	0.218E+01	0.218E+01	0.104E+01	0.168E+01	0.109E+01
24	0.3000	-0.544E+00	0.000E+00	0.329E+01	0.329E+01	0.153E+01	0.206E+01	0.109E+01
23	0.2667	-0.718E+00	0.000E+00	0.396E+01	0.396E+01	0.221E+01	0.254E+01	0.000E+00
22	0.2333	-0.850E+00	0.000E+00	0.525E+01	0.526E+01	0.308E+01	0.324E+01	0.109E+01
21	0.2000	0.000E+00	0.000E+00	0.668E+01	0.669E+01	0.378E+01	0.342E+01	0.109E+01
20	0.1667	0.000E+00	0.247E+01	0.822E+01	0.823E+01	0.494E+01	0.389E+01	0.109E+01
19	0.1333	0.291E+01	0.494E+01	0.991E+01	0.992E+01	0.603E+01	0.389E+01	0.109E+01
18	0.1000	0.130E+02	0.917E+01	0.115E+02	0.115E+02	0.721E+01	0.450E+01	0.109E+01
17	0.0667	0.201E+02	0.141E+02	0.122E+02	0.122E+02	0.774E+01	0.475E+01	0.155E+01
16	0.0333	0.212E+02	0.187E+02	0.123E+02	0.123E+02	0.860E+01	0.463E+01	0.109E+01
15	0.0000	0.222E+02	0.215E+02	0.129E+02	0.129E+02	0.902E+01	0.488E+01	0.155E+01
14	-0.0333	0.217E+02	0.209E+02	0.105E+02	0.105E+02	0.875E+01		
13	-0.0667	0.213E+02	0.198E+02	0.866E+01	0.866E+01	0.922E+01		
12	-0.1000	0.176E+02	0.162E+02	0.710E+01	0.710E+01	0.829E+01		
11	-0.1333	0.728E+01	0.999E+01	0.552E+01	0.553E+01	0.730E+01		
10	-0.1667	0.000E+00	0.724E+01	0.435E+01	0.436E+01	0.577E+01		
9	-0.2000	0.000E+00	0.367E+01	0.337E+01	0.338E+01	0.515E+01	0.330E+01	0.929E+00
8	-0.2333	-0.968E+00	0.131E+01	0.223E+01	0.223E+01	0.462E+01		
7	-0.2667	-0.104E+01	0.000E+00	0.000E+00	0.000E+00	0.316E+01		
6	-0.3000	-0.104E+01	0.000E+00	0.928E+00	0.928E+00	0.227E+01		
5	-0.3333	0.000E+00	0.000E+00	0.000E+00	0.000E+00	0.195E+01		
4	-0.3667	-0.880E+00	0.000E+00	0.000E+00	0.000E+00	0.131E+01		
3	-0.4000	0.000E+00	0.000E+00	0.000E+00	0.000E+00	0.929E+00	0.130E+01	0.109E+01
2	-0.4333	0.000E+00	0.000E+00	0.000E+00	0.000E+00	0.000E+00		
1	-0.4667	0.000E+00	0.000E+00	0.000E+00	0.000E+00	0.000E+00		

(c)  $u/u_{av}$



TABLE VIII (Continued)

J	Y	I =						
		1	2	3	4	5	6	7
	X =	0.0278	0.0833	0.1389	0.1944	0.2500	0.3056	0.4167
27	0.4000	0.000E+00	0.000E+00	-0.423E+00	-0.423E+00	0.000E+00	-0.803E+00	0.000E+00
26	0.3667	0.000E+00	0.000E+00	-0.423E+00	-0.423E+00	0.000E+00	-0.684E+00	0.000E+00
25	0.3333	-0.102E+01	0.000E+00	0.000E+00	0.000E+00	0.624E+00	-0.597E+00	0.000E+00
24	0.3000	-0.102E+01	0.000E+00	0.202E+00	0.202E+00	0.440E+00	-0.535E+00	0.000E+00
23	0.2667	-0.102E+01	0.000E+00	0.329E+00	0.329E+00	0.293E+00	-0.260E+00	0.000E+00
22	0.2333	-0.570E+00	0.000E+00	0.257E+00	0.257E+00	0.633E+00	0.000E+00	0.000E+00
21	0.2000	0.000E+00	0.000E+00	0.491E+00	0.491E+00	0.681E+00	0.000E+00	0.000E+00
20	0.1667	0.000E+00	0.263E+00	0.562E+00	0.562E+00	0.656E+00	0.000E+00	0.000E+00
19	0.1333	0.445E+00	0.525E+00	0.412E+00	0.412E+00	0.539E+00	0.000E+00	0.000E+00
18	0.1000	0.771E+00	0.510E+00	0.304E+00	0.304E+00	0.460E+00	0.000E+00	0.000E+00
17	0.0667	0.180E+00	0.202E+00	-0.498E+00	-0.499E+00	0.267E+00	0.000E+00	0.000E+00
16	0.0333	-0.318E+00	-0.279E+00	0.591E-01	0.591E-01	0.837E-01	0.000E+00	0.000E+00
15	0.0000	-0.790E+00	-0.151E+01	-0.174E+00	-0.174E+00	0.000E+00	0.000E+00	0.000E+00
14	-0.0333	-0.113E+01	-0.105E+01	-0.791E+00	-0.791E+00	-0.260E+00		
13	-0.0667	-0.133E+01	-0.196E+01	-0.990E+00	-0.991E+00	-0.578E+00		
12	-0.1000	-0.179E+01	-0.216E+01	-0.964E+00	-0.964E+00	-0.717E+00		
11	-0.1333	-0.162E+01	-0.189E+01	-0.932E+00	-0.932E+00	-0.873E+00		
10	-0.1667	0.000E+00	-0.103E+01	-0.991E+00	-0.991E+00	-0.109E+01		
9	-0.2000	0.000E+00	-0.997E+00	-0.903E+00	-0.904E+00	-0.108E+01	-0.108E+01	-0.569E+00
8	-0.2333	0.000E+00	-0.804E+00	-0.798E+00	-0.798E+00	-0.944E+00		
7	-0.2667	0.000E+00	0.000E+00	0.000E+00	0.000E+00	-0.113E+01		
6	-0.3000	0.000E+00	0.000E+00	-0.569E+00	-0.569E+00	-0.140E+01		
5	-0.3333	0.000E+00	0.000E+00	0.000E+00	0.000E+00	-0.883E+00		0.000E+00
4	-0.3667	-0.570E+00	0.000E+00	0.000E+00	0.000E+00	-0.805E+00		
3	-0.4000	0.000E+00	0.000E+00	0.000E+00	0.000E+00	-0.569E+00	-0.803E+00	0.000E+00
2	-0.4333	0.000E+00	0.000E+00	0.000E+00	0.000E+00	0.000E+00		
1	-0.4667	0.000E+00	0.000E+00	0.000E+00	0.000E+00	0.000E+00		

(d)  $v/u_{sv}$

TABLE VIII (Continued)

	I =	1	2	3	4	5	6	7
J	Y	X = 0.0278	0.0833	0.1389	0.1944	0.2500	0.3056	0.4167
27	0.4000	0.000E+00	0.000E+00	0.560E+00	0.560E+00	-0.659E-05	0.732E+00	-0.659E-05
26	0.3667	-0.887E+00	0.000E+00	0.780E+00	0.780E+00	0.000E+00	0.958E+00	-0.659E-05
25	0.3333	-0.671E+00	0.000E+00	0.206E+00	0.206E+00	-0.626E-05	0.113E+01	-0.659E-05
24	0.3000	-0.626E+00	0.000E+00	0.201E+00	0.201E+00	-0.921E-05	0.100E+01	-0.659E-05
23	0.2667	-0.414E+00	0.000E+00	0.242E+00	0.242E+00	-0.133E-04	0.124E+01	0.000E+00
22	0.2333	-0.378E+00	0.000E+00	0.128E+00	0.128E+00	-0.185E-04	0.455E+00	-0.659E-05
21	0.2000	0.000E+00	0.000E+00	0.163E+00	0.163E+00	-0.228E-04	0.480E+00	-0.659E-05
20	0.1667	0.000E+00	0.862E-02	-0.495E-04	-0.496E-04	-0.298E-04	0.547E+00	-0.659E-05
19	0.1333	0.204E+00	0.172E-01	-0.597E-04	-0.597E-04	-0.363E-04	0.547E+00	-0.659E-05
18	0.1000	0.454E+00	-0.553E-04	-0.690E-04	-0.691E-04	-0.434E-04	-0.271E-04	-0.659E-05
17	0.0667	0.702E-01	-0.850E-04	-0.735E-04	-0.735E-04	-0.466E-04	-0.286E-04	-0.932E-05
16	0.0333	0.371E-01	0.327E-01	-0.742E-04	-0.742E-04	-0.518E-04	-0.279E-04	-0.659E-05
15	0.0000	-0.134E-03	-0.129E-03	-0.775E-04	-0.776E-04	-0.543E-04	-0.294E-04	-0.932E-05
14	-0.0333	-0.130E-03	-0.126E-03	-0.631E-04	-0.631E-04	-0.527E-04		
13	-0.0667	0.000E+00	-0.119E-03	-0.151E+00	-0.151E+00	-0.555E-04		
12	-0.1000	0.000E+00	-0.568E-01	-0.124E+00	-0.124E+00	-0.499E-04		
11	-0.1333	0.127E+00	-0.350E-01	-0.964E-01	-0.965E-01	-0.440E-04		
10	-0.1667	0.000E+00	-0.253E-01	-0.760E-01	-0.761E-01	-0.348E-04		
9	-0.2000	0.000E+00	-0.128E-01	-0.589E-01	-0.590E-01	-0.311E-04	0.464E+00	-0.560E-05
8	-0.2333	0.515E+00	0.389E-01	-0.389E-01	-0.390E-01	-0.278E-04		
7	-0.2667	0.357E+00	0.000E+00	0.000E+00	0.000E+00	-0.190E-04		
6	-0.3000	0.357E+00	0.000E+00	-0.162E-01	-0.162E-01	-0.137E-04		
5	-0.3333	0.000E+00	0.000E+00	0.000E+00	0.000E+00	-0.117E-04		
4	-0.3667	0.303E+00	0.000E+00	0.000E+00	0.000E+00	-0.791E-05		
3	-0.4000	0.000E+00	0.000E+00	0.000E+00	0.000E+00	-0.559E-05	0.182E+00	-0.659E-05
2	-0.4333	0.000E+00	0.000E+00	0.000E+00	0.000E+00	0.000E+00		
1	-0.4667	0.000E+00	0.000E+00	0.000E+00	0.000E+00	0.000E+00		

(e)  $w/u_{av}$

APPENDIX E

FIGURES

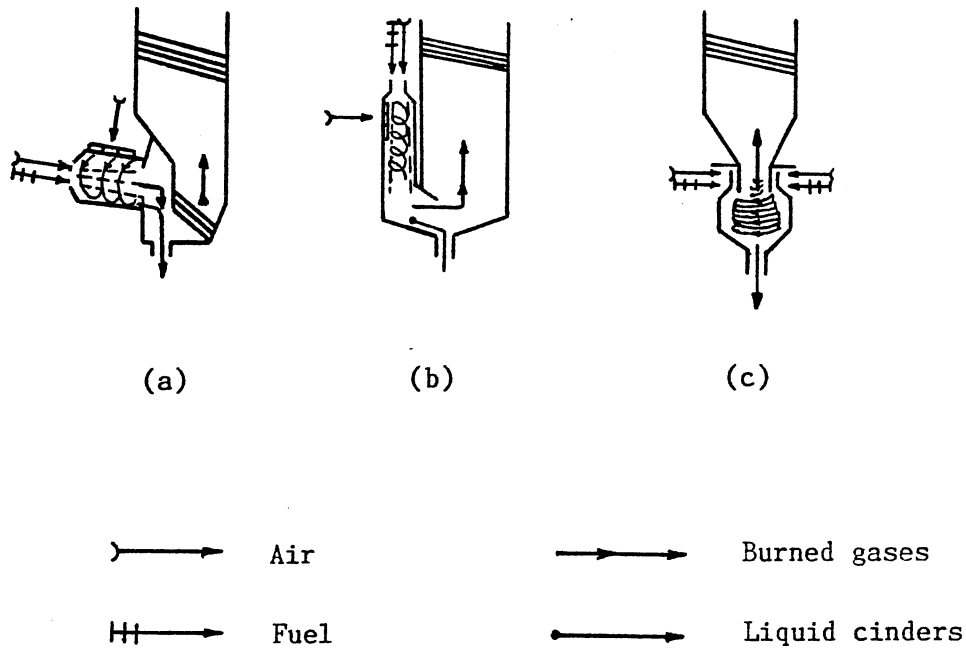


Figure 1. The Cyclone Furnace

- (a) Horizontal (or slightly inclined by 5-20°)
- (b) Vertical VTJ (USSR)
- (c) Vertical KSG

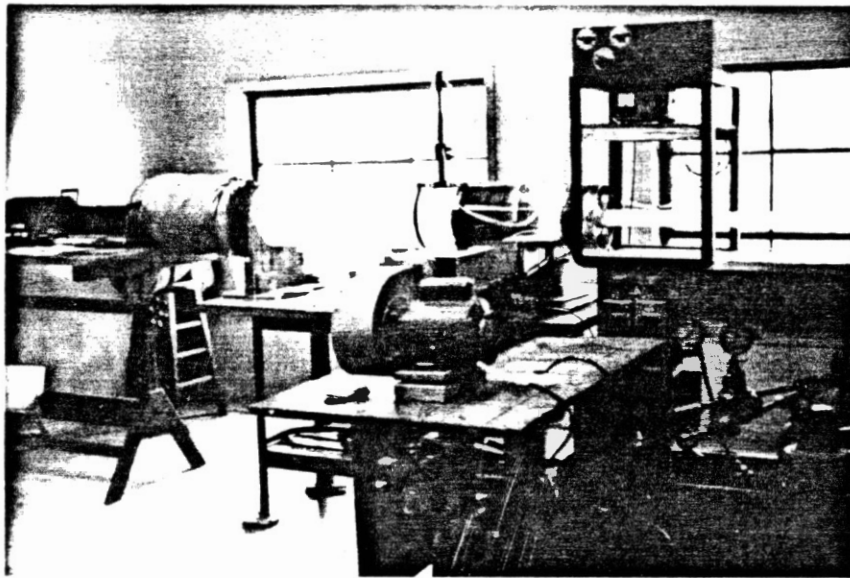


Figure 2. Photograph of the Overall Facility

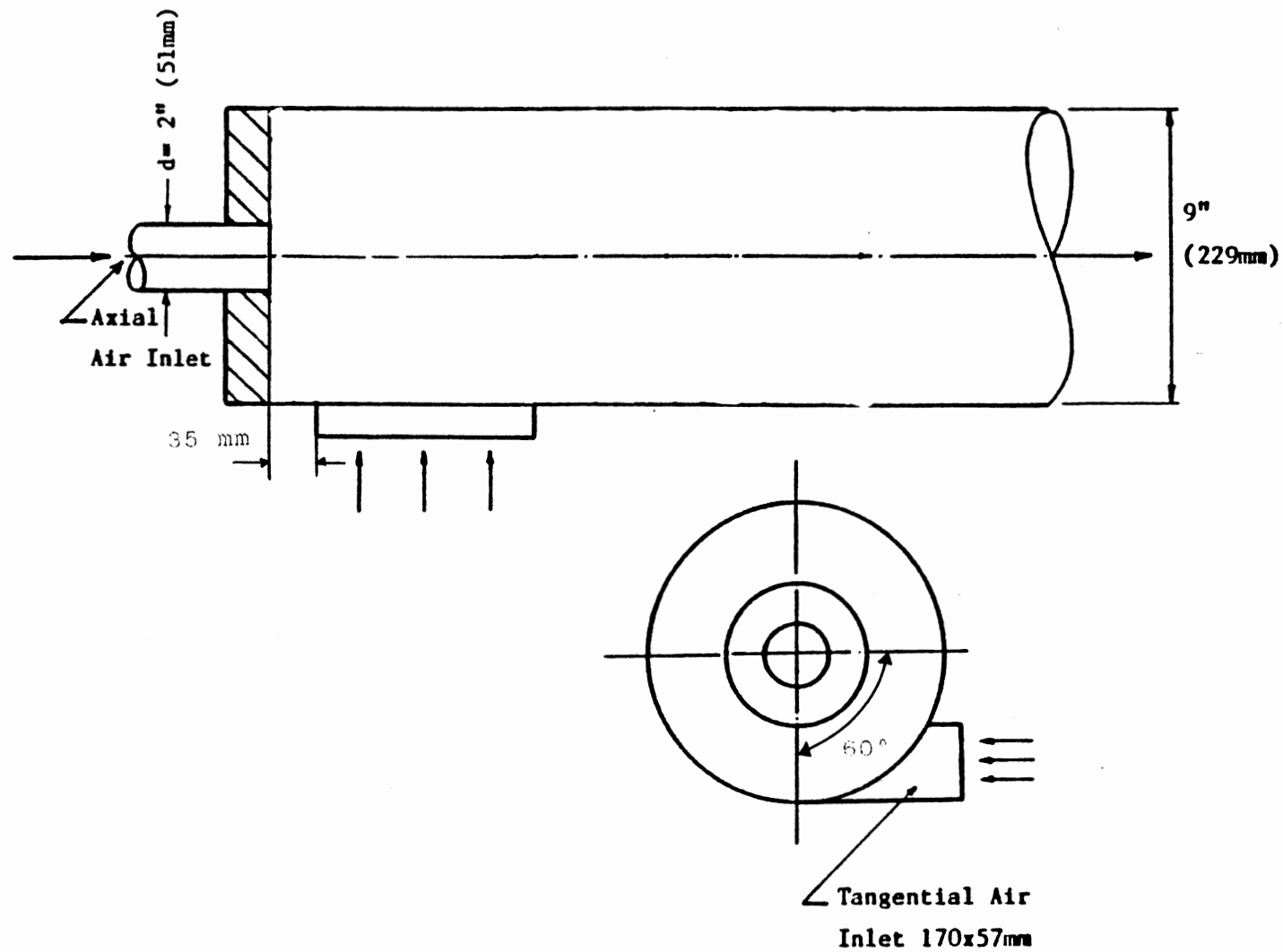
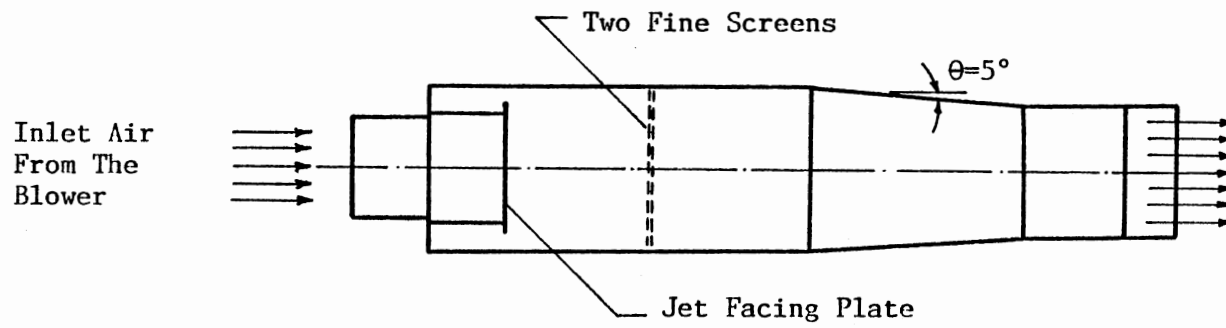
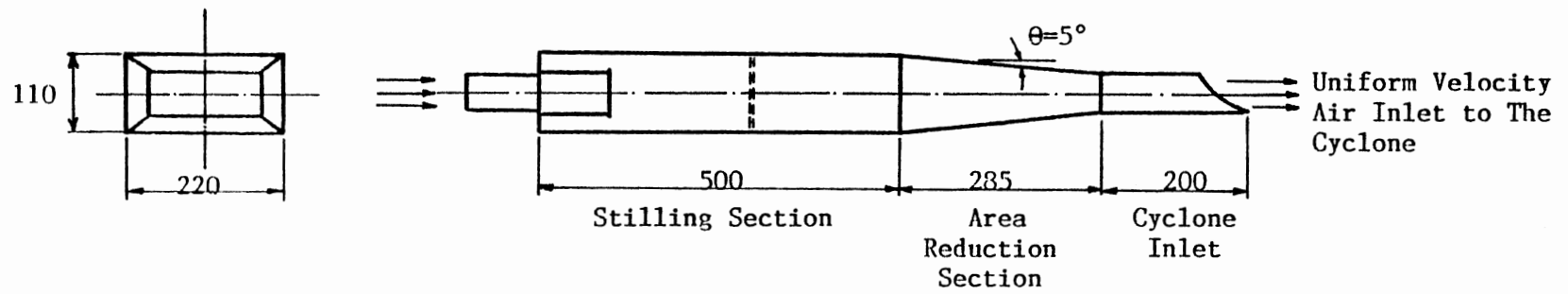


Figure 3. Geometry of strongly Swirling Flow Facility



All Dimensions in mm  
 Scale 1 : 10

Figure 4. Tangential Inlet Stilling Chamber

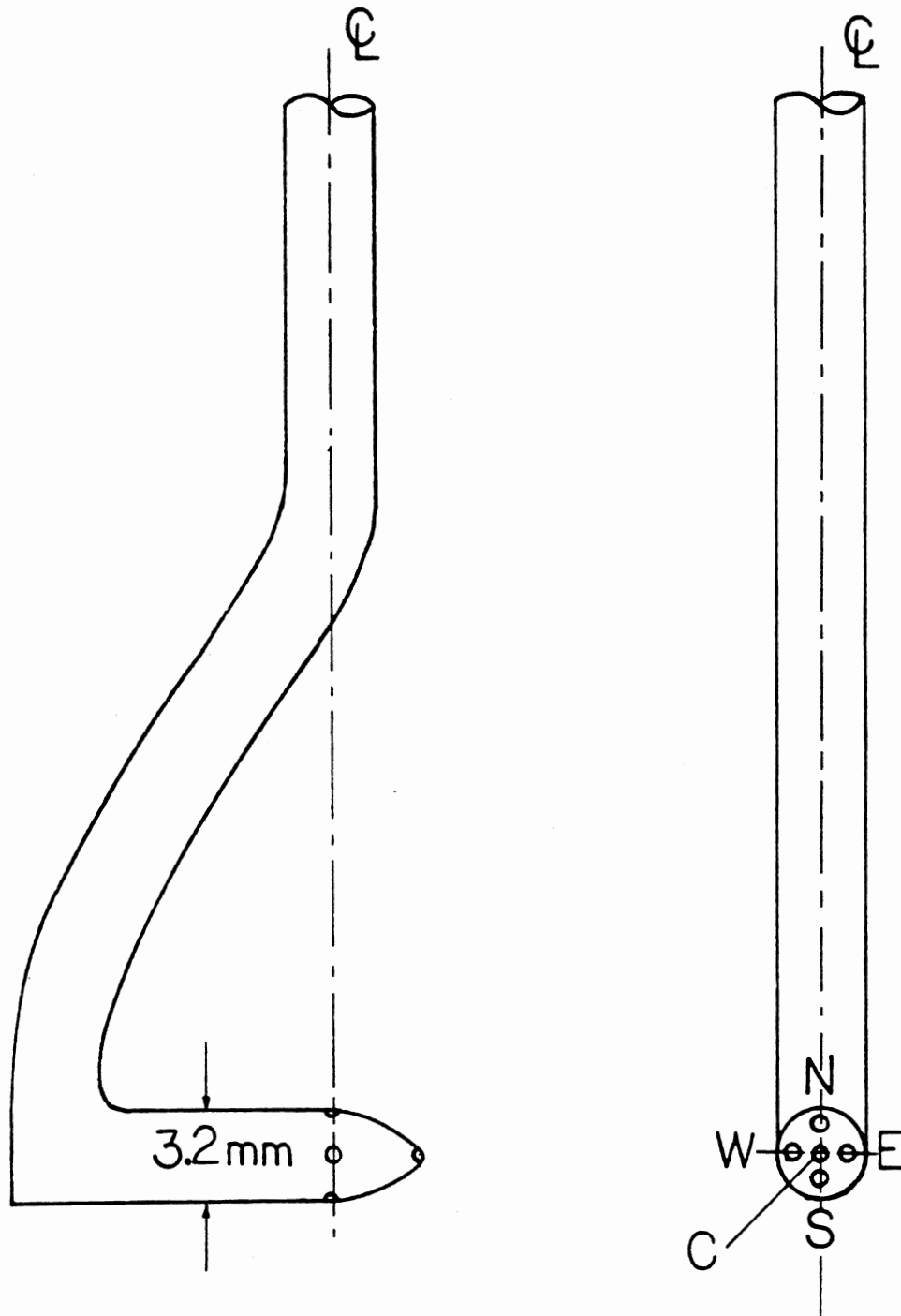


Figure 5. Five-Hole Pitot Probe



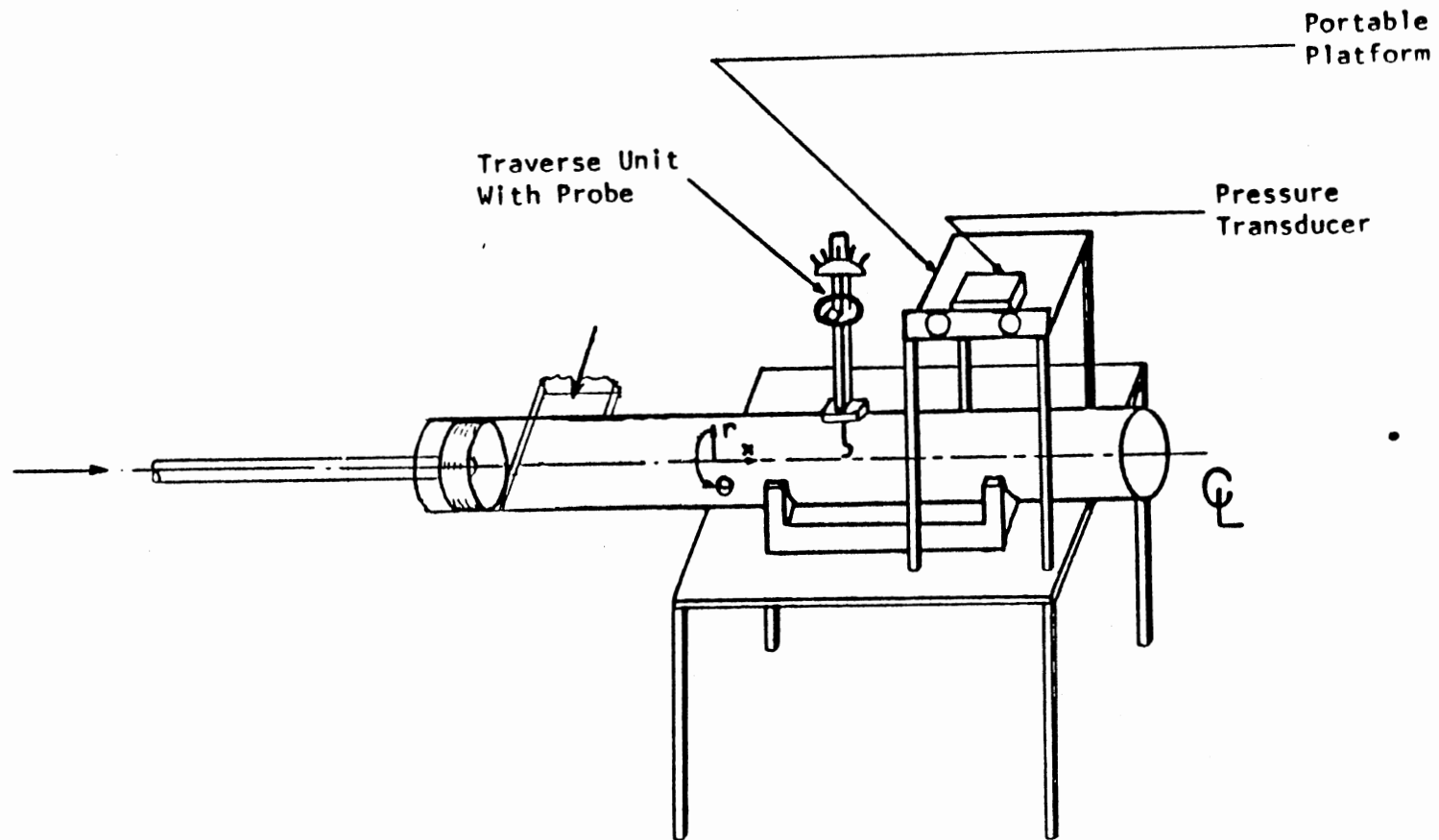


Figure 6. Apparatus for Time-Mean Velocity Measurements Using a Five-Hole Pitot Probe

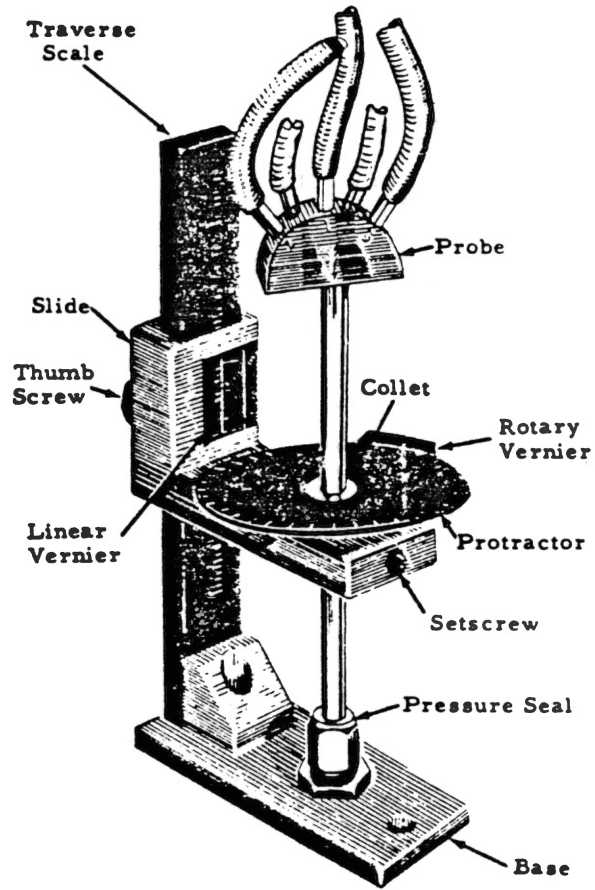


Figure 7. Manual Traverse Mechanism used for Five-Hole Pitot Probe Measurements

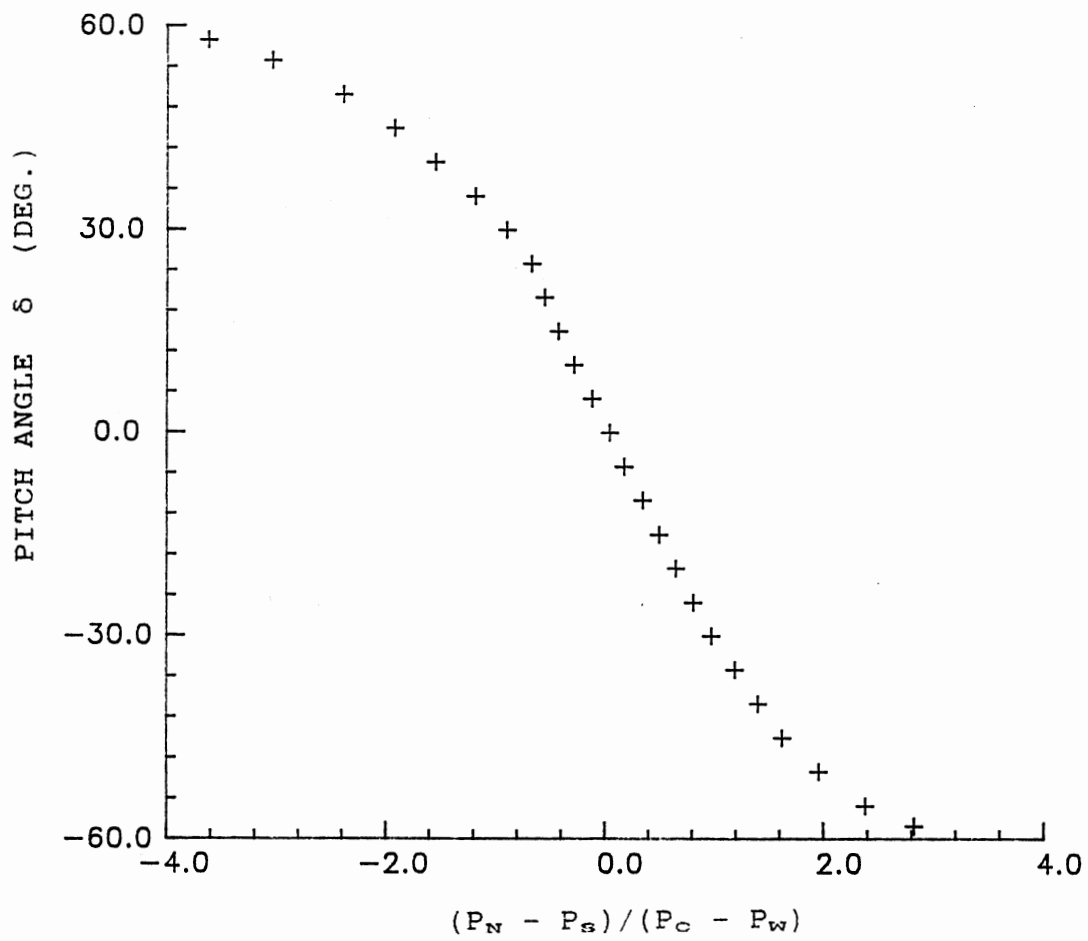


Figure 8. Pitch Angle Calibration Characteristic for Five-Hole Pitot Probe

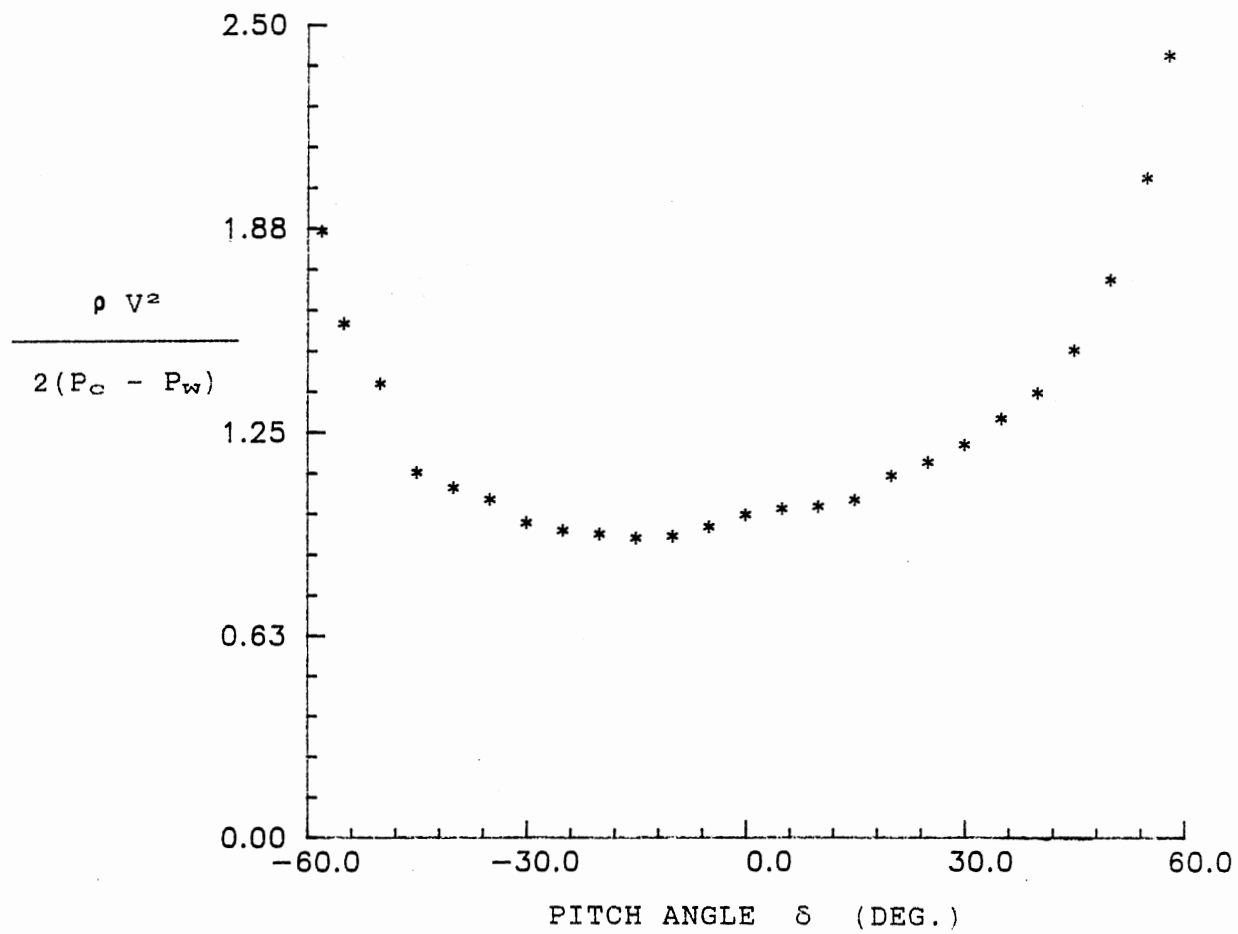


Figure 9. Velocity Coefficient Calibration Characteristic for Five-Hole Pitot Probe

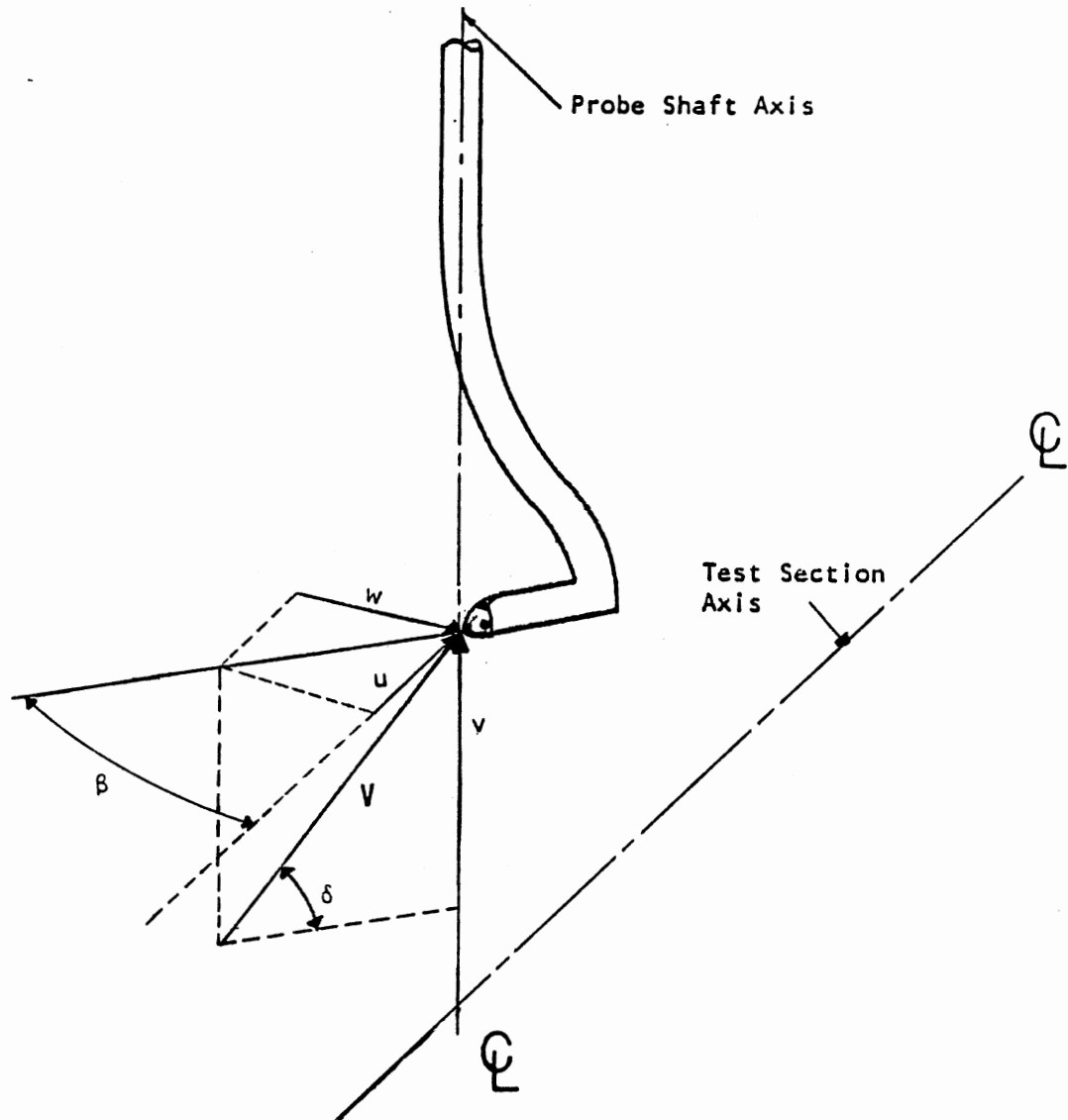


Figure 10. Velocity Components and Flow Direction Angles Associated with Five-Hole Pitot Probe Measurements

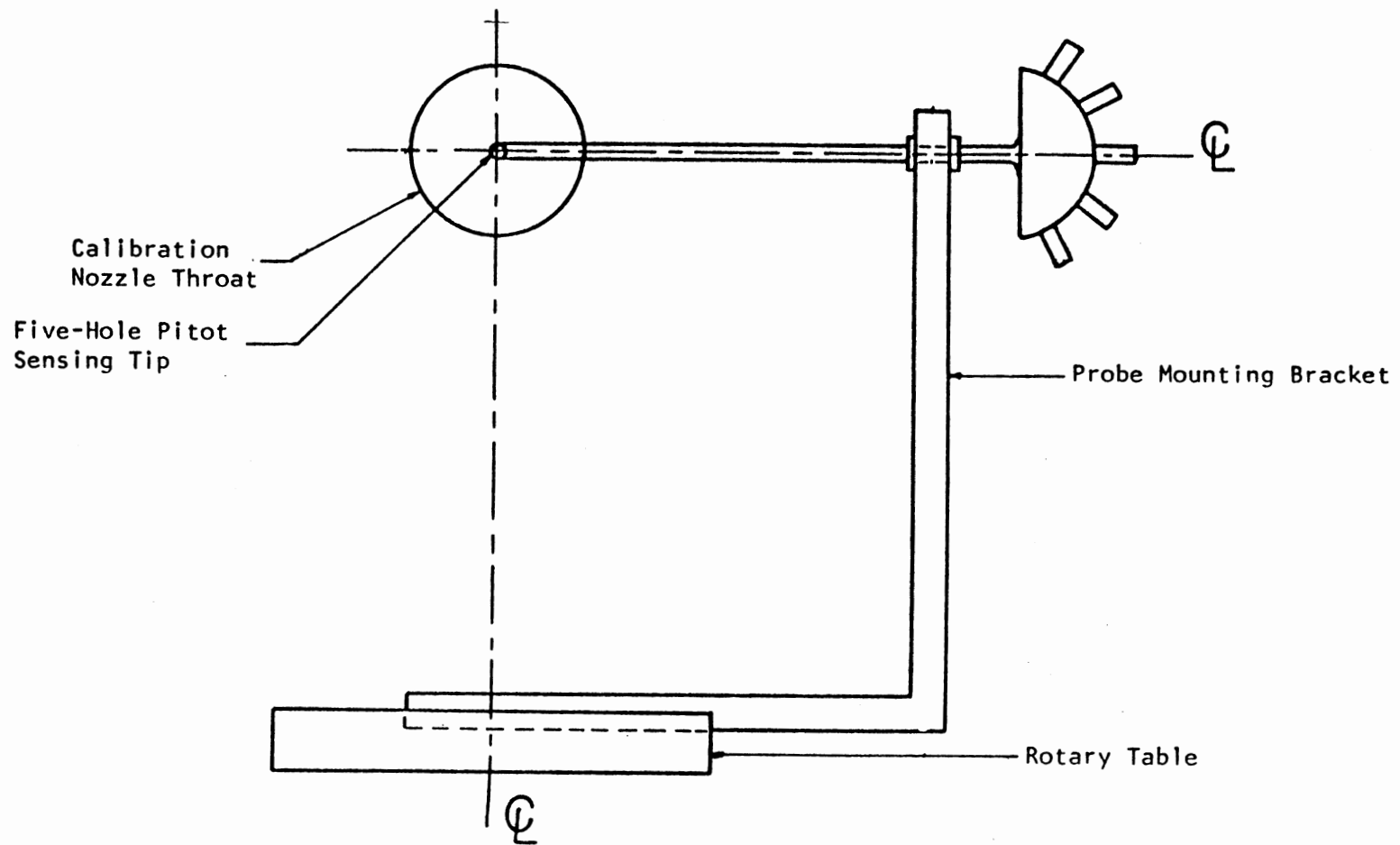
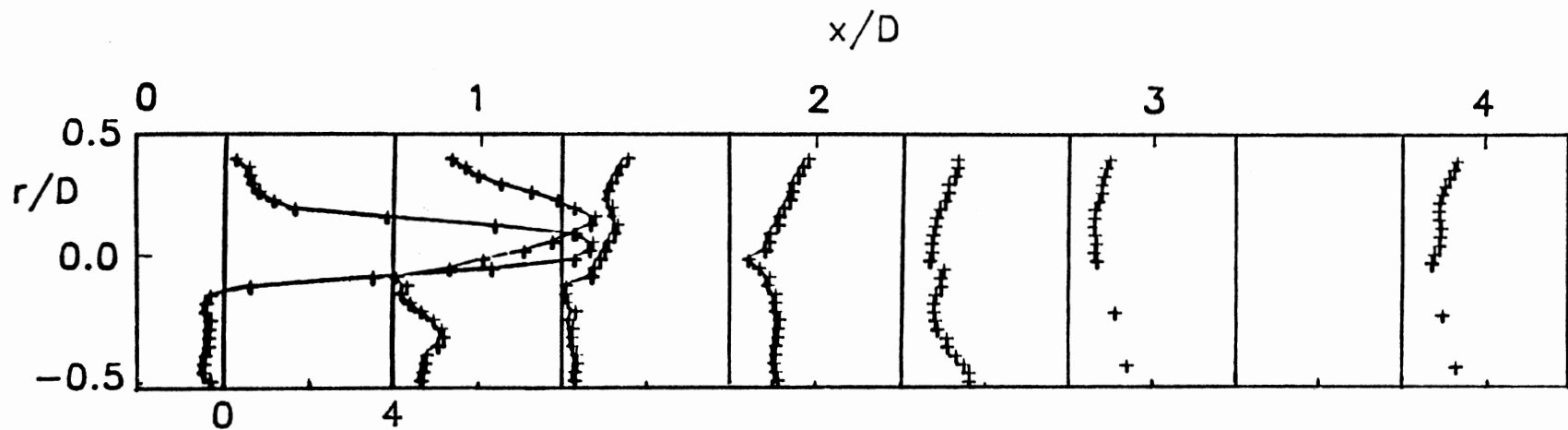
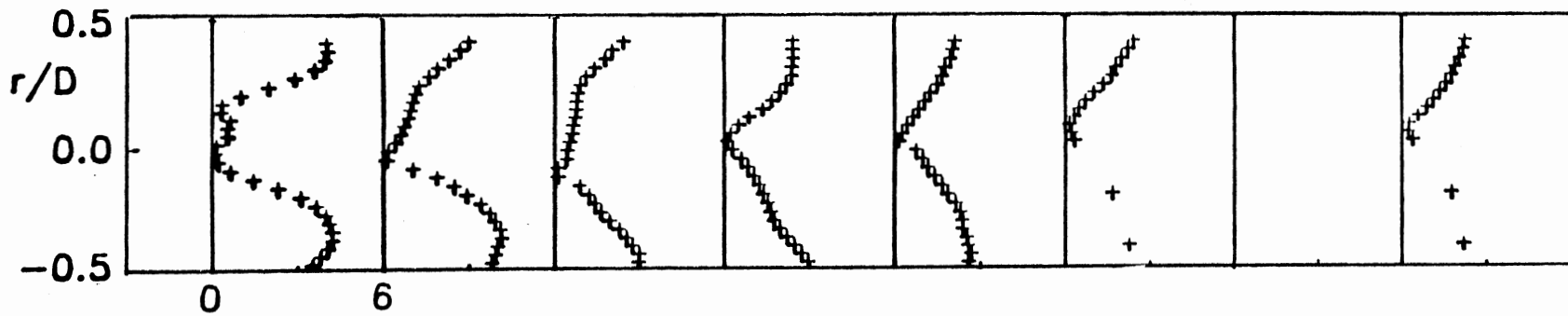


Figure 11. Calibration Apparatus with Five-Hole Pitot Probe

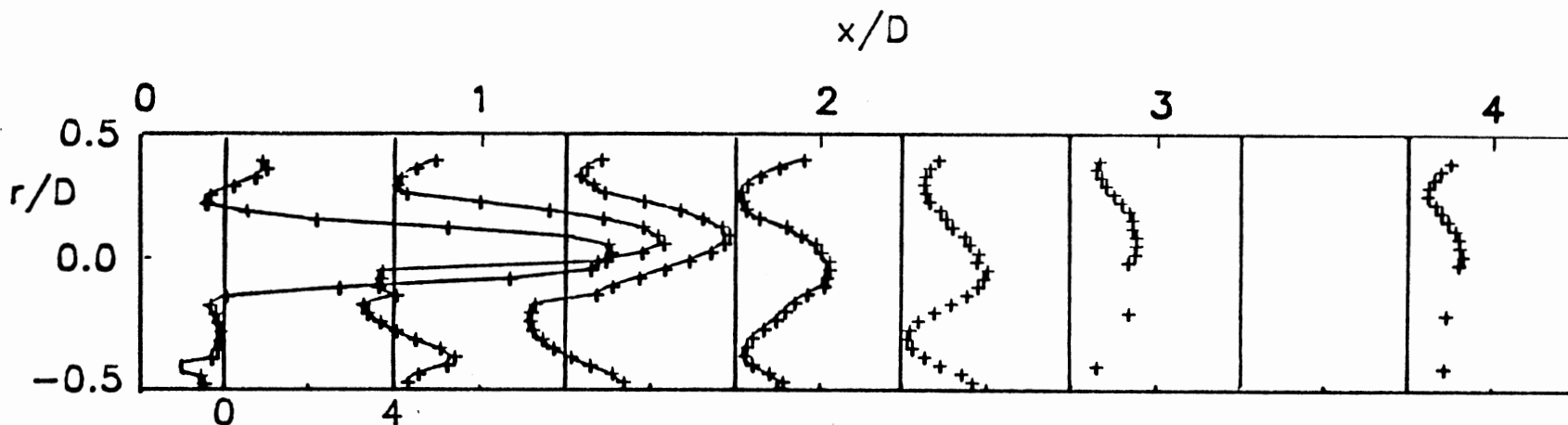


(a) Normalized Axial Velocity Profile  $u/u_{av}$

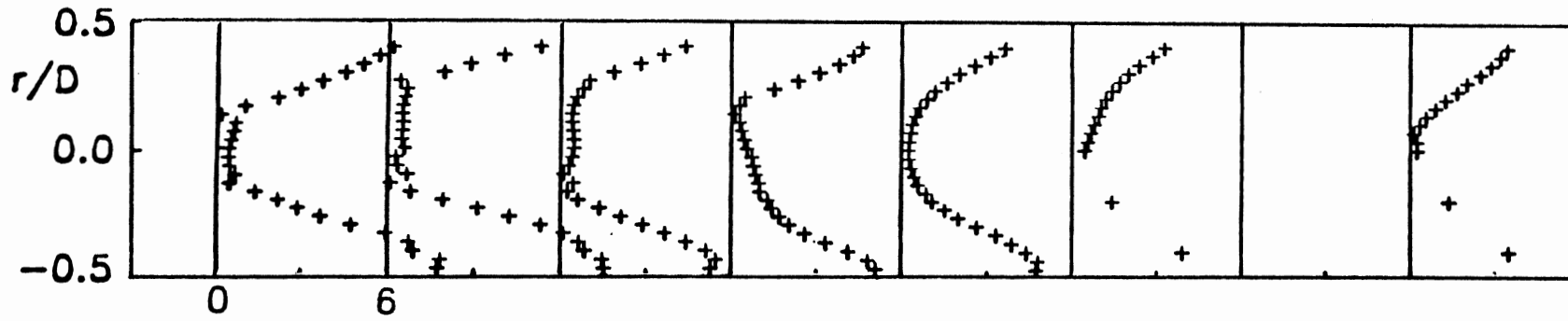


(b) Normalized Swirl Velocity Profile  $w/u_{av}$

Figure 12. Case 1 ( $m_t/m_a = 2$  and  $w_t/u_{av} = 2.83$ )



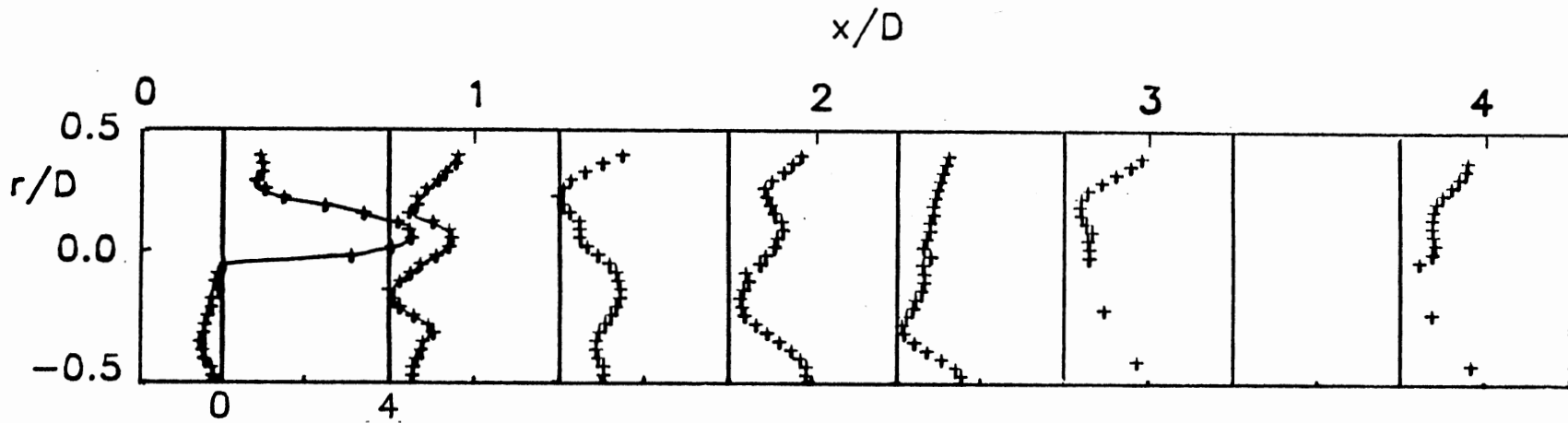
(a) Normalized Axial Velocity Profile  $u/u_{av}$



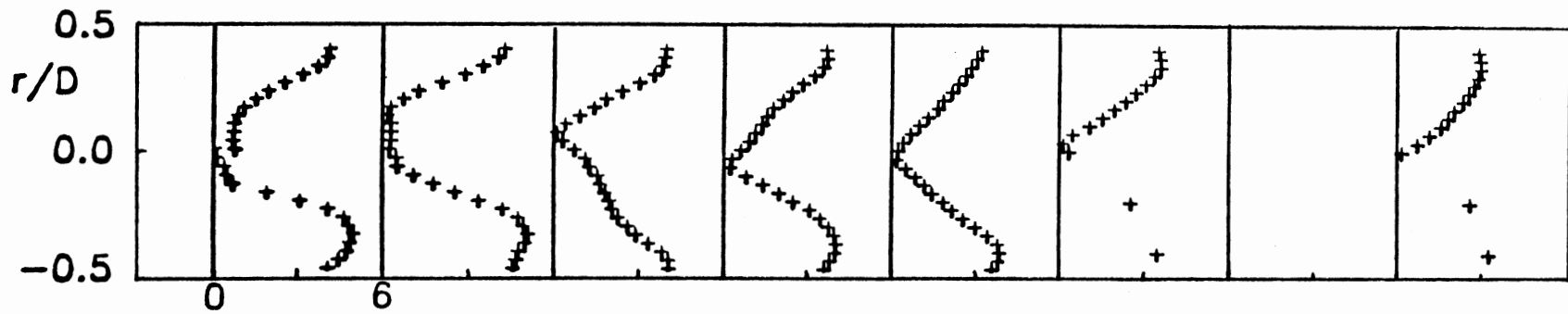
(b) Normalized Swirl Velocity Profile  $w/u_{av}$

Figure 13. Case 2 ( $m_t/m_a = 2$  and  $w_t/u_{av} = 5.64$ )



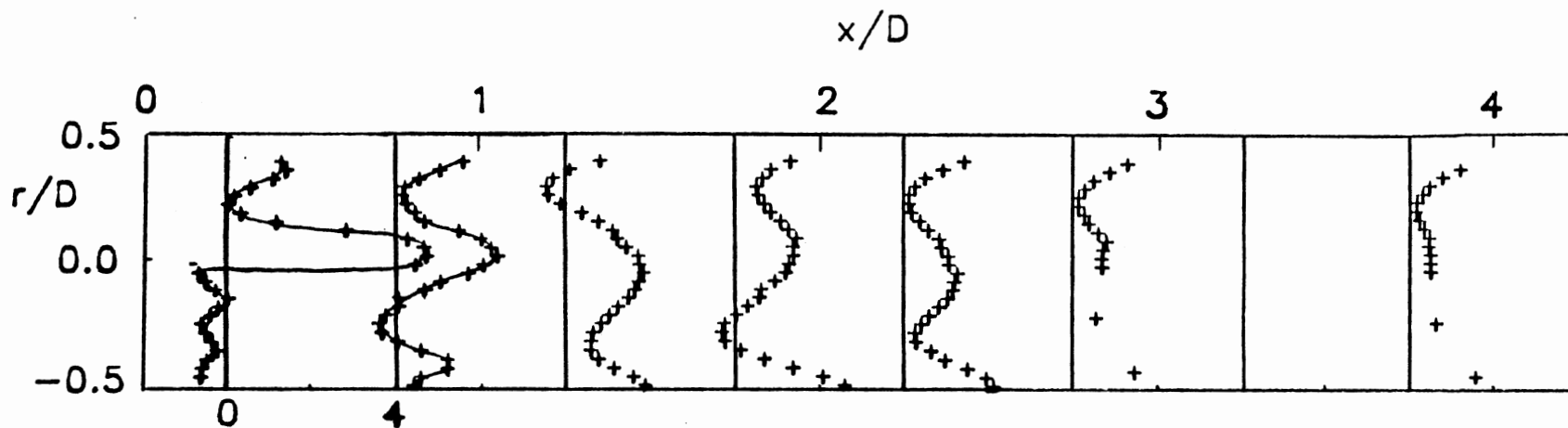


(a) Normalized Axial Velocity Profile  $u/u_{av}$

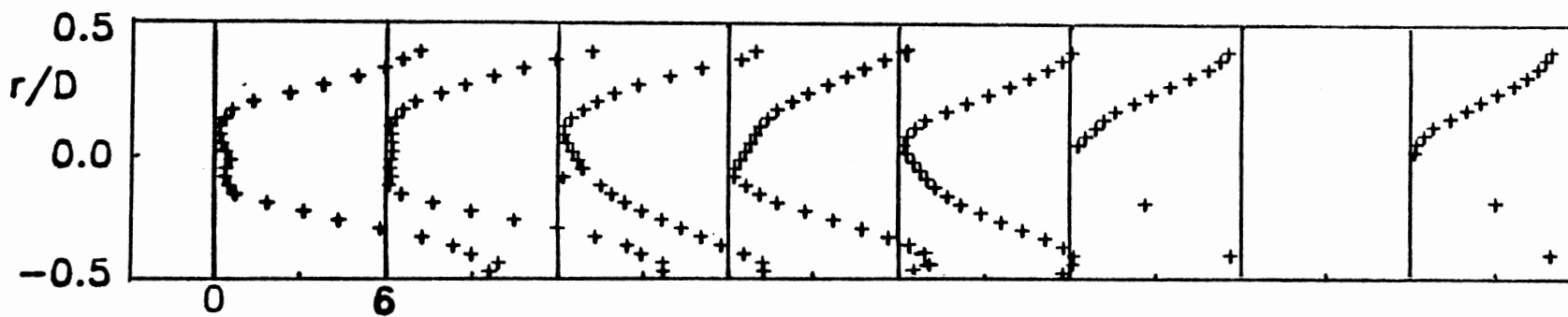


(b) Normalized Swirl Velocity Profile  $w/u_{av}$

Figure 14. Case 3 ( $m_t/m_n = 4$  and  $w_t/u_{av} = 3.39$ )

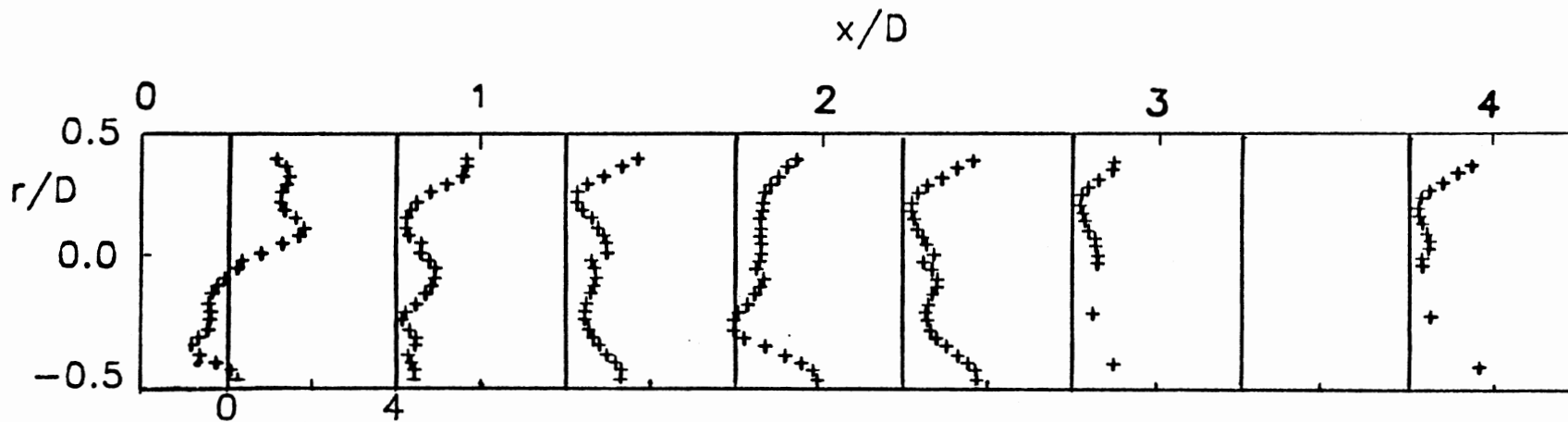


(a) Normalized Axial Velocity Profile  $u/u_{av}$

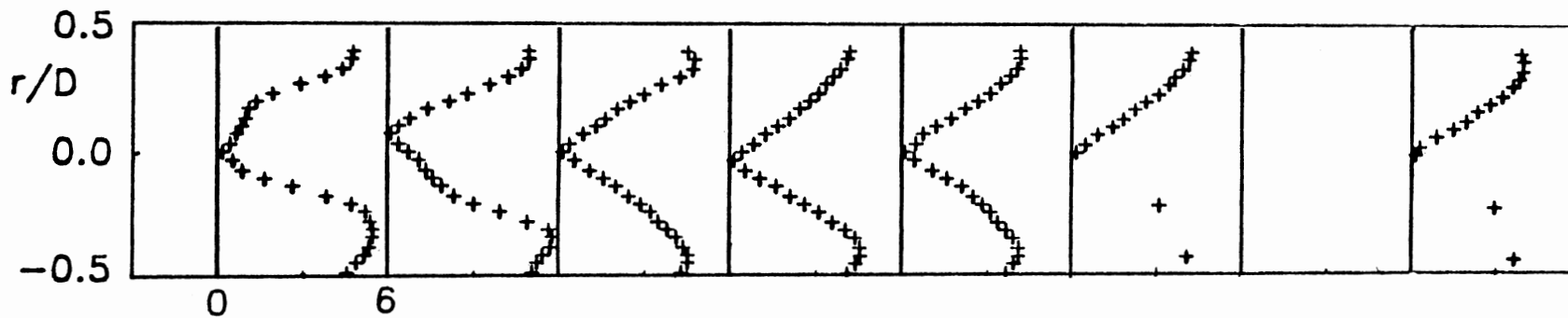


(b) Normalized Swirl Velocity Profile  $w/u_{av}$

Figure 15. Case 4 ( $m_t/m_a = 4$  and  $w_t/u_{av} = 6.78$ )

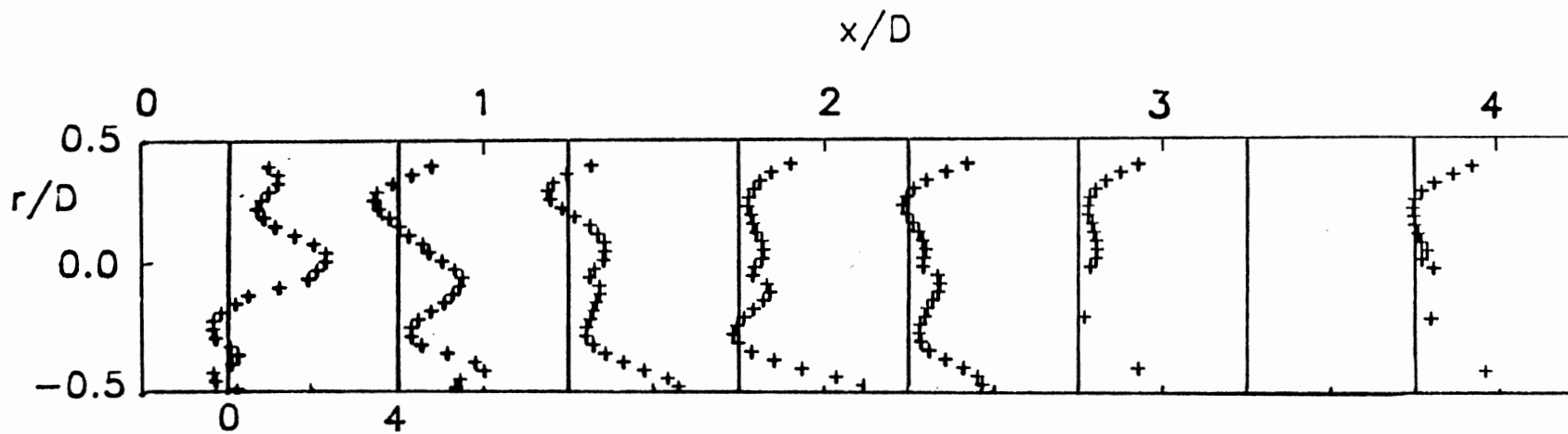


(a) Normalized Axial Velocity Profile  $u/u_{av}$

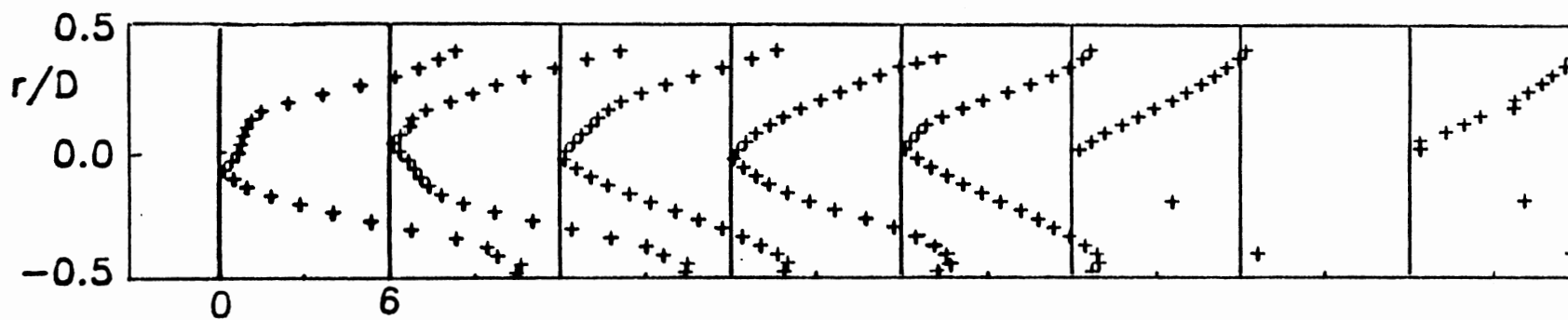


(b) Normalized Swirl Velocity Profile  $w/u_{av}$

Figure 16. Case 5 ( $m_t/m_a = 8$  and  $w_t/u_{av} = 3.77$ )

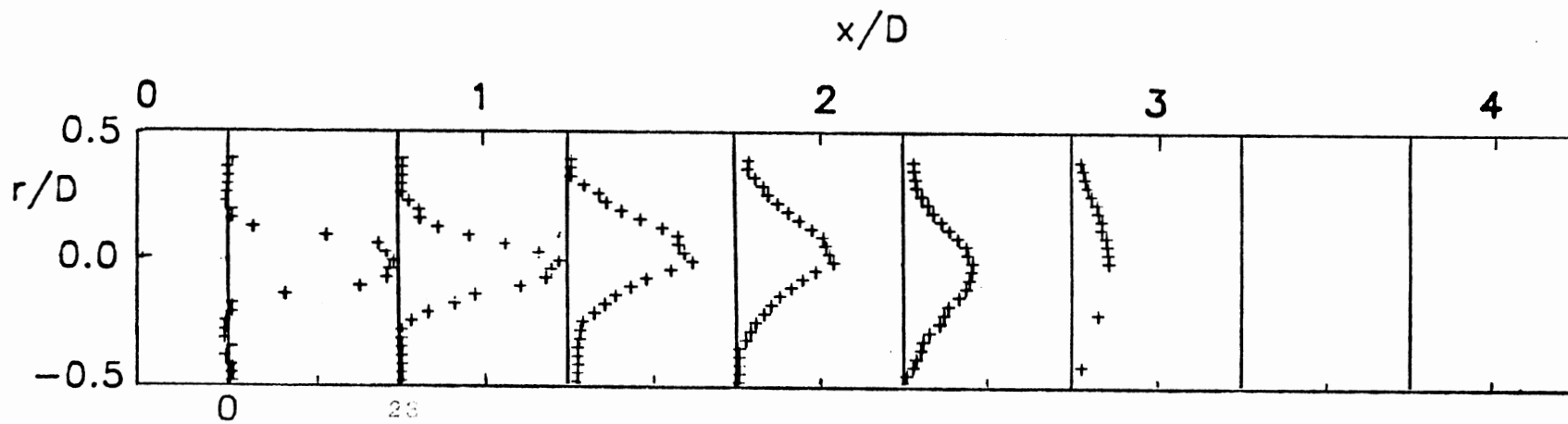


(a) Normalized Axial Velocity Profile  $u/u_{av}$

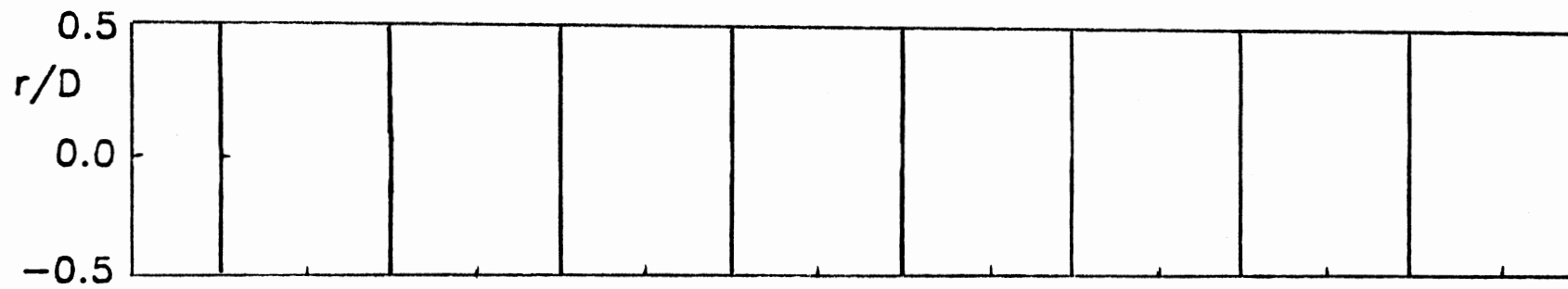


(b) Normalized Swirl Velocity Profile  $w/u_{av}$

Figure 17. Case 6 ( $m_t/m_a = 8$  and  $w_t/u_{av} = 7.51$ )



(a) Normalized Axial Velocity Profile  $u/u_{av}$



(b) Normalized Swirl Velocity Profile  $w/u_{av}$

Figure 18. Case 7 ( $m_t/m_a = 0$  and  $w_t/u_{av} = 0$ )

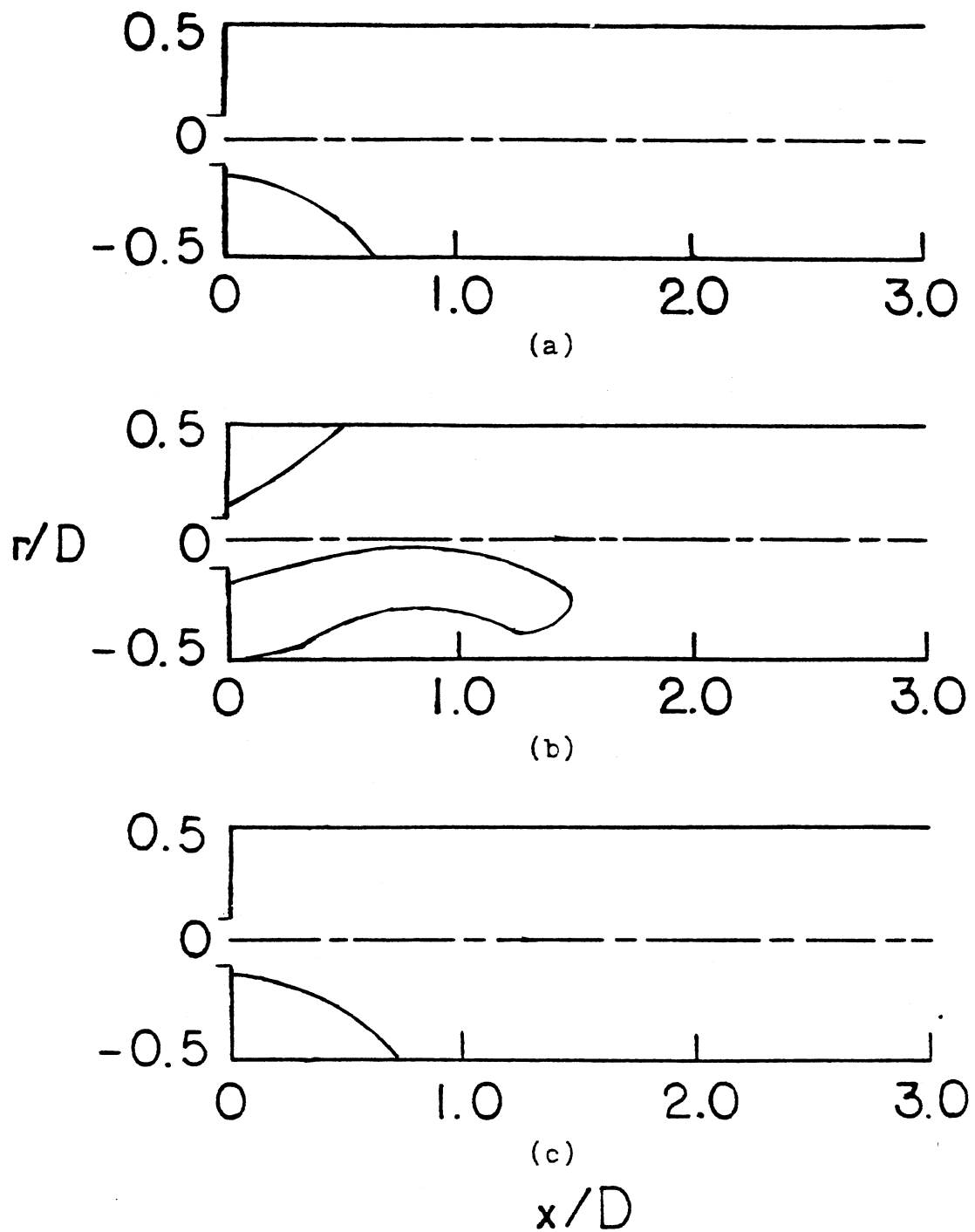


Figure 19. Sketch of Recirculation Zones: (a) Case 1  
 (b) Case 2 (c) Case 3

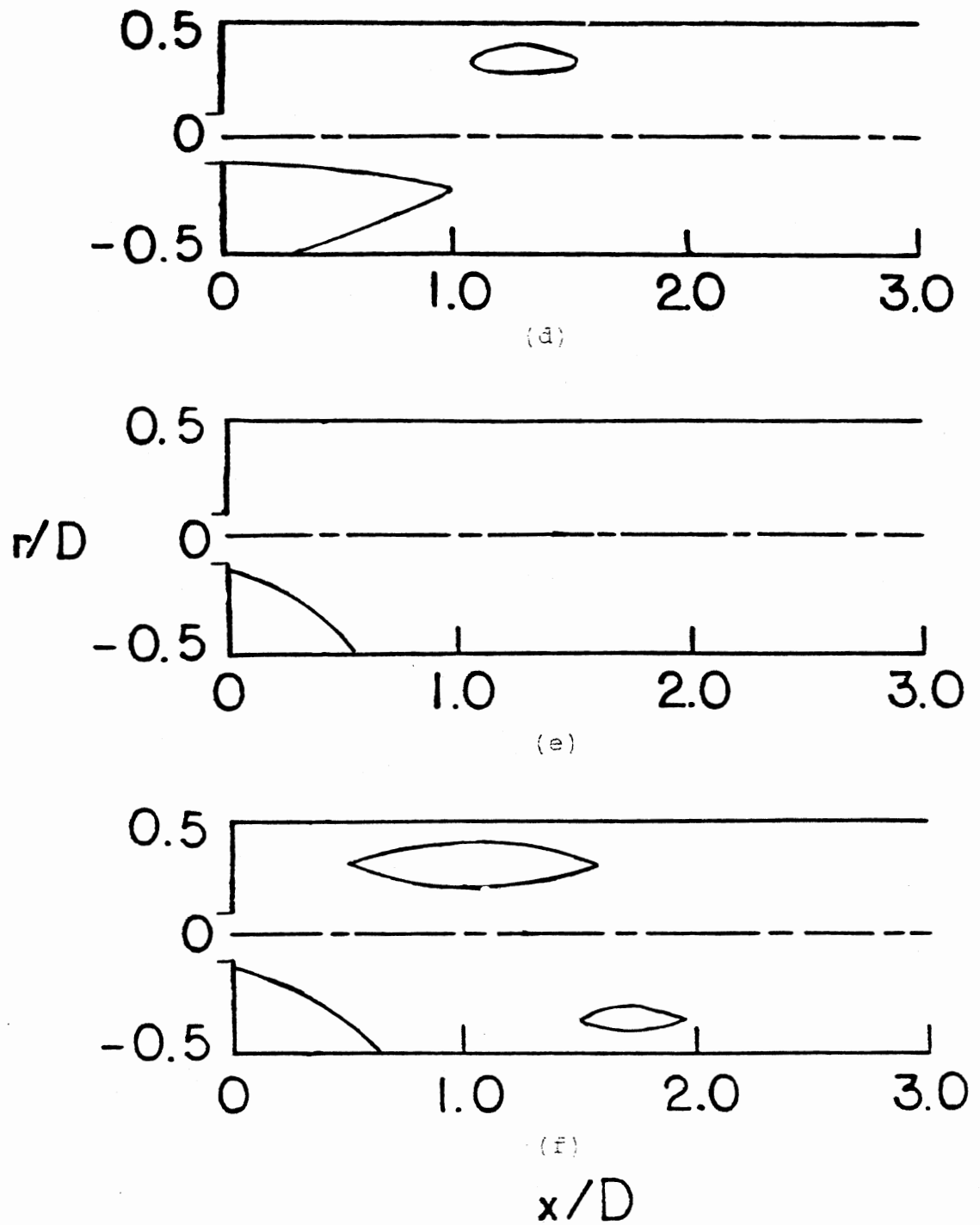


Figure 19. Continued: (d) Case 4 (e) Case 5  
(f) Case 6

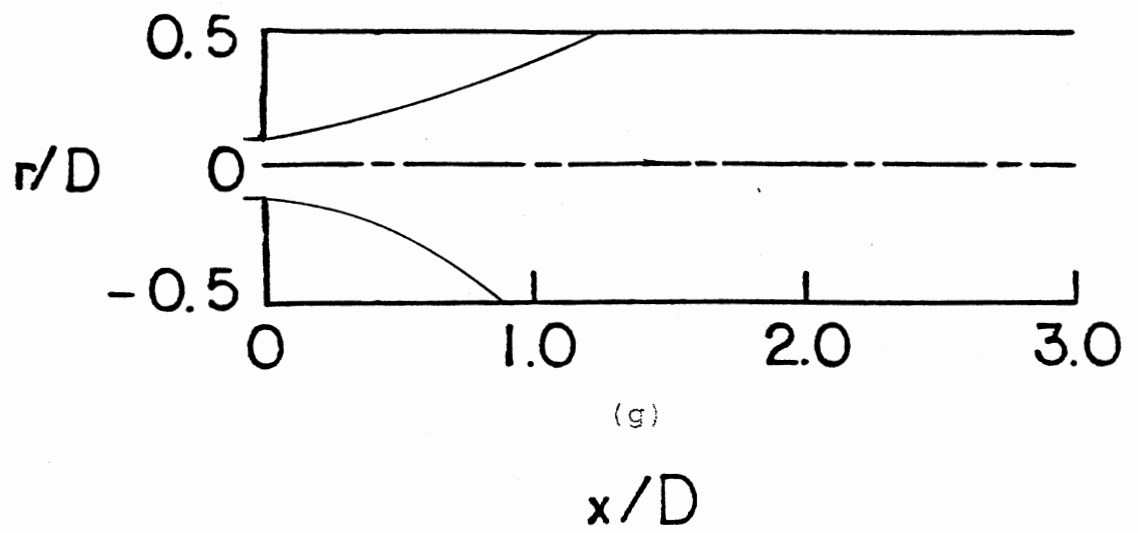


Figure 19. Continued: (g) Case 7



APPENDIX C

DATA REDUCTION COMPUTER PROGRAM AND CALIBRATION  
DATA FOR FIVE-HOLE PITOT PROBE MEASUREMENTS

\*\*\*\* TSO FOREGROUND HARDCOPY \*\*\*\*  
 DSNAME=U12107A.TEST1.FORT

```

C      SUBROUTINE MAIN                                0000000
C                                                    0000000
C*****0000000
C                                                    0000000
C                                                    0000000
C      A COMPUTER PROGRAM FOR DATA REDUCTION OF FIVE-HOLE PITOT 0000000
C      MEASUREMENTS IN TURBULENT, SWIRLING, RECIRCULATING FLOW 0000000
C      IN COMBUSTOR GEOMETRIES                                0000000
C                                                    0000000
C      MODIFIED VERSION FOR INTERACTIVE USE ON CYCLONE FACILITY 0000000
C      MAY, 1988                                             0000000
C                                                    0000000
C      MODIFICATIONS INCLUDE COMBINED RADIAL AND AZIMUTHAL CAPA- 0000000
C      BILITY, REDUCTION OF STATIC PRESSURE DATA, AND CALCULATION 0000000
C      OF MOMENTUM FLUXES AND SWIRL NUMBERS FOR RADIAL PROFILES. 0000000
C                                                    0000000
C      BASED ON A PROGRAM BY D. L. RHODE (PHD THESIS, OSU, 1981) 0000000
C                                                    0000000
C                                                    0000000
C      FIRST MODIFICATION   : G. F. SANDER (MS THESIS, OSU, 1983) 0000000
C      SECOND MODIFICATION  : L. H. ONG (MS THESIS, OSU, 1985)   0000000
C      THIRD MODIFICATION   : C. B. MCMURRY (MS THESIS, OSU, 1985) 0000000
C      FORTH MODIFICATION   : W. D. CHAI AND G. EGHNEIM           0000000
C                                                    0000000
C                                                    (MS THESIS, OSU, 1988) 0000000
C                                                    0000000
C      MECHANICAL AND AEROSPACE ENGINEERING                   0000000
C      OKLAHOMA STATE UNIVERSITY                               0000000
C      STILLWATER, OK      74078                               0000000
C                                                    0000000
C*****0000000
C---MAJOR FORTRAN VARIABLES IN MAIN PROGRAM (LISTED IN ORDER 0000000
C      OF FIRST OCCURRENCE IN THE PROGRAM):                   0000000
C                                                    0000000
C      C IWRITE - LOGICAL FLAG FOR WRITING INTO OUTPUT DATASET (UNFORMATTED) 0000000
C      C DIAGNS - FLAG FOR DIAGNOSTIC OUTPUT                   0000000
C      C IT - MAX NO. OF TRAVERSES ALLOWED; DIMENSION VALUE IN SUBROUTINES 0000000
C      C JT - MAX NO. OF POINTS ALLOWED PER TRAVERSE; ALSO DIMENSION VALUE 0000000
C      C HEDM ETC. - ALL VARIABLES STARTING WITH "HED" ARE ALPHANUMERIC ARRAYS 0000000
C      FOR OUTPUT HEADINGS                                     0000000
C      C NCAL - NO. OF CALIBRATION DATA POINTS                0000000
C      C CPITCH - CALIBRATION PITCH COEFF. -- (PN-PS)/(PC-PW) 0000000
C      C CDELTA - CAL. PITCH ANGLE -- STANDARD RANGE -58 TO +58 DEG. 0000000
C      C CVELCF - CAL. VELOCITY COEFF. -- (CAL. DYN. PRESS.)/(PC-PW) 0000000
C      C CPSTCF - CAL. STATIC PRESSURE COEFF. -- (PC-PA)/(PC-PW) 0000000
C      C HEDID1,HEDID2 - USER HEADINGS TO IDENTIFY THE RUN BEING REDUCED 0000000
C      C ALPHA - INLET SIDEWALL EXPANSION ANGLE                0000000
C      C PHI - SWIRL VANE ANGLE SETTING                        0000000
C      C DSINCH - INLET NOZZLE OR SWIRLER DIAMETER, DSMALL, IN INCHES 0000000
C      C DLINCH - TEST SECTION DIAMETER, DLARGE, INCHES       0000000
C      C AAFR - AXIAL AIR FLOW RATE,CFM                        0000000
C      C TAFR - TANGENTIAL AIR FLOW RATE,CFM                  0000000
C      C KRADTR - INTEGER FLAG FOR TRAVERSE TYPE -- 1 FOR RADIAL, 0 FOR AZIM. 0000000
C      C NSTATN - NO. OF TRAVERSES TO BE REDUCES              0000000
C      C MAXJPT - MAX NO. OF POINTS IN ANY OF THE TRAVERSES BEING REDUCED 0000000
C      C XINCHS - AXIAL POSITION OF EACH TRAVERSE, INCHES      0000000
C      C NDATA - NO. OF DATAPOINTS IN EACH TRAVERSE          0000000
C      C RDNPRS - INLET DYNAMIC PRESSURE (UPSTREAM OF SWIRLER), TORR 0000000
C      C PREF - REF. PRESS. USED TO CALC. PDIFF FOR SWIRL NUMBER, TORR 0000000

```

```

C FANSPD - FAN SPEED, RPM 0000000
C TFLOW - TEMPERATURE OF AIR IN TEST SECTION, DEG. CELSIUS 0000000
C PATM - ATMOSPHERIC PRESSURE, TORR 0000000
C BZOFF - BETA ZERO-OFFSET FOR YAW ANGLE READINGS 0000000
C RINCHS - RADIAL POS. OF DATAPPOINT, INCHES (THETA FOR AZIM. TRAVERSES) 0000000
C RBETA - RAW VALUE OF YAW ANGLE BETA, DEG. 0000000
C RPNMPS - MEAS. VALUE OF PNORTH - PSOUTH PRESS. DIFF, TORR 0000000
C RPCMPW - MEAS. VALUE OF PCENTER - PWEST, TORR 0000000
C RPCMPA - MEAS. VALUE OF PCENTER - PATMOSPHERE, TORR 0000000
C RSMALL - INLET NOZZLE OR SWIRLER RADIUS, METERS 0000000
C RLARGE - TEST SECTION RADIUS, METERS 0000000
C X - AXIAL POSITION OF TRAVERSE, METERS 0000000
C R - RADIAL POSITION OF DATAPPOINT, METERS 0000000
C IDID - FLAG TO USE ENTRY POINT SP IN SPLINE INTERPOLATION ROUTINE 0000000
C PICHCF - REDUCED PITCH COEFF. FOR EACH DATAPPOINT 0000000
C DELTA - REDUCED PITCH ANGLE FOUND BY INTERPOLATION USING PICHCF 0000000
C VELCF - REDUCED VELOCITY COEFF. FROM INTERPOLATION USING DELTA 0000000
C PSTCF - REDUCED STATIC PRESS. COEFF. FROM INTERPOLATION USING DELTA 0000000
C RHO - DENSITY FOR EACH TRAVERSE, FROM IDEAL-GAS LAW 0000000
C BETA - REDUCED VALUE FOR PROBE YAW ANGLE, DEG. 0000000
C VTOTAL - TOTAL VELOCITY VECTOR MAGNITUDE, M/S 0000000
C U - AXIAL COMPONENT OF VELOCITY, M/S 0000000
C V - RADIAL COMP. OF VELOCITY, M/S 0000000
C W - TANGENTIAL (SWIRL) VELOCITY, M/S 0000000
C P - REDUCED VALUE OF STATIC PRESSURE, N/SQ. M (GAGE) 0000000
C XND - NONDIMENSIONAL AXIAL POSITION, X/DLARGE 0000000
C UIN - INLET REFERENCE VELOCITY (CALC. FROM RDNPRS), M/S 0000000
C MASFLO - INLET MASS FLOW RATE (ASSUMING UNIFORM AXIAL VELOCITY), KG/S 0000000
C VTSTAR - NONDIM. TOTAL VELOCITY MAGNITUDE, VTOTAL/UIN 0000000
C USTAR - NONDIM. AXIAL VELOCITY, U/UIN 0000000
C VSTAR - NONDIM. RADIAL VELOCITY, V/UIN 0000000
C WSTAR - NONDIM. TANGENTIAL VEL., W/UIN 0000000
C PSTAR - NONDIM. STATIC PRESSURE, P/RDNPRS 0000000
C RND - NONDIM. RADIAL POS., R/DLARGE; ALSO THETA FOR AZIM. TRAVERSES 0000000
C DYPS - "DELTA-Y, POINT-SOUTH" (FOR RADIAL INTEGRATION; FROM STARPIC) 0000000
C DYNP - "DELTA-Y, NORTH-POINT" (SIM. TO DYPS) 0000000
C SNS - "SMALL NORTH-SOUTH" FROM STARPIC; USED AS DELTA-R FOR INTEGR. 0000000
C PDIFF - PRESS. DIFF. P - PREF USED TO CALCULATE SWIRL NUMBER, N/SQ. M 0000000
C AREA1 - AREA OF DISC ELEMENT AT CENTER OF INTEGRATION REGION 0000000
C FLOW - SUMMATION FOR MASS FLOW THROUGH RING ELEMENTS 0000000
C WMOM - SUMMATION FOR ANGULAR MOMENTUM FLUX 0000000
C U MOM - SUMMATION FOR DYNAMIC AXIAL MOM. FLUX (NEGL. PRESS. TERM) 0000000
C U MOMP - SUMMATION FOR AXIAL MOMENTUM FLUX, INCL. PRESSURE DIFF. TERM 0000000
C AREAJ - AREA OF EACH RING ELEMENT, SQ. M 0000000
C MASS - INTEGRATED MASS FLOW RATE, KG/S 0000000
C UMEAN - INTEGRATED MEAN AXIAL VELOCITY, M/S 0000000
C AXGMOM - INTEGRATED AXIAL FLUX OF ANGULAR MOMENTUM, N-M 0000000
C AXMOM - INT. AXIAL FLUX OF DYNAMIC AXIAL MOM., N (NEGL. PRESS. TERM) 0000000
C AXMOMP - INT. AXIAL FLUX OF AXIAL MOMENTUM, N (INCL. PRESSURE TERM) 0000000
C SPRIME - SWIRL NUMBER CALC. USING DYNAMIC AXIAL MOMENTUM FLUX 0000000
C S - SWIRL NUMBER CALC. USING FULL AXIAL MOM. FLUX (INCL. PRESS.) 0000000
C USTAVG - AVERAGE OF USTAR VALUES FOR AZIM. TRAV., OVER ONE BLADE SPACE 0000000
C VSTAVG - AVG. OF VSTAR VALUES 0000000
C WSTAVG - AVG. OF WSTAR VALUES 0000000
C PDFAVG - AVG. OF PDIFF VALUES 0000000
C VISCOS - LAMINAR ABS. VISCOSITY CALCULATED FOR EACH TRAVERSE, KG/M*S 0000000
C REDIN - INLET REYNOLDS NUMBER, CALC. USING VISCOSITY FOR EACH TRAV. 0000000
C 0000000
C 0000000
C *****0000000
CHAPTER 0 0 0 0 0 0 0 0 PRELIMINARIES 0 0 0 0 0 0 0 0 0000000
C 0000000
    DIMENSION HEDM(9),HEDUMN(9),HEDNMS(9),HEDCMW(9),HEDCMA(9),
    #HEDU(9),HEDV(9),HEDW(9),HEDVT(9),HEDUST(9),
    #HEDVST(9),HEDWST(9),HEDPST(9),HEDDEL(9),HEDBET(9),
    #HEDMMF(9),HEDMIV(9),HEDMIP(9),HEDAM(9),
    0000000
    0000000
    0000000
    0000000
    0000000

```

```

#HEDAX(9),HEDAXP(9),HEDSPR(9),HEDS(9),HEDP(9),HEDPDF(9),HEDRED(9), 0000000
#HEDID1(18),HEDID2(18),HEDUSA(9),HEDVSA(9),HEDWSA(9),HEDPDA(9), 0000000
#HEDFAN(9),HEDTFL(9),HEDPAT(9),HEDRHO(9),HEDVIS(9),HEDCAL(9) 0000000
C 0000000
C 0000000
COMMON 0000000
#/CALIB/CPITCH(26),CDELTA(26),CVELCF(26),CPSTCF(26) 0000000
#/MEASUR/RBETA(8,24),RPNMPS(8,24),RPCMPW(8,24),RPCMPA(8,24), 0000000
#  NDATA(8),MAXJPT,RDNPRS(8), 0000000
#  FANSPD(8),TFLOW(8),PATM(8),BZOFF(8) 0000000
#/GEOM/X(8),R(24),XND(8),RND(24),DYPS(24),DYNP(24), 0000000
#  SNS(24),NSTATN,XINCHS(8),RINCHS(24) 0000000
#/CALC/VTOTAL(8,24),U(8,24),V(8,24),W(8,24),P(8,24), 0000000
#  VTSTAR(8,24),USTAR(8,24),VSTAR(8,24),WSTAR(8,24), 0000000
#  PICHCF(8,24),VELCF(8,24),DELTA(8,24),BETA(8,24), 0000000
#  ANGMOM(8),UMEAN(8),UIN(8),RMASS(8),RMASFL(8), 0000000
#  PSTAR(8,24),PSTCF(8,24),AXMOM(8),AXMOMP(8), 0000000
#  SPRIME(8),S(8),REDIN(8),FREF(8),RHO(8),VISCOS(8), 0000000
#  USTAVG(8,24),VSTAVG(8,24),WSTAVG(8,24),PSTAVG(8,24) 0000000
#/OUTPUT/STORE(8) 0000000
C 0000000
LOGICAL IWRITE,DIAGNS 0000000
C 0000000
C---SET IWRITE=.TRUE. FOR WRITING SOLN. ON DISK STORAGE; 0000000
C SET DIAGNS=.TRUE. TO ACTIVATE DIAGNOSTIC WRITE STATEMENTS 0000000
C 0000000
IWRITE=.TRUE. 0000000
DIAGNS=.TRUE. 0000000
IT=8 0000000
JT=24 0000000
C 0000000
C---READ CHARACTER DATA FOR HEADINGS USED BY SUBROUTINES 0000000
C WRITE AND PRINT (ALSO CALIBRATION HEADING) 0000000
C 0000000
READ(7,205) HEDM,HEDUMN,HEDU,HEDV,HEDW, 0000000
#  HEDVT,HEDUST,HEDVST,HEDWST,HEDPST,HEDEL,HEDBET, 0000000
#  HEDNMS,HEDCMW,HEDCMA,HEDMMF,HEDMIV,HEDMIP,HEDAM, 0000000
#  HEDAX,HEDAXP,HEDSPR,HEDS,HEDP,HEDPDF,HEDRED, 0000000
#  HEDFAN,HEDTFL,HEDPAT,HEDRHO,HEDVIS, 0000000
#  HEDUSA,HEDVSA,HEDWSA,HEDPDA,HEDCAL 0000000
205 FORMAT(9A4) 0000000
C 0000000
C-----INITIALIZE VARIABLES TO ZERO 0000000
C 0000000
CALL INIT 0000000
C 0000000
C-----READ FIVE-HOLE PITOT CALIBRATION DATA 0000000
C 0000000
NCAL=25 0000000
DO 10 I=1,NCAL 0000000
READ(7,210) CPITCH(I),CDELTA(I),CVELCF(I),CPSTCF(I) 0000000
10 CONTINUE 0000000
210 FORMAT(4F10.5) 0000000
IF(DIAGNS) WRITE(8,400) (CPITCH(I),I=1,25) 0000000
IF(DIAGNS) WRITE(8,400) (CDELTA(I),I=1,25) 0000000
IF(DIAGNS) WRITE(8,400) (CVELCF(I),I=1,25) 0000000
IF(DIAGNS) WRITE(8,400) (CPSTCF(I),I=1,25) 0000000
400 FORMAT(///,1X,13(F8.4,1X),//,5X,12(F8.4)) 0000000
C 0000000
C---READ RAW MEASURED DATA TO BE REDUCED 0000000
C 0000000
READ(7,215) HEDID1,HEDID2 0000000
215 FORMAT(18A4) 0000000
READ(7,216) ALPHA,PHI,DSINCH,DLINCH,AAFR,TAFR 0000000
216 FORMAT(6F10.5) 0000000
READ(7,217) KRADTR,NSTATN,MAXJPT 0000000

```

```

217 FORMAT(3I10)
DO 30 I=1,NSTATN
READ(7,230) XINCHS(I),NDATA(I),RDNPRS(I),PREF(I)
READ(7,216) FANSPD(I),TFLOW(I),PATM(I),BZOFF(I)
JPTS=NDATA(I)
DO 20 J=1,JPTS
READ(7,220) RINCHS(J),RBETA(I,J),RPNMPS(I,J),RPCMPW(I,J),
# RPCMPA(I,J)
20 CONTINUE
30 CONTINUE
C
C-----CONVERT X'S AND R'S FROM INCHES TO METERS
C
RSMALL=DSINCH*0.0254/2.0
RLARGE=DLINCH*0.0254/2.0
DO 35 I=1,NSTATN
X(I)=XINCHS(I)*0.0254
JPTS=NDATA(I)
DO 32 J=1,JPTS
R(J)=RINCHS(J)*0.0254
32 CONTINUE
35 CONTINUE
220 FORMAT(7F10.5)
230 FORMAT(1F10.5,1I10,2F10.5)
IF(DIAGNS) WRITE(8,470) (NDATA(I),I=1,NSTATN)
IF(DIAGNS) WRITE(8,450) (X(I),I=1,NSTATN)
IF(DIAGNS) WRITE(8,500) (R(J),J=1,JPTS)
DO 37 I=1,NSTATN
IF(DIAGNS) WRITE(8,500) (RBETA(I,J),J=1,JPTS)
IF(DIAGNS) WRITE(8,500) (RPNMPS(I,J),J=1,JPTS)
IF(DIAGNS) WRITE(8,500) (RPCMPW(I,J),J=1,JPTS)
IF(DIAGNS) WRITE(8,500) (RPCMPA(I,J),J=1,JPTS)
37 CONTINUE
450 FORMAT(/,40X,1(F8.4,1X))
470 FORMAT(///,40X,1(I8,1X))
500 FORMAT(///,20X,10(F8.4))
C
CHAPTER 1 1 1 1 1 DATA REDUCTION 1 1 1 1 1 1
C
C-----CALC PICHCF AND INTERPOLATE FOR DELTA FROM
C----- PITOT CALIBRATION CURVE
C
IDID=0
DO 50 I=1,NSTATN
JPTS=NDATA(I)
DO 40 J=1,JPTS
IF((RPCMPW(I,J).EQ.0.0).AND.(RPNMPS(I,J).EQ.0.0)) GO TO 38
PICHCF(I,J)=RPNMPS(I,J)/(RPCMPW(I,J)+1.E-6)
IF((PICHCF(I,J).GT.2.544).OR.(PICHCF(I,J).LT.-3.769)) GO TO 38
IF(IDID.EQ.0) DELTA(I,J)=SPLINE(CPITCH,
# CDELTA,NCAL,PICHCF(I,J),IDID)
IF(IDID.GT.0) DELTA(I,J)=SPLINE(CPITCH,CDELTA,
# NCAL,PICHCF(I,J),IDID)
IDID=1
GO TO 40
38 CONTINUE
DELTA(I,J)=0.0
WRITE(8,850) I,J
850 FORMAT(20X,'PICHCF IS OUT OF RANGE OF CALIBRATION AT I=
# ',I3,' AND J=',I3)
40 CONTINUE
50 CONTINUE
C
C-----INTERPOLATE FOR VELCF AND PSTCF FROM PITOT CALIBRATION DATA
C
IDID=0

```

```

DO 80 I=1,NSTATN                                0000000
  JPTS=NDATA(I)                                  0000000
  DO 70 J=1,JPTS                                  0000000
    IF((RPCMPW(I,J).EQ.O.O).AND.(RPNMPS(I,J).EQ.O.O)) GO TO 65 0000000
    IF((ABS(DELTA(I,J))) .GT. 58.O) GO TO 65      0000000
    IF(IDID .EQ. O) VELCF(I,J)=SPLINE(CDELTA,    0000000
#     CVELCF,NCAL,DELTA(I,J),IDID)              0000000
    IF(IDID .GT. O) VELCF(I,J)=SPLINE(CDELTA,CVELCF, 0000000
#     NCAL,DELTA(I,J),IDID)                    0000000
    IF(IDID .EQ. O) PSTCF(I,J)=SPLINE(CDELTA,    0000000
#     CPSTCF,NCAL,DELTA(I,J),IDID)            0000000
    IF(IDID .GT. O) PSTCF(I,J)=SPLINE(CDELTA,CPSTCF, 0000000
#     NCAL,DELTA(I,J),IDID)                  0000000
    IDID=1                                         0000000
    GO TO 70                                       0000000
65  CONTINUE                                       0000000
    VELCF(I,J)=O.O                                0000000
    PSTCF(I,J)=O.O                                0000000
    WRITE(8,890) I,J                              0000000
890  FORMAT(20X,'DELTA IS OUT OF RANGE OF CALIBRATION DATA 0000000
#        AT I=',I3,' AND J=',I3)                0000000
70  CONTINUE                                       0000000
80  CONTINUE                                       0000000
C
  DO 85 I=1,NSTATN                                0000000
    IF(DIAGNS) WRITE(8,500) (PICHCF(I,J),J=1,JPTS) 0000000
    IF(DIAGNS) WRITE(8,500) (DELTA(I,J),J=1,JPTS) 0000000
    IF(DIAGNS) WRITE(8,500) (VELCF(I,J),J=1,JPTS) 0000000
    IF(DIAGNS) WRITE(8,500) (PSTCF(I,J),J=1,JPTS) 0000000
85  CONTINUE                                       0000000
C
C-----CALC MAGNITUDE OF TOTAL MEAN VELOCITY VECTOR,      0000000
C-----      U, V, & W COMPONENTS, AND STATIC PRESSURE 0000000
C
  PI=3.14159                                       0000000
  DO 100 I=1,NSTATN                                0000000
    RHO(I)=PATM(I)*(133.33)/(286.94*(TFLOW(I)+273.15)) 0000000
    JPTS=NDATA(I)                                  0000000
    DO 90 J=1,JPTS                                  0000000
      BETA(I,J)=360.+BZOFF(I)-RBETA(I,J)          0000000
      IF((RPCMPW(I,J).EQ.O.O).AND.(RPNMPS(I,J).EQ.O.O))BETA(I,J)=O.00000000
      VTOTAL(I,J)=SQRT(ABS(2.O/RHO(I)*VELCF(I,J)*RPCMPW(I,J)*133.9))0000000
      U(I,J)=VTOTAL(I,J) * COS(DELTA(I,J)*PI/180.O) * 0000000
#     COS(BETA(I,J)*PI/180.O)                    0000000
      V(I,J)=VTOTAL(I,J) * SIN(DELTA(I,J)*PI/180.O) 0000000
#     W(I,J)=VTOTAL(I,J) * COS(DELTA(I,J)*PI/180.O) * 0000000
#     SIN(BETA(I,J)*PI/180.O)                  0000000
      P(I,J)=(RPCMPA(I,J)-PSTCF(I,J)*RPCMPW(I,J))*133.33 0000000
90  CONTINUE                                       0000000
100 CONTINUE                                       0000000
    IF(DIAGNS) WRITE(8,500)(VTOTAL(I,J),J=1,JPTS) 0000000
    IF(DIAGNS) WRITE(8,500)(U(I,J),J=1,JPTS)      0000000
    IF(DIAGNS) WRITE(8,500)(V(I,J),J=1,JPTS)      0000000
    IF(DIAGNS) WRITE(8,500)(W(I,J),J=1,JPTS)      0000000
    IF(DIAGNS) WRITE(8,500)(P(I,J),J=1,JPTS)      0000000
C
CHAPTER 2 2 2 2 2 2 AUXILIARY CALCULATIONS 2 2 2 2 2 0000000
C
C-----NONDIMENSIONALIZE LENGTHS AND VELOCITIES          0000000
C
  DO 150 I=1,NSTATN                                0000000
    XND(I)=X(I)/(2.O*RLARGE)                      0000000
    JPTS=NDATA(I)                                  0000000
    UIN(I)=AAFR*4.7195/(10000.O * PI * RSMALL**2) 0000000
    UAV=(AAFR+TAFR)*4.7195/(10000.O * PI *RLARGE**2) 0000000
    RMAFL(I)=PI*RHO(I)*UIN(I)*RSMALL**2          0000000

```

```

IF(DIAGNS) WRITE(8,450) (JIN(II),II=1,NSTATN)
IF(DIAGNS) WRITE(8,450) (RMASFL(II),II=1,NSTATN)
  DO 140 J=1,JPTS
    VTSTAR(I,J)=VTOTAL(I,J)/UAV
    USTAR(I,J)=U(I,J)/UAV
    VSTAR(I,J)=V(I,J)/UAV
    WSTAR(I,J)=W(I,J)/UAV
    PSTAR(I,J)=P(I,J)/(RDNPRS(I)*133.33)
140  CONTINUE
150  CONTINUE
    DO 160 J=1,MAXJPT
      RND(J)=R(J)/(2.0*RLARGE)
      IF(KRADTR.EQ.O) RND(J)=RINCHS(J)
      IF(KRADTR.EQ.O) R(J)=RINCHS(J)
160  CONTINUE
C
      IF(KRADTR.EQ.O) GO TO 135
C
C---FOR RADIAL PROFILES: NUMERICAL INTEGRATION TO CALC. MASS
C FLOW AND MOMENTUM FLUXES FOR SWIRL NUMBER
C
C FOR PROFILES AT AND UPSTREAM OF EXPANSION CORNER, RSMALL
C IS USED IN EXPRESSIONS FOR DYNP AND UMEAN; DOWNSTREAM OF
C EXPANSION, RLARGE IS USED.
C
    DO 130 I=1,NSTATN
      JPTS=NDATA(I)
      JPTSM1=JPTS-1
      PREF(I)=P(I,JPTS)
      DYPS(1)=0.0
      DYNP(JPTS)=2.0*(RSMALL-R(JPTS))
C
      DO 110 J=1,JPTSM1
        DYNP(J)=R(J+1)-R(J)
        DYPS(J+1)=DYNP(J)
110  CONTINUE
      DO 115 J=1,JPTS
        SNS(J)=0.5*(DYNP(J)+DYPS(J))
        PSTAR(I,J)=P(I,J)-PREF(I)
115  CONTINUE
C
C----INNER 3 (HUB) VALUES OF PSTAR SET TO ZERO FOR SWIRLER
C EXIT-PLANE PROFILES: FOR DOWNSTREAM PROFILES, MAKE THESE
C STATEMENTS COMMENTS.
C
C      PSTAR(I,1)=0.0
C      PSTAR(I,2)=0.0
C      PSTAR(I,3)=0.0
C
IF(DIAGNS) WRITE(8,500) (DYNP(J),J=1,JPTS)
IF(DIAGNS) WRITE(8,500) (SNS(J),J=1,JPTS)
AREA1=PI*SNS(1)**2
ARSUM=AREA1
FLOW=RHO(I)*U(I,1)*AREA1
WMOM=W(I,1)*R(2)/4.*FLOW
UMOM=U(I,1)*FLOW
UMOMP=(RHO(I)*U(I,1)**2+PSTAR(I,1))*AREA1
IF(DIAGNS) WRITE(8,2030) AREA1,ARSUM, FLOW, WMOM, UMOM, UMOMP
DO 120 J=2,JPTS
  AREAJ=2.*PI*R(J)*SNS(J)
  ARSUM=ARSUM+AREAJ
  FLOW=FLOW+RHO(I)*U(I,J)*AREAJ
  UMOM=UMOM+RHO(I)*U(I,J)**2*AREAJ
  UMOMP=UMOMP+(RHO(I)*U(I,J)**2+PSTAR(I,J))*AREAJ
  WMOM=WMOM+RHO(I)*U(I,J)*W(I,J)*R(J)*AREAJ
IF(DIAGNS) WRITE(8,2040) AREAJ,ARSUM, FLOW, WMOM, UMOM, UMOMP

```

```

120  CONTINUE                                0000000
      RMASS(I)=FLOW                          0000000
      UMEAN(I)=RMASS(I)/(RHO(I)*PI*RSMALL**2) 0000000
      ANGMOM(I)=WMOM                          0000000
      AXMOM(I)=UMOM                           0000000
      AXMOMP(I)=UMOMP                          0000000
      IF(DIAGNS) WRITE(8,2050) UMEAN(I),RMASS(I),ANGMOM(I),AXMOM(I),
#      AXMOMP(I)                               0000000
C
2030  FORMAT(/4X,'AREAJ',5X,'ARSUM',5X,'FLOW',6X,'WMOM',6X,
#      'UMOM',6X,'UMOMP'/'/'',6E10.3)         0000000
2040  FORMAT(' ',6E10.3)                     0000000
2050  FORMAT(/14X,'UMEAN',5X,'MASS',6X,'ANGMOM',4X,'AXMOM',
#      5X,'AXMOMP'/'/'',11X,5E10.3)         0000000
C
      SPRIME(I)=ANGMOM(I)/(AXMOM(I)*RSMALL)   0000000
      S(I)=ANGMOM(I)/(AXMOMP(I)*RSMALL)       0000000
130  CONTINUE                                0000000
      IF(DIAGNS) WRITE(8,450) (UMEAN(I),I=1,NSTATN) 0000000
      IF(DIAGNS) WRITE(8,450) (RMASS(I),I=1,NSTATN) 0000000
      IF(DIAGNS) WRITE(8,450) (ANGMOM(I),I=1,NSTATN) 0000000
      IF(DIAGNS) WRITE(8,450) (AXMOM(I),I=1,NSTATN) 0000000
      IF(DIAGNS) WRITE(8,450) (AXMOMP(I),I=1,NSTATN) 0000000
      IF(DIAGNS) WRITE(8,450) (SPRIME(I),I=1,NSTATN) 0000000
      IF(DIAGNS) WRITE(8,450) (S(I),I=1,NSTATN)     0000000
135  CONTINUE                                0000000
C
      IF(KRADTR.EQ.1) GO TO 180                0000000
C---FOR AZIMUTHAL TRAVERSES:  CALC. PSTAR=(P-PREF) USING SUPPLIED
C  VALUES OF PREF(I).                        0000000
C
      DO 178 I=1,NSTATN                        0000000
        JPTS=NDATA(I)                          0000000
        DO 177 J=1,JPTS                        0000000
          PSTAR(I,J)=P(I,J)-PREF(I)*133.33     0000000
177  CONTINUE                                0000000
178  CONTINUE                                0000000
C
C---CALC. AVERAGE VALUES FOR AZIMUTHAL TRAVERSES -- NREP IS NO. OF
C  POINTS IN REPEATING CYCLE ACROSS ONE BLADE; NAVE IS NO. OF
C  AVERAGES POSSIBLE CONTAINING NREP CONSECUTIVE POINTS.
C
      NREP=6                                    0000000
      DO 180 I=1,NSTATN                        0000000
        NAVE=NDATA(I)-NREP+1                   0000000
        DO 175 K=1,NAVE                        0000000
          NAVEND=K+NREP-1                      0000000
          USUM=0.                               0000000
          VSUM=0.                               0000000
          WSUM=0.                               0000000
          PSUM=0.                               0000000
          DO 174 J=K,NAVEND                    0000000
            USUM=USUM+USTAR(I,J)               0000000
            VSUM=VSUM+VSTAR(I,J)               0000000
            WSUM=WSUM+WSTAR(I,J)               0000000
            PSUM=PSUM+PSTAR(I,J)               0000000
174  CONTINUE                                0000000
          USTAVG(I,K)=USUM/NREP                 0000000
          VSTAVG(I,K)=VSUM/NREP                 0000000
          WSTAVG(I,K)=WSUM/NREP                 0000000
          PSTAVG(I,K)=PSUM/NREP                 0000000
175  CONTINUE                                0000000
180  CONTINUE                                0000000
C
C---CALCULATE VISCOSITY AND INLET REYNOLDS NUMBER (BOTH TRAVERSE TYPES)
C

```



```

C---VISCOSITY FORMULA FROM LAN & ROSKAM, AIRPLANE AERODYNAMICS      000000
C & PERFORMANCE, P.42.                                             000000
C                                                                      000000
C      DO 162 I=1,NSTATN                                           000000
C          DENOM=TFLOW(I)+273.15+110.4                             000000
C          VISCOS(I)=(1.458E-06)*(TFLOW(I)+273.15)**1.5/DENOM     000000
C          REDIN(I)=UIN(I)*2.*RSMALL*RHO(I)/VISCOS(I)              000000
C      162 CONTINUE                                                000000
C                                                                      000000
CHAPTER 3 3 3 3 3 OUTPUT 3 3 3 3 3 3 3                             000000
C                                                                      000000
C      IF(.NOT. IWRITE) GO TO 165                                  000000
C      DO 168 I=1,NSTATN                                           000000
C          WRITE(11,163) XINCHS(I)                                 000000
C          WRITE(11,163) UIN(I)                                   000000
C          WRITE(11,163) PREF(I)                                  000000
C          DO 168 J=1,MAXJPT                                       000000
C              WRITE(11,166) RINCHS(J), USTAR(I,J), VSTAR(I,J),   000000
C              & BETA(I,J), DELTA(I,J), PSTAR(I,J)                000000
C          WRITE(11,163) RINCHS                                   000000
C          WRITE(11,163) USTAR                                    000000
C          WRITE(11,163) VSTAR                                    000000
C          WRITE(11,163) WSTAR                                    000000
C          WRITE(11,163) BETA                                     000000
C          WRITE(11,163) DELTA                                   000000
C          WRITE(11,163) PSTAR                                    000000
C      163 FORMAT(E10.3)                                           000000
C      166 FORMAT(7E10.3)                                          000000
C      168 CONTINUE                                                000000
C                                                                      000000
C      165 CONTINUE                                                000000
C          WRITE(8,311)                                             000000
C          WRITE(8,312) HEDID1,HEDID2,HEDCAL                      000000
C          WRITE(8,325) ALPHA                                       000000
C          WRITE(8,330) PHI                                           000000
C          WRITE(8,335) RSMALL                                       000000
C          WRITE(8,340) RLARGE                                       000000
C          CALL WRITE(1,1,NSTATN,1,IT,JT,XINCHS,RINCHS,FANSPD,HEDFAN) 000000
C          CALL WRITE(1,1,NSTATN,1,IT,JT,XINCHS,RINCHS,TFLOW,HEDTFL) 000000
C          CALL WRITE(1,1,NSTATN,1,IT,JT,XINCHS,RINCHS,PATM,HEDPAT) 000000
C          CALL WRITE(1,1,NSTATN,1,IT,JT,XINCHS,RINCHS,RHO,HEDRHO) 000000
C          CALL WRITE(1,1,NSTATN,1,IT,JT,XINCHS,RINCHS,VISCOS,HEDVIS) 000000
C          CALL WRITE(1,1,NSTATN,1,IT,JT,XINCHS,RINCHS,RDNPRS,HEDMIP) 000000
C          CALL WRITE(1,1,NSTATN,1,IT,JT,X,R,UIN,HEDMIV)           000000
C          CALL WRITE(1,1,NSTATN,1,IT,JT,X,R,RMASFL,HEDMMF)        000000
C          CALL WRITE(1,1,NSTATN,1,IT,JT,X,R,REDIN,HEDRED)         000000
C                                                                      000000
C          IF(KRADTR.EQ.0) GO TO 170                                000000
C          CALL WRITE(1,1,NSTATN,1,IT,JT,X,R,RMASS,HEDM)           000000
C          CALL WRITE(1,1,NSTATN,1,IT,JT,X,R,UMEAN,HEDUMN)         000000
C          CALL WRITE(1,1,NSTATN,1,IT,JT,X,R,ANGMOM,HEDAM)         000000
C          CALL WRITE(1,1,NSTATN,1,IT,JT,X,R,AXMOMP,HEDAXP)        000000
C          CALL WRITE(1,1,NSTATN,1,IT,JT,X,R,AXMOM,HEDAX)         000000
C          CALL WRITE(1,1,NSTATN,1,IT,JT,X,R,S,HEDS)              000000
C          CALL WRITE(1,1,NSTATN,1,IT,JT,X,R,SPRIME,HEDSPR)        000000
C                                                                      000000
C      170 CONTINUE                                                000000
C          CALL PRINT(1,1,NSTATN,MAXJPT,IT,JT,X,R,U,HEDU)          000000
C          CALL PRINT(1,1,NSTATN,MAXJPT,IT,JT,X,R,V,HEDV)          000000
C          CALL PRINT(1,1,NSTATN,MAXJPT,IT,JT,X,R,W,HEDW)          000000
C          CALL PRINT(1,1,NSTATN,MAXJPT,IT,JT,X,R,P,HEDP)          000000
C          CALL PRINT(1,1,NSTATN,MAXJPT,IT,JT,X,R,DELTA,HEDDEL)    000000
C          CALL PRINT(1,1,NSTATN,MAXJPT,IT,JT,X,R,BETA,HEDBET)    000000
C          CALL PRINT(1,1,NSTATN,MAXJPT,IT,JT,X,R,VTOTAL,HEDVT)    000000
C          CALL PRINT(1,1,NSTATN,MAXJPT,IT,JT,XND,RND,USTAR,HEDUST) 000000
C          CALL PRINT(1,1,NSTATN,MAXJPT,IT,JT,XND,RND,VSTAR,HEDVST) 000000

```



```

RPNMPS(I,J)=0.0      0000000
RPCMPW(I,J)=0.0      0000000
RPCMPA(I,J)=0.0      0000000
PICHCF(I,J)=0.0      0000000
VELCF(I,J)=0.0       0000000
PSTCF(I,J)=0.0       0000000
DELTA(I,J)=0.0       0000000
USTAVG(I,J)=0.0      0000000
VSTAVG(I,J)=0.0      0000000
WSTAVG(I,J)=0.0      0000000
PSTAVG(I,J)=0.0      0000000
10  CONTINUE          0000000
20  CONTINUE          0000000
    RETURN            0000000
    END                0000000
C                      0000000
    FUNCTION SPLINE(X, FX, N, X1, IDID) 0000000
C*****                0000000
C    CUBIC SPLINE CURVE FITTING IN 2 DIMENSIONAL DATA PLANE 0000000
C    INPUT VALUES : 0000000
C    X, FX      DATA ARRAYS, ONE DIMENSIONAL, X IN INCREASING ORDER 0000000
C    N          NUMBER OF DATA POINTS IN X, MAX 26 0000000
C    X1         POINT OF INTEREST, WHERE F(X1) IS TO BE FOUND 0000000
C                      0000000
C    RETURN VALUE : 0000000
C    SPLINE = F(X1) 0000000
C    THIS ROUTINE ACTIVATES ROUTINE ABUILD, H, AND GAUSS. 0000000
C    FOR INTERPOLATION OF A LARGE NUMBER OF DATA POINTS, FUNCTION 0000000
C    SPLINE MAY BE CALLED ONLY ONCE , AND SUBSEQUENT CALLS MAY USE 0000000
C    ENTRY POINT AT STATEMENT 36. 0000000
C*****                0000000
    DIMENSION X(1), FX(1), A(26,27) 0000000
C                      0000000
C-----CONSTRUCT SPLINE MATRIX 0000000
C                      0000000
    IF (IDID .GT. 0)GO TO 36 0000000
    N1=N+1 0000000
    DO 10 I=1, N 0000000
        DO 10 J=1, N1 0000000
10      A(I,J)=0. 0000000
        M1=N-1 0000000
        DO 20 I=2, M1 0000000
20      CALL ABUILD(X, FX, A, N, I) 0000000
        A(1,1)=H(X,2) 0000000
        A(1,2)=-H(X,1)-H(X,2) 0000000
        A(1,3)=H(X,1) 0000000
        M2=N-2 0000000
        A(N,M2)=H(X,M1) 0000000
        A(N,M1)=-H(X,M2)-H(X,M1) 0000000
        A(N,N)=H(X,M2) 0000000
C                      0000000
C-----FIND SECOND DERIVATIVES 0000000
C                      0000000
    CALL GAUSS(A, N, N1) 0000000
C                      0000000
C-----FIND F(X1) 0000000
C                      0000000
36  CONTINUE 0000000
    DO 40 I=1, M1 0000000
        I1=I+1 0000000
        IF(X1 .EQ. X(I)) GO TO 50 0000000
        IF(X1 .LT. X(I) .AND. X1 .GT. X(I1)) GO TO 41 0000000
        IF(X1 .GT. X(I) .AND. X1 .LT. X(I1) ) GO TO 41 0000000
40  CONTINUE 0000000
    IF(X1 .EQ. X(N)) GO TO 60 0000000

```

```

WRITE(8, 42) X1
42  FORMAT(' X1=', G14.7, ' OUT OF INTERPOLATION RANGE, RETURNED VALUE' 000000
    *='0') 000000
    SPLINE=0. 000000
    STOP 000000
C 000000
41  CONTINUE 000000
    I1=I+1 000000
    HI=H(X,I) 000000
    HX=X(I1)-X1 000000
    HX2=X1-X(I) 000000
    FX1=HX**3/HI-HI*HX 000000
    FX1=FX1*A(I,N1) 000000
    STO=HX2**3/HI - HI*HX2 000000
    FX1=(FX1+STO*A(I1,N1) )/6. 000000
    SPLINE=(FX(I)*HX+FX(I1)*HX2)/HI+FX1 000000
    RETURN 000000
C 000000
50  CONTINUE 000000
    SPLINE=FX(I) 000000
    RETURN 000000
C 000000
60  CONTINUE 000000
    SPLINE=FX(N) 000000
    RETURN 000000
    END 000000
C 000000
    FUNCTION H(X,I) 000000
C***** 000000
C  CALCULATE DELTA X WHICH IS USUALLY CALLED H. 000000
C***** 000000
    DIMENSION X(1) 000000
    I1=I+1 000000
    H=X(I1)-X(I) 000000
    RETURN 000000
    END 000000
C 000000
    SUBROUTINE ABUILD(X, F, A, N, I) 000000
C***** 000000
C  CONSTRUCT SPLINE MATRIX FOR FINDING 2ND DERIVATIVES. 000000
C***** 000000
    DIMENSION X(1), F(1), A(26,27) 000000
    IM1=I-1 000000
    I1=I+1 000000
    N1=N+1 000000
    STO=H(X,I) 000000
    HIM1=H(X,IM1) 000000
    A(I,IM1)=HIM1 000000
    A(I,I)=2.*(HIM1+STO) 000000
    A(I,I1)=STO 000000
    A(I,N1)=( (F(I1)-F(I))/STO - (F(I)-F(IM1))/HIM1 ) *6. 000000
    RETURN 000000
    END 000000
C 000000
    SUBROUTINE GAUSS(A, K, M) 000000
C***** 000000
C  GAUSS-JORDAN ELIMINATION 000000
C***** 000000
    DIMENSION A(26,27) 000000
    M1=M-1 000000
    K1=K-1 000000
    DO 3 L=1, K1 000000
      L1=L+1 000000
      DO 3 I=L1, K 000000
        CONST=A(I,L)/A(L,L) 000000
        DO 3 J=L, M 000000

```

```

3      A(I,J)=A(I,J)-CONST*A(L,J)          0000000
DO 6 I=1, K1                               0000000
  I1=I+1                                    0000000
  DO 6 L=I1, M1                             0000000
    CONST=A(I,L)/A(L,L)                    0000000
    DO 6 J=I, M                             0000000
6      A(I,J)=A(I,J)-CONST*A(L,J)          0000000
DO 10 I=1, K                               0000000
  A(I,M)=A(I,M)/A(I,I)                    0000000
10     A(I,I)=1.                            0000000
      RETURN                                0000000
      END                                    0000000

C
C      SUBROUTINE PRINT(ISTART,JSTART,NI,NJ,IT,JT,X,Y,PHI,HEAD) 0000000
C*****0000000
C
C      DIMENSION PHI(IT,JT),X(IT),Y(JT),HEAD(9) 0000000
COMMON /OUTPUT/ STORE(8) 0000000
      ISKIP=1 0000000
      JSKIP=1 0000000
      WRITE(8,110)HEAD 0000000
      ISTA=ISTART-10 0000000
100    CONTINUE 0000000
      ISTA=ISTA+10 0000000
      IEND=ISTA+9 0000000
      IF(NI.LT.IEND)IEND=NI 0000000
      WRITE(8,111)(I,I=ISTA,IEND,ISKIP) 0000000
      WRITE(8,114)(X(I),I=ISTA,IEND,ISKIP) 0000000
      WRITE(8,112) 0000000
      DO 101 JJ=JSTART,NJ,JSKIP 0000000
        J=JSTART+NJ-JJ 0000000
        DO 120 I=ISTA,IEND 0000000
          A=PHI(I,J) 0000000
          IF(ABS(A).LT.1.E-20) A=0.0 0000000
120      STORE(I)=A 0000000
101    WRITE(8,113)J,Y(J),(STORE(I),I=ISTA,IEND,ISKIP) 0000000
      IF(IEND.LT.NI)GO TO 100 0000000
      RETURN 0000000
110    FORMAT(1HO,17(2H*-),7X,9A4,7X,17(2H-*)) 0000000
111    FORMAT(1HO,15H      I =      ,I2,9I11) 0000000
112    FORMAT(8HO J      Y) 0000000
113    FORMAT(I3,OPF8.4,1X,10(1X,E10.3)) 0000000
114    FORMAT(13H      X = ,F8.4,9F11.4) 0000000
      END 0000000

C
C      SUBROUTINE WRITE(ISTART,JSTART,NI,NJ,IT,JT,X,Y,PHI,HEAD) 0000000
C
C      COMMON /OUTPUT/ STORE(8) 0000000
DIMENSION PHI(IT),X(IT),Y(JT),HEAD(9) 0000000
      ISKIP=1 0000000
      JSKIP=1 0000000
      WRITE(8,110)HEAD 0000000
      ISTA=ISTART-12 0000000
100    CONTINUE 0000000
      ISTA=ISTA+12 0000000
      IEND=ISTA+11 0000000
      IF(NI.LT.IEND)IEND=NI 0000000
      WRITE(8,111)(I,I=ISTA,IEND,ISKIP) 0000000
      WRITE(8,114)(X(I),I=ISTA,IEND,ISKIP) 0000000
      DO 101 JJ=JSTART,NJ,JSKIP 0000000
        J=JSTART+NJ-JJ 0000000
        DO 120 I=ISTA,IEND 0000000
          A=PHI(I) 0000000
          IF(ABS(A).LT.1.E-20) A=0.0 0000000
120      STORE(I)=A 0000000
101    WRITE(8,113) (STORE(I),I=ISTA,IEND,ISKIP) 0000000

```

```
IF(IEND.LT.NI)GO TO 100
RETURN
110 FORMAT(1H0,17(2H*-),7X,9A4,7X,17(2H-*))
111 FORMAT(1H0,15H          I =          ,I2,9I11)
113 FORMAT(/12X,1P10E11.3)
114 FORMAT(13H          X = ,F8.4,9F11.4)
END
```

```
0000000
0000000
0000000
0000000
0000000
0000000
0000000
```

\*\*\*\* TSO FOREGROUND HARDCOPY \*\*\*\*  
 DSNNAME=U11316A.PI4126.DATA

COMPUTED MASS FLOW RATE (KG/S)	0000010
COMPUTED MEAN AXIAL VELOCITY (M/S)	0000020
U VELOCITY (M/S)	0000030
V VELOCITY (M/S)	0000040
W VELOCITY (M/S)	0000050
TOTAL VELOCITY MAGNITUDE (M/S)	0000060
DIMENSIONLESS U VELOCITY	0000070
DIMENSIONLESS V VELOCITY	0000080
DIMENSIONLESS W VELOCITY	0000090
DIMENSIONLESS STATIC PRESS. P/RDNPRS	0000100
PROBE PITCH ANGLE (DEG.)	0000110
PROBE YAW ANGLE (DEG.)	0000120
P(NORTH) - P(SOUTH) (VOLTS)	0000130
P(CENTER) - P(WEST) (VOLTS)	0000140
P(CENTER) - P(ATM.) (VOLTS)	0000150
MEAS. INLET MASS FLOW RATE (KG/S)	0000160
MEAS. INLET AXIAL VELOCITY (M/S)	0000170
MEAS. INLET DYNAMIC PRESS. (TORR)	0000180
AXIAL FLUX OF ANGULAR MOMENTUM (N-M)	0000190
AXIAL FLUX OF AXIAL MOM. (NEGL. PST)	0000200
AXIAL FLUX OF AXIAL MOM. (INCL. PST)	0000210
SWIRL NO. S-PRIME (NEGL. PST)	0000220
SWIRL NO. S (INCL. PST)	0000230
STATIC PRESSURE, GAGE (N/SQ. M)	0000240
STAT. PRESS. DIFF., P-PREF (N/SQ.M)	0000250
INLET REYNOLDS NUMBER	0000260
FAN SPEED (RPM)	0000270
REP. FLOW TEMP. (DEG CELSIUS)	0000280
ATMOSPHERIC PRESSURE (TORR)	0000290
DENSITY (KG/CU. M)	0000300
ABS. (LAM.) VISCOSITY (KG/M-S)	0000310
AVERAGES OF NONDIM. U-VELOCITY	0000320
AVERAGES OF NONDIM. V-VELOCITY	0000330
AVERAGES OF NONDIM. W-VELOCITY	0000340
AVERAGES OF STATIC PRESS. DIFFERENCE	0000350
-----	0000351
CALIBRATION DATA FOR FIVE-HOLE PITOT PROBE	0000352
-----	0000360
-----	0000361
(PN-PS) PITCH VELOCITY PC-PA	0000362
(PC-PW) ANGLE COEFFICIENT PC-PW	0000363
-----	0000364
2.780 -58.0 1.869 -0.655	0000365
2.343 -55.0 1.586 -0.414	0000370
1.920 -50.0 1.402 -0.125	0000380
1.580 -45.0 1.130 0.129	0000390
1.360 -40.0 1.083 0.345	0000400
1.150 -35.0 1.047 0.480	0000410
0.940 -30.0 0.975 0.590	0000420
0.770 -25.0 0.952 0.745	0000430
0.610 -20.0 0.940 0.814	0000440
0.455 -15.0 0.929 0.850	0000450
0.300 -10.0 0.935 0.893	0000460
0.135 -5.0 0.963 0.893	0000470
0.000 0.0 1.000 0.930	0000480
-0.163 5.0 1.020 0.993	0000490
-0.327 10.0 1.026 0.980	0000500
-0.470 15.0 1.047 0.900	0000510
	0000520

-0.600	20.0	1.121	0.910		00000530
-0.710	25.0	1.163	0.844		00000540
-0.940	30.0	1.212	0.698		00000550
-1.220	35.0	1.298	0.570		00000560
-1.590	40.0	1.377	0.351		00000570
-1.960	45.0	1.510	0.086		00000580
-2.430	50.0	1.725	-0.176		00000590
-3.080	55.0	2.039	-0.532		00000600
-3.700	58.0	2.416	-0.985		00000610
RAD TRAV. AT X/D=2.25 FOR PHI=0, EXIT PLANE(NO NOZZLE)					
MEAS. 11/8/87 BY CHAI DATAFILE NAME 'PI4225'					
90.0	0.0	2.0	9.0	20.0	80.0
	1	1	12		
	2.25	12	0.068	746.0	
	0000.	15.0	746.0	0.0	
0.0	320.0	-3.000	0.520	-0.220	00000620
0.3	307.0	-0.293	0.450	-0.205	00000630
0.6	300.2	-0.231	0.570	0.220	00000640
0.9	291.5	-0.148	0.478	0.370	00000650
1.2	281.5	-0.087	0.390	0.484	00000660
1.5	275.0	-0.056	0.348	0.555	00000670
1.8	274.0	-0.038	0.289	0.583	00000680
2.1	275.5	-0.021	0.236	0.600	00001100
2.4	275.5	-0.014	0.198	0.606	00001200
2.7	275.5	-0.005	0.170	0.610	00001300
3.0	278.2	-0.003	0.147	0.613	00001400
3.3	282.0	0.000	0.132	0.617	00001500
					00001600
					00001700
					00001800
					00001900
					00002000
					00002100
					00002100



\*\*\*\* TSD FOREGROUND HARDCOPY \*\*\*\*  
 DSNAME=U11316A.B.DATA

O U VELOCITY (M/S)

O

O

I = 1

X = 0.0572

O J Y

12	0.0838	0.113E+01
11	0.0762	0.815E+00
10	0.0686	0.589E+00
9	0.0610	0.637E+00
8	0.0533	0.696E+00
7	0.0457	0.563E+00
6	0.0381	0.772E+00
5	0.0305	0.188E+01
4	0.0229	0.379E+01
3	0.0152	0.561E+01
2	0.0076	0.599E+01
1	0.0000	0.824E+01

O

O

V VELOCITY (M/S)

O

O

I = 1

X = 0.0572

O J Y

12	0.0838	0.000E+00
11	0.0762	0.700E-01
10	0.0686	0.107E+00
9	0.0610	0.268E+00
8	0.0533	0.362E+00
7	0.0457	0.577E+00
6	0.0381	0.765E+00
5	0.0305	0.112E+01
4	0.0229	0.172E+01
3	0.0152	0.251E+01
2	0.0076	0.410E+01
1	0.0000	0.000E+00

O

O

W VELOCITY (M/S)

O

O

I = 1

X = 0.0572

O J Y

12	0.0838	0.530E+01
11	0.0762	0.566E+01
10	0.0686	0.612E+01
9	0.0610	0.661E+01
8	0.0533	0.723E+01
7	0.0457	0.805E+01
6	0.0381	0.882E+01
5	0.0305	0.923E+01
4	0.0229	0.962E+01
3	0.0152	0.965E+01
2	0.0076	0.795E+01
1	0.0000	0.692E+01

O

O

STATIC PRESSURE, GAGE (N/SQ. M)

O

O

I = 1

X = 0.0572

O J Y

```

12 0.0838 0.659E+02
11 0.0762 0.634E+02
10 0.0686 0.601E+02
9 0.0610 0.556E+02
8 0.0533 0.497E+02
7 0.0457 0.399E+02
6 0.0381 0.280E+02
5 0.0305 0.124E+02
4 0.0229 -0.136E+02
3 0.0152 -0.414E+02
2 0.0076 -0.810E+02
1 0.0000 -0.938E+02
O
O PROBE PITCH ANGLE (DEG.)
O
O I = 1
X = 0.0572
O J Y
12 0.0838 0.000E+00
11 0.0762 0.702E+00
10 0.0686 0.100E+01
9 0.0610 0.231E+01
8 0.0533 0.286E+01
7 0.0457 0.409E+01
6 0.0381 0.494E+01
5 0.0305 0.675E+01
4 0.0229 0.943E+01
3 0.0152 0.127E+02
2 0.0076 0.224E+02
1 0.0000 0.000E+00
O
O PROBE YAW ANGLE (DEG.)
O
O I = 1
X = 0.0572
O J Y
12 0.0838 0.780E+02
11 0.0762 0.818E+02
10 0.0686 0.845E+02
9 0.0610 0.845E+02
8 0.0533 0.845E+02
7 0.0457 0.860E+02
6 0.0381 0.850E+02
5 0.0305 0.785E+02
4 0.0229 0.685E+02
3 0.0152 0.598E+02
2 0.0076 0.530E+02
1 0.0000 0.400E+02
O
O TOTAL VELOCITY MAGNITUDE (M/S)
O
O I = 1
X = 0.0572
O J Y
12 0.0838 0.542E+01
11 0.0762 0.571E+01
10 0.0686 0.614E+01
9 0.0610 0.665E+01
8 0.0533 0.728E+01
7 0.0457 0.809E+01
6 0.0381 0.889E+01
5 0.0305 0.949E+01
4 0.0229 0.105E+02
3 0.0152 0.114E+02
2 0.0076 0.108E+02
1 0.0000 0.108E+02

```

O  
O DIMENSIONLESS U VELOCITY  
O

O I = 1  
O X = 0.2500  
O J Y  
12 0.3667 0.980E+00  
11 0.3333 0.709E+00  
10 0.3000 0.512E+00  
9 0.2667 0.554E+00  
8 0.2333 0.606E+00  
7 0.2000 0.489E+00  
6 0.1667 0.671E+00  
5 0.1333 0.163E+01  
4 0.1000 0.329E+01  
3 0.0667 0.488E+01  
2 0.0333 0.521E+01  
1 0.0000 0.717E+01

O  
O DIMENSION V VELOCITY  
O

O I = 1  
O X = 0.2500  
O J Y  
12 0.3667 0.000E+00  
11 0.3333 0.609E-01  
10 0.3000 0.934E-01  
9 0.2667 0.233E+00  
8 0.2333 0.315E+00  
7 0.2000 0.502E+00  
6 0.1667 0.666E+00  
5 0.1333 0.970E+00  
4 0.1000 0.149E+01  
3 0.0667 0.219E+01  
2 0.0333 0.357E+01  
1 0.0000 0.000E+00

O  
O DIMENSION W VELOCITY  
O

O I = 1  
O X = 0.2500  
O J Y  
12 0.3667 0.461E+01  
11 0.3333 0.492E+01  
10 0.3000 0.532E+01  
9 0.2667 0.575E+01  
8 0.2333 0.629E+01  
7 0.2000 0.700E+01  
6 0.1667 0.767E+01  
5 0.1333 0.803E+01  
4 0.1000 0.836E+01  
3 0.0667 0.839E+01  
2 0.0333 0.691E+01  
1 0.0000 0.601E+01

END

VITA 2

Woon Don Chai

Candidate for the Degree of  
Master of Science

Thesis: TIME-MEAN VELOCITY MEASUREMENTS IN SUDDEN  
EXPANSION CONFINED FLOW WITH  
TANGENTIAL INJECTION

Major Field: Mechanical Engineering

Biographical:

Personal Data: Born in Seoul, Korea, May 13,  
1962, the son of the Mr. and Mrs. Chang S.  
Chae.

Education: Graduated from Han Sung High  
School, Seoul, Korea, in March 1981;  
received Bachelor of Science degree in  
Mechanical Engineering from Sung Kyun Kwan  
University, February, 1985; completed  
requirements for the Master of Science  
degree at Oklahoma State University in  
May, 1988.

Professional Experience: Research Assistant,  
School of Mechanical Engineering, Oklahoma  
State University, Stillwater, Oklahoma,  
1987

Professional Society: AIAA